Transmit and Multiuser Diversity Techniques in Wireless Communications

Vom Fachbereich 18
Elektrotechnik und Informationstechnik
der Technischen Universität Darmstadt
zur Erlangung der Würde eines
Doktor-Ingenieurs (Dr.-Ing.)
genehmigte Dissertation

von

Dipl.-Ing. **Liang Li**

Geboren am 02. Nov. 1981 in Taiyuan, China

Referent:	Prof. Dr.-Ing. Marius Pesavento
Korreferent:	Prof. Dr. Constantinos B. Papadias
Tag der Einreichung:	07. Feb. 2012
Tag der mündlichen Prüfung:	02. May 2012

D17

Darmstädter Dissertation

2012

To my family

Abstract

Recently, the demand for high-rate wireless data service has increased enormously. To meet this growing demand, many new techniques have been developed in wireless communications. Among them, techniques based on transmit and multiuser diversity have attracted much attention due to their ability to provide reliable high data rate services. This thesis is aimed at developing and analyzing advanced communication techniques making use of transmit and multiuser diversity.

In this thesis, we consider a cellular network where data transmissions are controlled and coordinated at the base station. We study a variety of special cases of this cellular network including point-to-point communication over the multiple-input and single-output channel, multiuser communication in the downlink from the base station to multiple mobile users, and cognitive communication in an unlicensed secondary network. In the first part of this thesis, we consider the case that a single user is scheduled and there are multiple antennas at the base station. We investigate the communication reliability in terms of the symbol error rate. In particular, we propose several techniques relying on the transmit diversity including different combinations of transmit antenna selection, space-time coding and power allocation. In the second part of this thesis, we study the opportunistic scheduling scheme and determine the potential performance improvement provided by multiuser diversity in terms of the symbol error rate (SER). Two scaling laws on the asymptotic behavior are derived for this system. In the first regime of a large average signal-to-noise ratio (SNR) denoted by A and a fixed number of users K, a SER asymptotically proportional to A^{-K} can be achieved. In the second regime of a large number of users K and a fixed average SNR value A, the SER asymptotically decreases as fast as K^{-A}. In the third part of this thesis, we focus on the

underlay cognitive radio network and study a cognitive broadcast scenario where one secondary transmitter and several secondary receivers share the same spectral resource with the primary users. We investigate the opportunistic scheduling scheme at the secondary transmitter which takes advantage of the multiuser diversity and meanwhile controls the interference at the primary receiver. The sum capacity of such a system is computed and scaling laws of the sum capacity are derived for two asymptotic regimes. In the first asymptotic regime of a large number of secondary receivers (SRs) K and a fixed number of primary receivers (PRs) U, we show that the ergodic sum capacity C scales as $\ln \ln K$. In the second asymptotic regime, where we have a large number of U and a fixed number of K, we show that C decreases as a function of $\ln U$ and asymptotically converges to a certain finite limit. Further, we analyze the symbol error rate performance of this cognitive scenario. Our study shows that the opportunistic scheduling scheme exploiting the multiuser diversity can significantly enhance the performance of the secondary network while limiting the interference caused to the primary system.

Kurzfassung

In letzter Zeit ist die Nachfrage nach drahtlosen Diensten mit Datenraten rasant gestiegen. Um dieser wachsenden Nachfrage gerecht zu werden, sind verschiedene neuartige Verfahren im Bereich der drahtlosen Kommunikation entwickelt worden. Unter ihnen haben Verfahren, die auf Sende- und Mehrnutzerdiversität beruhen, besondere Aufmerksamkeit auf sich gezogen, da sie zuverlässige Dienste mit hohen Datenraten ermöglichen. Ziel dieser Arbeit ist es, fortschrittliche nachrichtentechnische Verfahren unter Verwendung von Sende- und Mehrnutzer- Diversität zu entwickeln und zu analysieren.

In dieser Arbeit betrachten wir Mobilfunknetze, in dem die Datenübertragung an der Basisstation gesteuert und koordiniert wird. Darüber hinaus untersuchen wir eine Vielzahl von Spezialfällen dieses Mobilfunknetze einschließlich der Punkt-zu-Punkt Kommunikation mittels multipler Antennen an der Sende- und Empfangsseite, der Mehrnutzer- Kommunikation in der Abwärtsstrecke von der Basisstation zu mehreren mobilen Teilnehmern, sowie der kognitive Kommunikation in einem nicht-lizenzierten Sekundär-Netzwerk. Im ersten Teil dieser Arbeit betrachten wir die Punkt-zu-Punkt Kommunikation zwischen einer Basisstation mit mehreren Sendeantennen und einem einzelnen mobilen Teilnehmer mit einer einzelnen Empfangsantenne. Wir untersuchen die Zuverlässigkeit der Kommunikation in Bezug auf die Symbolfehlerrate (SER). Insbesondere schlagen wir mehrere auf senderseitiger Diversität basierende Verfahren vor, darunter verschiedene Kombinationen von Verfahren zur Sendeantennenauswahl, Raum-Zeit-Kodierung und Leistungsregelung. Im zweiten Teil dieser Arbeit untersuchen wir die opportunistische Zeitschlitzverwaltung und bestimmen die Grenzen der Reduktion der Symbolfehlerrate, die sich unter Ausnutzung von Mehrnutzerdiversität erreichen läss t. Zwei Gesetzemässigkeiten des asymptotischen Verhaltens werden in diesem

Zusammenhang hergeleitet. Im Bereich eines großen Bei einem hohen durchschnittlichen Signal-Rausch-Verhältnis (SNR), bezeichnet mit A und einer festen Anzahl von Nutzern K, kann eine SER erzielt werden, die asymptotisch proportional gemäß A^{-K} abfällt. Im Falle einer großen Anzahl von Nutzern K und eines konstanten SNR A reduziert sich die SER asymptotisch gemäß K^{-A}. Im dritten Teil dieser Arbeiten wird ein kognitives Funknetzwerk zugrundegelegt, in dem der informationstheoretische Broadcast-Szenario betrachtet wird, in dem sich Sekundärnutzer die spektralen Ressourcen mit den Teilnehmern eines lizensierten Primärnetzwerk teilen. Wir untersuchen die opportunistische Ressourcenvergabe am Sender des Sekundärnetzwerks, welcher die Vorteile der Mehrenutzerdiversität ausnutzt und gleichzeitig die erzeugten Interferenzen im Primärnetzwerk kontrolliert. Störung der primären Nutzern reguliert. Es wird die Summenkapazität eines solchen Kommunikationssystems berechnet und dessen asymptotisches Verhalten bestimmt. Für den ersten asymptotischen Bereich, in dem die Anzahl K der sekundären Empfänger (SRs) hoch und die Anzahl U der primären Empfänger (PRs) fest gehalten wird, zeigen wir, dass die ergodische Summenkapazität C mit $\ln \ln K$ anwächst. Für den zweiten asymptotischen Bereich, in dem bei festem K die Anzahl U der PRs ist, zeigen wir, dass C als eine Funktion von $\ln U$ abfällt und asymptotisch gegen einen endliche Grenzwert konvergiert. Danach analysieren wir die Symbolfehlerrate in dem betrachteten kognitiven Szenario. Unsere Untersuchungen ergeben, dass Systeme mit opportunistischer Ressourcenverwaltung unter Ausnutzung von Mehrnutzerdiversität, erheblich die Leistungsfähigkeit des sekundären Netzwerkes steigern können und sich gleichzeitig die Störung, die dem primären Netzwerk zugeführt wird, begrenzt werden kann.

Acknowledgements

First and foremost, I would like to thank my supervisor Prof. Dr.-Ing. Marius Pesavento for supporting and guiding my research. His effort in creating an excellent academic atmosphere in the Communication Systems Group has been a key factor in success of mine.

I would also like to thank my co-supervisor Prof. Dr. Constantinos B. Papadias for his time and interest in my work. It is a fortune to be able to work with him on the CROWN project. I have benefited a lot from his knowledge and insights during the last three years.

I am grateful to my former supervisor Prof. Alex B. Gershman, who passed away on 12 August 2011. He was a brilliant scientist and an outstanding advisor. He introduced me to the field of MIMO and multiuser communications and gave me the freedom to explore new ideas.

I am indebted to a number of colleagues for valuable discussions and support. Most notably, I am grateful to Professor Sergiy Vorobyov, Nils Bornhorst, Yong Cheng, Dana Ciochina, Dr.-Phys. Mohammed Nabil El Korso, Adrian Schad, Christian Steffens, Nima Sarmadi and Imran Wajid.

Above all, I am grateful to my parents and my wife Wen. Their unconditional love has been the strongest support to me. I would like to thank my parents for giving me the opportunity to study in Germany. Special thanks go to my wife Wen. Compared with her techniques to create happiness diversity to me, all diversity techniques I have spent years to develop become trivial.

Liang Li

Darmstadt, Germany

Feb. 2012

Nomenclature

Abbreviation	Description
AC	**A**lamouti **C**ode
AoA	**A**ngles **o**f **A**rrival
AoD	**A**ngles **o**f **D**eparture
AWGN	**A**dditive **W**hite **G**aussian **N**oise
BC	**B**roadcast **C**hannel
BER	**B**it **E**rror **R**ate
bps	**b**it **p**er **s**ymbol
BPSK	**B**inary **P**hase-**S**hift **K**eying
cdf	**c**umulative **d**istribution **f**unction
CLT	**C**entral **L**imit **T**heorem
CQI	**C**hannel **Q**uality **I**ndicator
CR	**C**ognitive **R**adio
CS	**C**omplementary **S**lackness
CSI	**C**hannel **S**tate **I**nformation
dB	**d**ecibel
FDD	**F**requency-**D**ivision **D**uplexing
HSPA	**H**igh-**S**peed **P**acket **A**ccess
ICT	**I**nformation and **C**ommunication **T**echnologies
IEEE	**I**nstitute of **E**lectrical and **E**lectronics **E**ngineers
i.i.d.	**i**ndependent and **i**dentically **d**istributed
IPC	**I**nterference **P**ower **C**onstraint

Abbreviation	Description
ISNR	**I**nstantaneous **S**ignal-to-**N**oise **R**atio
KKT	**K**arush-**K**uhn-**T**ucker
LOS	**L**ine-**O**f-**S**ight
LTE	**L**ong-**T**erm **E**volution
MAP	**M**aximum **A** posteriori **P**robability
MGF	**M**oment **G**enerating **F**unction
MIMO	**M**ultiple-**I**nput and **M**ultiple-**O**utput
MISO	**M**ultiple-**I**nput and **S**ingle-**O**utput
ML	**M**aximum **L**ikelihood
OFDM	**O**rthogonal **F**requency-**D**ivision **M**ultiplexing
OSTBC	**O**rthogonal **S**pace-**T**ime **B**lock **C**ode
PA	**P**ower **A**llocation
pdf	**p**robability **d**ensity **f**unction
PR	**P**rimary **R**eceiver
PT	**P**rimary **T**ransmitter
PSD	**P**ower **S**pectral **D**ensity
PSK	**P**hase-**S**hift **K**eying
SER	**S**ymbol **E**rror **R**ate
SIMO	**S**ingle-**I**nput and **M**ultiple-**O**utput
SINR	**S**ignal-to-**I**nterference-plus-**N**oise **R**atio
SISO	**S**ingle-**I**nput and **S**ingle-**O**utput
SNR	**S**ignal-to-**N**oise **R**atio
SR	**S**econdary **R**eceiver
ST	**S**econdary **T**ransmitter
STBC	**S**pace-**T**ime **B**lock **C**ode
STC	**S**pace-**T**ime **C**oding
TAS	**T**ransmit **A**ntenna **S**election
TDD	**T**ime-**D**ivision **D**uplexing

Abbreviation	Description
TIA	**T**elecommunications **I**ndustry **A**ssociation
TPC	**T**ransmitted **P**ower **C**onstraint
US	**U**nited **S**tates

Symbols

τ_{coh}	channel coherence time
B_{coh}	coherence bandwidth
Δf_m	maximum Doppler shift
$\Delta\tau$	delay spread
B	signal bandwidth
T_s	symbol duration
$\Delta\theta_r$	angle spread at the receiver
$\Delta\theta_t$	angle spread at the transmitter
D_{coh}	coherence distance
$\binom{n}{i}$	binomial coefficient
$\beta(k,n)$	beta function
$\log_b$	logarithm to base b
$\ln$	natural logarithm
$\mathbf{0}_{m\times n}$	$m \times n$ matrices with all entries equal to 0
$\mathbf{1}_{m\times n}$	$m \times n$ matrices with all entries equal to 1
$\mathbf{e}_i$	a vector with the ith entry equal to 1 and all other entries equal to 0
$\lceil x \rceil$	the smallest integer larger than or equal to x
$[x]^+$	the maximum of x and 0
$\mathcal{N}(\mu, \sigma^2)$	Gaussian distribution with mean μ and variance σ^2
$\mathcal{M}(x)$	MGF
$\Gamma(x)$	gamma function
$\mathrm{Re}(x)$	real part of x

$\mathrm{Im}(x)$	imaginary part of x
$\mathrm{rank}\{\cdot\}$	rank of a matrix
$\mathrm{tr}\{\cdot\}$	trace of a matrix
$\mathrm{E}\{\cdot\}$	statistical expectation
$\mathrm{E}_X\{\cdot\}$	statistical expectation taken with respect to the random variable X
γ_e	Euler's constant

Table of Contents

List of Figures

List of Tables

Chapter 1

Introduction

Wireless communication has been deeply embedded in our daily life. Nowadays services provided by wireless communication devices such as cellular phones and Wi-Fi modems are almost indispensable to the modern life. According to the TIA's 2010 ICT market review and forecast, the wireless services revenue in the US achieved $161.1 billion dollars in 2009 and is expected to increase to $210.7 billion dollars in 2013 [1]. As a necessary supplement to the traditional voice services, data services play an important role on the wireless market. Currently, data services are the driving force behind the growth of wireless services. The aim of this thesis is to develop and analyze advanced transmission and scheduling techniques that enable high-performance wireless data services. In this introductory chapter, we give a brief overview of the concepts and topics addressed in this thesis and outline the contributions.

1.1 Features of Wireless Communication

Wireless communication is facilitated by the radiation of electromagnetic waves from the transmitter to the receiver. Compared with wired communication such as cable television and fiber-optic communication, wireless communication has its specific characteristics.

Firstly, the propagation of an electromagnetic wave through a wireless channel is a phenomenon that is generally difficult to be described with simple models. The natural and artificial objects in the environment cause reflection, diffraction and scattering of electro-

magnetic waves. A wireless channel is generally characterized by three aspects which are path loss, shadowing and multipath fading. The pass loss is the decay of signal power related to the distance between the transmitter and the receiver. A small path loss is preferred in general. Shadowing, also called large-scale fading, represents the slow variations of the average local signal strength which results from the presence of large objects such as buildings, hills and vehicles. According to empirical studies, the attenuation of signal strength due to shadowing can often be described by so-called log-normal distributions. Multipath fading, also referred to as small-scale fading, stands for the rapid variations of the signal attenuation caused by the multipath propagation, where electromagnetic waves arrive at the receiver from many different directions with different delays. As a consequence of the above mentioned phenomena, which depend on frequency, time and space, a wireless channel can hardly be described by any deterministic model. Instead, a stochastic model is often applied to characterize the propagation environment. Comprehensive surveys of characterizing and modeling of wireless communication can be found in [2]-[6].

Secondly, several wireless devices often access the same medium and they may cause severe interference to each other. Hence, in the design and regulation of wireless communication systems, the issue of co-channel interference must be carefully addressed. A traditional way of avoiding co-channel interference is to assign different frequencies to different wireless systems. Although this way can effectively reduce the co-channel interference, it leads to inefficient spectrum usage especially if multiple antennas are available and produces a heavy regulatory burden preventing further increase of the worldwide wireless services. This background has motivated the emergence and rapid development of cognitive radio (CR) technologies [7]-[9].

1.1.1 Multipath Fading

The focus of this thesis is to develop advanced transmission and scheduling techniques to, on one hand, combat multipath fading, and, on the other hand, exploit the associated diversity gains. In this section, we will provide a more detailed description of fading due to multipath propagation as illustrated in Fig. 1.1). According to the rate at which the channel gains

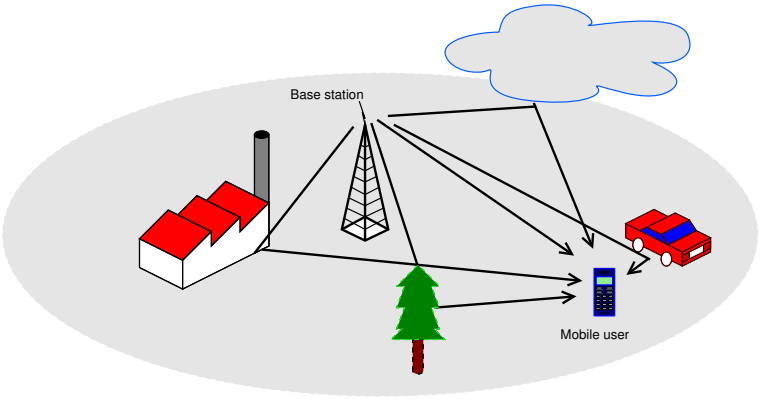

Figure 1.1: Multipath propagation

vary as compared to the symbol rate, the multipath fading can be classified into fast and slow fading. Considering its spectral properties as compared to the signal bandwidth, the multipath fading can be categorized as flat or frequency-selective fading. According to its spatial properties, the multipath fading can be further classified as space-selective and space-non-selective fading.

To describe fast and slow fading, we introduce the notion of Doppler spread and its relation to the channel coherence time. The Doppler shift describes the phenomenon that the signal frequency is shifted when there is relative motion between the transmitter and the receiver. In the case of multipath propagation, signals traveling along different paths may experience different Doppler shifts, resulting a Doppler spread of the signal at the receiver. Denoting the difference between the maximum and minimum Doppler shift encountered in the received signal as Δf, the channel coherence time τ_{coh} is equal to

$$\tau_{coh} = \frac{1}{\Delta f}. \tag{1.1}$$

The channel coherence time τ_{coh} represents the time duration during which the signal components are highly correlated and during which the channel can be assumed to be approximately constant. If the signal bandwidth is much larger than the maximum Doppler shift, or equivalently, if the symbol duration T_s is much less than the channel coherence time τ_{coh}, i.e., $T_s \ll \tau_{coh}$, the channel fading is called slow fading. If the channel coherence time is small relative to the symbol duration T_s, i.e., $T_s \gg \tau_{coh}$, the fading in this case is called fast fading.

The spectral properties of multipath fading are determined by the coherence bandwidth B_{coh}, where coherence bandwith is defined as the bandwidth over which the channel can be considered as approximately constant, i.e., over which two signals with different frequencies are likely to experience correlated amplitude fading. The delay spread $\Delta\tau$ is usually defined as the time delay between the first and the last arrivals of significant signal components. The coherence bandwidth is inversely proportional to the delay spread $\Delta\tau$, i.e.,

$$B_{coh} \sim \frac{1}{\Delta\tau}. \tag{1.2}$$

If the signal bandwidth B is less than the coherence bandwith, i.e., $B < B_{coh}$, the channel fading is called flat fading. On the other hand, if the the signal bandwidth is larger than the coherence bandwidth, i.e., $B > B_{coh}$, the fading is called frequency-selective fading.

The spatial properties of the multipath fading can be similarly identified as its spectral properties. Angle spread at the receiver, $\Delta\theta_r$, is defined as the spread of the angles of arrival (AoAs) of the multipath signals. Likewise, angle spread at the transmitter, $\Delta\theta_t$, refers to the spread of the angles of departure (AoDs) of the multipath signals. The angle spread can cause spatial selectivity of fading, which is characterized by the coherence distance D_{coh}. The coherence distance represents the maximum distance for which the channel responses at two antennas are strongly correlated. Generally, a larger angle spread will result in a shorter coherence distance. If multiple transmit antennas are separated sufficiently far ($\gg D_{coh}$) from each other, the signal transmitted from these antennas to a common receive antenna will experience uncorrelated (space-selective) fading . Similarly, if multiple receive antennas are separated sufficiently far ($\gg D_{coh}$) from each other, the signal transmitted from a common transmit antenna to these receive antennas will experience space-selective fading.

A wireless communication channel is frequently modeled as a fading channel [3]. Conventionally, in single-antenna point-to-point communication systems, channel fading is considered as a kind of channel impairment which is harmful to the wireless communication. This point of view is to a large extent due to the fact that a wireless channel is frequently in deep fading, where deep fading refers to strongly destructive superpositions of the multipath signal components at the receiver. Also, the existence of fading makes channel equalization more expensive. However, recent research has shown that with the introduction of multiple

antenna systems [10] and advanced scheduling schemes, fading should be reconsidered as a kind of precious resources which should be optimally utilized to maximize the overall system performance [2] [11] [12]. In this thesis, we will focus on slow, flat, but space-selective fading channels and develop diversity-based techniques to combat or exploit fading. Rayleigh fading will be used as the statistical model to represent the multipath fading envelope. The Rayleigh distribution is often used to model the multipath fading channel without a direct line-of-sight (LOS) path [3]. In the following two sections, we will give a brief survey of techniques making use of diversity.

1.2 Traditional Diversity Techniques

The reliability of wireless communication depends on the quality of fading channel. In general, there is a significant probability that a signal path is in deep fading. Diversity-based techniques are commonly used to combat the adverse impacts of the fading. The original motivation for applying diversity techniques is that if multiple versions of the same transmitted signal pass through independently fading paths, compared with the case of single signal path, the probability that all these versions experience deep fade reduces dramatically [6]. A wireless communication system relying on diversity techniques can guarantee reliable communication as long as one of the multiple signal paths is strong.

Diversity can be achieved in time, frequency and space domain. Diversity in time domain can be obtained by repeatedly transmitting multiple versions of the same signal at different time instants affected by different fading states. Repetition code is the simplest form of applying time diversity. Frequency diversity can be similarly achieved by transmitting multiple versions of the same signal on different carrier frequencies affected by frequency-selective fading. In wireless communication, time and frequency diversity are frequently exploited together with forward error correction coding and interleaving [13] [14], where the information message is firstly encoded and the codewords are then spread over different time instants and/or carrier frequencies by means of interleaving. In this way, different parts of a codeword experience independent fading channels and error bursts are effectively avoided. Orthogonal Frequency-Division Multiplexing (OFDM) [11] [12] [15] and frequency hopping [16] [17]

are two typical examples of applying time and frequency diversity together with channel coding. Space diversity can be acquired by equipping multiple antennas at the transmitter and/or the receiver. Signal paths which experience independent fading can then be created by placing the equipped antennas sufficiently far apart. A well-known diversity technique performed in the space domain is beamforming [18] [19], where signal components received at different antennas are constructively combined while the components of the interference signal are destructively combined. According to the site of implementation, space diversity can be further classified into transmit diversity and receive diversity and the transmit diversity is one focus of this thesis. Certainly, a diversity technique can exploit diversity in multiple domains. A perfect example of such a technique is space-time coding (STC) which exploits diversity in both time and space domains [20] [21]. More information about the traditional diversity techniques can be found in [15]-[23] and references therein.

As next, we will provide a more detailed discussion on the concept of transmit diversity. The applicability of diverse transmit diversity techniques crucially depends on the amount of channel state information (CSI) available at the transmitter. In the extreme cases of full and no CSI at the transmitter, transmit beamforming and space-time block code (STBC) [24] [25], respectively, are commonly used. In the context of this thesis, full CSI means the exact values of complex channel gains in baseband signal model. Unlike the receiver, which can estimate the channel based on known training (pilot) signals, the transmitter usually does not have instantaneous CSI unless this information is either fed back from the receiver[1] or estimated at the transmitter based on the channel reciprocity[2]. In practical systems, the CSI feedback can cause significant signal overhead and in general, only a quantized version of instantaneous CSI can be fed back to the transmitter. This fact motivates the study of diversity techniques that rely on partial CSI at the transmitter [26]-[30], where partial CSI stands for a quantized version of CSI which may represent an index of power level, a quantized channel gain, an index of a beamformer, etc. Traditionally, the partial CSI is provided to the transmitter by means of the limited feedback [32] [33]. An example of diversity techniques based

[1] In the case of frequency-division duplexing (FDD).

[2] The channel reciprocity can be maintained, for example, in some time-division duplexing (TDD) systems. However, the estimated CSI may be outdated if the channel varies rapidly.

on partial CSI at the transmitter is the transmit antenna selection (TAS) [34]. By applying the TAS, the selection diversity [6], which is conventionally exploited at the receiver [39] [40], can also be achieved at the transmitter. For example, in [28], it has been proposed to use diagonally weighted orthogonal space-time block codes (OSTBCs) with feedback-driven weights. The results in [28] have shown that the performance of such a diagonally weighted OSTBC scheme is substantially better than that of the conventional OSTBC scheme without any feedback. In [29], a combined strategy based on antenna selection and OSTBCs has been compared with the conventional OSTBC-based scheme. Different transmission techniques based on TAS and power allocation (PA) in one-bit-feedback-based Alamouti-type wireless systems have been studied in [30]. Further extensions of the approach of [30] to single-antenna OFDM-based systems have been reported in [31]. Some other works relating to the fundamental capacity limits can be found in [32]-[38].

1.3 Evolution of Diversity-Based Techniques

The principle of diversity has been widely adopted in many wireless communication systems. In current research activities, the applications of diversity-based techniques are extended beyond the traditional point-to-point setting to multiuser, cooperative and CR scenarios. As already mentioned in Section 1.1.1, fading, to a large extent, has been reconsidered as natural resources to utilize, rather than an artefact to combat.

1.3.1 Multiuser Diversity

In a multiuser wireless system, the antennas of different users are often located sufficiently far from each other such that channels of different users experience space-selective (independent) fading. If there is a large number of users in the system, then at any time instant, it is likely that the channel of at least one user exhibits a strong gain. If the scheduler can be provided with the CSI of each individual user, by scheduling the user(s) with good channel quality opportunistically, the overall system performance can be enhanced. In literature, the increase of spectral efficiency and system reliability associated with the opportunistic

scheduling and opportunistic beamforming [42] is generally referred to as multiuser diversity [2]. A rapidly growing interest in applying multiuser diversity in practical systems is motivated by the importance of delay-tolerant high-rate data services widely used in the third- and fourth-generation communication systems [41], where the users can tolerate longer delay and wait for good channel conditions to appear. In modern cellular radio access technologies, the scheduler is a key system element which to a large extent determines the overall system performance. To date, the channel-aware dynamic scheduling which takes advantage of multiuser diversity has already been adopted in the Long-Term Evolution (LTE) and LTE Advanced standards [11] [12]. In forthcoming radio access technologies, further supporting mechanisms are provisioned for enhanced dynamic scheduling.

Up to date, the increase of spectral efficiency in terms of channel capacity has already been widely studied for the multiuser diversity. In [43], it has been shown that in the case of multiple single-antenna users, the optimal scheduling scheme in the uplink case is always to schedule the user with the strongest channel. Similar results have been obtained for the downlink case as well [44]. Further results on recent progress in multiuser diversity techniques can be found in [42]-[47] and references therein. Conventionally, the multiuser diversity schemes are evaluated in terms of the achievable system throughput and as a measure, the channel capacity has been extensively studied. However, little work has been devoted to analyze and quantify the system reliability of a multiuser system in terms of symbol error rate (SER). This important issue will be addressed in this thesis.

1.3.2 Cooperative Diversity

Recently, cooperative communication has drawn considerable attention in the field of wireless communication. By relaying signals using antennas belonging to different nodes, another kind of spatial diversity, the so-called cooperative diversity, can be achieved [57]-[59]. In modern wireless networks, users may cooperate and relay messages of other users to realize the cooperative diversity. The most frequently considered relaying methods include amplify-and-forward, decode-and-forward and compress-and-forward [60]. By exploiting cooperative diversity, the system performance in terms of throughput or reliability can be

significantly improved. Recent works on the performance analysis of cooperative diversity can be found in [60]-[70] and references therein.

1.3.3 Diversity Techniques in Cognitive Radio

CR is another emerging field in wireless communication where various diversity-based techniques find their way to practical applications. As a promising technology, CR aims to increase the current inefficient spectrum usage and has shown great potential to further increase the worldwide wireless services. Since proposed by Mitola [7], the idea of CR has generated significant interest in academic community, industry, standardization bodies, and regulatory agencies [8] [9]. Despite its relatively short history, the CR has already been adopted by the standardization bodies [71], [72]. Based on the regulatory restrictions, the CR systems are commonly classified into three categories, namely interweave, underlay and overlay [73]. In the following, we will briefly introduce these three categories.

The interweave category has originally been proposed in [7]. In an interweave CR system, the unlicensed secondary users opportunistically access the radio resources, i.e., spectrum, time and space, complementary to the resources occupied by the licensed users. In such a system, a variety of diversity techniques can be applied by the secondary users in their occupied resources.

In contrast to the interweave, the underlay and the overlay systems explicitly permit coexistence of licensed primary users and secondary users and the adjunctive interference caused by the secondary users is tolerated as long as it remains harmless for the primary users. In underlay CR systems [73] [74], radio access is granted to the secondary devices under the premise that the interference created at the primary users falls below some acceptable threshold. In an underlay CR scenario with multiple secondary users, the benefit of multiuser diversity can still be achieved by advanced scheduling schemes. As an intuitive example, a cognitive scheduler may select the secondary users according to the following two criteria: 1) A scheduled secondary user should have good channel quality relative to its average channel quality. 2) A scheduled secondary user must induce relatively low interference to the primary receivers (PRs). In practice, a compromise between the two criteria

needs to be found.

In the overlay CR category [73] [75] [76], the secondary users can facilitate the primary user's data transmission so that the primary user's communication does not deteriorate. In comparison with the underlay CR, an overlay CR system is often allowed to create higher interference to the primary system due to its ability to increase the desired signal strength at the PUs. In an overlay CR system, the secondary user may apply cooperative diversity by relaying the primary user's signal to compensate the interference caused at the primary user. Certainly, the concepts of time, frequency and space diversity can also be applied in an overlay CR system. In contrast to the underlay CR, overlay CR requires knowledge on primary user's codebook, CSI of the primary user, and often non-causal knowledge of the primary user's data, etc., therefore, the overlay CR depicts an advanced model of CR.

One focus of this thesis is to study the underlay CR system. In particular, opportunistic scheduling scheme will be investigated in a CR broadcast scenario. In an underlay CR system, the opportunistic scheduler can both enhance the performance of the secondary users and reduce the interference caused at the PRs. While the channel capacity of the traditional (non-cognitive) broadcast channel (BC) has been intensively studied [48]-[53], many important questions regarding the capacity of CR systems remain open. The underlay cognitive BC, where additional interference power constraints (IPCs) apply to the primary users, has been considered in [54] and its ergodic sum capacity has been investigated based on the uplink-downlink duality results of [55]. It has been shown in [54] that the optimal user scheduling scheme is to select the user with the best channel condition. Further, the ergodic sum capacity is maximized by the power allocation scheme obtained from the constrained water-filling solution. A comprehensive overview of the recent progress in exploring capacity limits of the CR system can be found in [73]. Compared with the works on spectral efficiency, a thorough study on the system reliability of CR in terms of SER is still lacking in literature. Some attempts on this topic can be found in [88] and [89] where the error rate is analyzed in frequency selective fading and multiple-antenna transmission scenarios, respectively.

1.4 Thesis Overview and Contributions

This thesis is structured as follows. Chapter 2 provides the system model and background knowledge required in this thesis. In Section 2.1, we introduce the general system model. Section 2.2 is devoted to describe two widely used performance measures, namely, the average SER and the channel capacity. In Section 2.3, we outline important definitions and theorems in the statistics and probability theory which are essential to this thesis. In Chapter 3, we study the transmission techniques which make use of transmit diversity to improve the link-level performance. The system-level performance and the problem of scheduler design in multiuser systems are addressed in Chapters 4-6. While Chapter 4 focuses on the application of multiuser diversity in a non-cognitive scenario, Chapter 5 and Chapter 6 are devoted to analyze and quantify the potential performance gains provided by multiuser diversity in the emerging area of CR.

The contributions of this thesis are outlined in the following. In Chapter 3, we focus on the application of multiple transmit antennas and investigate the link-level SER performance. Several transmit diversity techniques based on limited feedback are reviewed and further developed. In particular, we design advanced techniques exploiting transmit diversity where different combinations of TAS, PA and OSTBC in a multiple-input and single-output (MISO) communication link are studied. The performance of diversity techniques based on these combinations is then analyzed. We derive the exact analytical expressions of the average SER which allows us to compare the performance of different techniques. In this chapter, we consider both the cases of error-free and erroneous feedback and show that the performance of the developed transmission strategies substantially depends on the feedback quality. The results presented in this chapter show the potential benefits that can be obtained by embedding the proposed transmit diversity techniques into the upcoming standards. The contributions of Chapter 3 have been published in [99] and [100].

Chapter 4 is dedicated to the study of multiuser diversity and scheduler design in the cellular downlink scenario. In this chapter, we quantify the benefits of applying opportunistic scheduling by deriving analytical SER expressions. Exact bit error rate (BER) expressions for the cases of both full and partial (quantized) CSI feedback are derived for the binary

phase-shift keying (BPSK) modulation. Using these expressions, we further study the problem of designing the CSI feedback parameters. Other contributions in this chapter include the derivation of the asymptotic BER behavior and the BER analysis in the case of erroneous feedback. The asymptotic behavior of the BER is derived in two limiting case. In the first case, we consider the regime of a large signal-to-noise ratio (SNR) denoted by A and a fixed number of users K. In the second case, we consider the regime of a large number of users K and a fixed SNR value A. We prove that under both the full and quantized CSI feedback, a BER proportional to A^{-K} and K^{-A} can be correspondingly achieved in these two asymptotic cases. This result shows that the maximal diversity order is equal to K, whereas the maximal multiuser diversity gain, as defined in (4.4), is equal to the SNR value A. In the case of erroneous feedback, our results show that the benefit of multiuser diversity can be obtained even in highly erroneous low-rate feedback channels. The results provided in Chapter 4 emphasize the benefits of channel-aware dynamic scheduling and show the performance gains in terms of the system reliability. The contributions of Chapter 4 have been published in [101] and [102].

In Chapter 5, we study the fundamental capacity limits of the underlay CR BC. We compute the sum capacity under different IPCs at the PRs. In a fading environment, we formulate the average sum capacity as the solution of a convex optimization problem and derive the ergodic sum capacity in the limiting case where the number of fading states tends to infinity. Further, we investigate the asymptotic ergodic sum capacity in the homogeneous Rayleigh fading case. Two asymptotic regimes are considered. In the first asymptotic regime, where the number of PRs U is kept constant and the number of secondary receivers (SRs) $K \to \infty$ is considered, we show that in this regime, the ergodic sum capacity C scales as $\ln \ln K$ if the number of SRs $K \to \infty$. In the second asymptotic regime, we let $U \to \infty$ for fixed K. We observe that C decreases with increasing U and asymptotically converges to a certain finite limit. This capacity limit is then evaluated for both the average and the peak IPCs, respectively. The contributions of this chapter have been published in [103]- [105].

The SER performance of the considered underlay CR BC is studied in Chapter 6. This chapter can be viewed as an extension of the study in Chapter 4 to the case of underlay

CR. Under the peak IPC at the single PR, SER expressions for the phase-shift keying (PSK) modulations are derived. Our work in this chapter serves as an early attempt to study the system reliability of the CR. The results in this chapter have been presented in [106].

This thesis is summarized in Chapter 7 where conclusions are drawn and future work is outlined.

1.5 Notations

The following common notations will be used throughout this thesis. Lower case and upper case letters are used to denote scalars. Bold face lower case letters denote vectors. Bold face upper case letters denote matrices. For matrices, $(\cdot)^T$, $(\cdot)^*$, $(\cdot)^H$ and $(\cdot)^{-1}$ denote transpose, conjugate, Hermitian transpose, and inverse, respectively.

Chapter 2

System Model and Theoretical Background

In this chapter, we introduce the system model and revise the theoretical background in communications and statistical signal processing on which the following chapters of this thesis are built. The general system model used throughout this thesis is presented in Section 2.1. In Section 2.2, we introduce two widely established performance measures which play a prominent role in this thesis. In Section 2.3, we provide some useful theorems and definitions from probability theory and statistical analysis.

2.1 System Model

The wireless cellular network is probably the most significant network structure for the terrestrial wireless communications to date. Traditionally, each cell is formed by a base station which organizes the data transmission of the associated mobile users. The results presented in this thesis are based on the cellular network structure. As illustrated in Fig. 2.1, the data transmission within a cell may cause interference to the mobile users in a neighboring cell. It is important to note that the scenario depicted in Fig. 2.1 in fact covers a wide range of cellular communication systems. In different communication scenarios, the cells illustrated in the figure may represent neighboring macrocells, femto, or picocells. In the context of

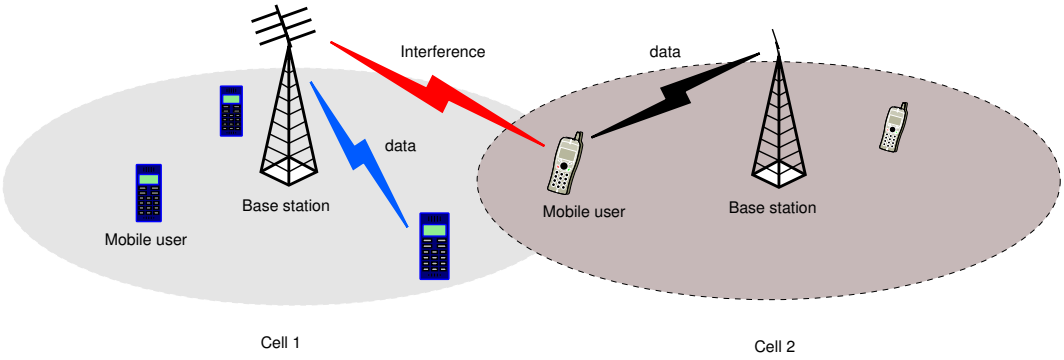

Figure 2.1: Cellular network

cognitive radio, Cell 1 in Fig. 2.1 may represent a cognitive radio cell as specified by the IEEE 802.22 standard and the mobile users in Cell 2 may represent the licensed primary users.

According to the existing and upcoming wireless communication standards such as LTE and LTE-Advanced , the base stations and mobile users can be equipped with multiple antennas which enable the advanced spatial processing and scheduling techniques to meet the increasing need for data service. In the sequel, we denote the number of antennas at the base station as M and assume that there are K active mobile users associated with this base station. Each mobile user is assumed to be equipped with a single antenna.

Assuming flat and slow fading channels, let us define the complex baseband channel coefficient from the ith ($1 \leq i \leq M$) antenna at the base station to the kth ($1 \leq k \leq K$) mobile user as $h_{i,k}$. In the downlink case, where the base station in Cell 1 transmits signal to its associated mobile users as shown in the Fig. 2.1, the digital baseband signal received by the kth mobile user in the time index t can be expressed as

$$r_k(t) = \sum_{i=1}^{M} h_{i,k}(t)s_i(t) + n_k(t), \tag{2.1}$$

where $s_i(t)$ denotes the signal transmitted by the ith antenna at the base station and $n_k(t)$ represents the additive noise received by the kth mobile user. Similarly, if we define the channel gain between the ith antenna at the base station and a mobile user l in the neighboring

Cell 2 as $g_{i,l}$, the interference received by this user can be expressed as

$$y_l(t) = \sum_{i=1}^{M} g_{i,l}(t)s_i(t). \tag{2.2}$$

Unless explicitly mentioned otherwise, we will assume Rayleigh fading channels and additive white Gaussian noise (AWGN) throughout this thesis. The variances of channel gains $h_{i,k}$ and $g_{i,l}$ are denoted as $\sigma_{h_{i,k}}$ and $\sigma_{g_{i,k}}$, respectively. The noise power received by the user k is denoted as σ_{n_k}.

In the uplink case, let us define the complex baseband channel coefficient from the kth ($1 \leq k \leq K$) mobile user to the ith ($1 \leq i \leq M$) antenna at the base station as $w_{i,k}$. The digital baseband signal received by the ith antenna of the base station in Cell 1 from its K associated mobile users in the time index t can be expressed as

$$v_i(t) = \sum_{k=1}^{K} w_{i,k}(t)u_k(t) + z_i(t), \tag{2.3}$$

where in this case, $u_k(t)$ denotes the signal transmitted by the kth mobile user and $z_i(t)$ is the noise received by the $i$the antenna. The interference received by the user l in the neighboring Cell 2 can be correspondingly expressed as

$$y_l(t) = \sum_{k=1}^{K} \eta_{k,l}(t)u_k(t), \tag{2.4}$$

where $\eta_{k,l}$ in the uplink case denotes the channel gain between the kth mobile user in Cell 1 and the mobile user l in Cell 2.

In this thesis, we will focus on the downlink case, however, after suitable modifications, some of the developed techniques and the provided analyses also apply in the uplink case. Throughout this thesis, we will assume that the channel coefficients corresponding to different transmitters or receivers are mutually independent (space-selective fading).

2.2 Performance Measures

Reliability and data throughput are two important aspects for characterizing the performance of wireless data service. Apart from high data throughput, a high-performance wireless system is required to provide reliable communication which means that the error rate should be

maintained at an acceptable level. A straightforward measure that reveals the communication reliability is the average received SER. Considering the data throughput, it is important to determine the maximal data rate of a system. From the famous work of Shannon [77], we know that channel capacity is the maximal achievable data rate of a reliable communication link, where a reliable link means that a communication link will result in an arbitrarily small error probability if we can use channel coding with infinitely long codewords. In the sequel, we will adopt the channel capacity as a performance measure for the data throughput. However, it should be noted that channel capacity is an idealized upper bound of the data throughput which is generally not achievable due to the imperfect CSI, finite codeword length, computational complexity constraints and inexact channel distributions, etc. As next, we discuss these two performance measures in detail.

2.2.1 Average SER

The SER of the demodulated signal is frequently used as a performance measure for the link reliability. In the sequel, we will compute the average SER of the uncoded signals. Beyond the computational tractability, considering uncoded signal can provide useful insight into the SER gain resulted from the spatial diversity as opposed to the SER gain obtained from the channel coding. Obviously, both the considered techniques based on transmit or multiuser diversity and the conventional error correction coding techniques can improve the SER performance and both techniques can be combined to accumulated their benefits. By considering the uncoded signal, we can illustrate the net performance improvement gained by the diversity-based techniques. In all analyses of SER carried out in this thesis, we consider the case of ideal coherent detection. Detailed discussions on non-coherent detection can be found in [3] and [16]. Although we will concentrate on the PSK modulation for the presentational simplicity, our results can be extended to other modulation types by using the corresponding SER expressions provided, for example, in [3].

As next, let us briefly introduce the detector for the ideal coherent signal detection. In this section, we consider the case of $K = 1$ and omit the subscript k in (2.1) for simplicity. In this thesis, we assume that each symbol has the same a priori probability. Thus, the

maximum a posteriori probability (MAP) detector is equivalent to the maximum likelihood (ML) detector [16]. As the channel gain is assumed to be known at the receiver, in the case of $M = 1$, omitting the subscripts i in (2.1), the signal at the input of the detector can be normalized by $h(t)$ and equivalently expressed as a signal passing through an AWGN channel, i.e.,

$$\hat{r}(t) = s(t) + \hat{n}(t), \tag{2.5}$$

where $\hat{r}(t)$ and $\hat{n}(t)$ are the equivalent received signal and the equivalent noise. If $s(t)$ is modulated by PSK and transmitted with power P, the SNR of $\hat{r}(t)$ can be expressed as $\frac{|h(t)|^2 P}{\sigma_n^2}$, where σ_n^2 denotes the noise power. In [16, Section 5.1.3], it has been shown that the ML detector for (2.5) is equivalent to a minimum distance detector which consists in finding the closest symbol to the equivalent received signal $\hat{r}(k)$.

In the case of Alamouti code (AC), we have $M = 2$, $s_1(1) = c_1$, $s_2(1) = c_2$, $s_1(2) = -c_2^*$, and $s_2(2) = c_1^*$, where c_1 and c_2 denote the two symbol to be transmitted [24]. The channel gains in this case must satisfy $h_i(1) = h_i(2) = h_i$ for $i = 1, 2$, i.e., a channel gain must remain constant during two symbol durations. The received signal according to (2.1) can be expressed as

$$\begin{bmatrix} r(1) \\ r(2) \end{bmatrix} = \begin{bmatrix} c_1 & c_2 \\ -c_2^* & c_1^* \end{bmatrix} \begin{bmatrix} h_1 \\ h_2 \end{bmatrix} + \begin{bmatrix} n(1) \\ n(2) \end{bmatrix}. \tag{2.6}$$

Rewriting (2.6) as

$$\begin{bmatrix} r(1) \\ r^*(2) \end{bmatrix} = \begin{bmatrix} h_1 & h_2 \\ h_2^* & -h_1^* \end{bmatrix} \begin{bmatrix} c_1 \\ c_2 \end{bmatrix} + \begin{bmatrix} n(1) \\ n^*(2) \end{bmatrix} \tag{2.7}$$

and multiplying

$$\begin{bmatrix} h_1 & h_2 \\ h_2^* & -h_1^* \end{bmatrix}^H$$

on both side of (2.7), we have

$$\begin{bmatrix} \hat{r}(1) \\ \hat{r}(2) \end{bmatrix} = \begin{bmatrix} c_1 \\ c_2 \end{bmatrix} + \begin{bmatrix} \hat{n}(1) \\ \hat{n}(2) \end{bmatrix} \tag{2.8}$$

with

$$\begin{bmatrix} \hat{r}(1) \\ \hat{r}(2) \end{bmatrix} = \frac{1}{|h_1|^2 + |h_2|^2} \begin{bmatrix} h_1 & h_2 \\ h_2^* & -h_1^* \end{bmatrix}^H \begin{bmatrix} r(1) \\ r^*(2) \end{bmatrix} \tag{2.9}$$

and

$$\begin{bmatrix} \hat{n}(1) \\ \hat{n}(2) \end{bmatrix} = \frac{1}{|h_1|^2 + |h_2|^2} \begin{bmatrix} h_1 & h_2 \\ h_2^* & -h_1^* \end{bmatrix}^H \begin{bmatrix} n(1) \\ n^*(2) \end{bmatrix}. \tag{2.10}$$

Hence, following (2.8), in the case of AC, we can still detect the signal in a symbol-by-symbol manner as in the case of $M = 1$. Detection of higher order OSTBCs is introduced in [20], which is similar to the case of AC and lies beyond the scope of this thesis. Thus, we omit the introduction of detection of higher order OSTBCs here for brevity.

In the fading environment, we are interested in the SER averaged over all fading states, which is referred to as the average SER. Within a given fading state, where the channel gain remains constant, we denote the SNR at the receiver as the received instantaneous SNR (ISNR). The average SER can be computed by the approach based on the moment generating function given in [3]. Denoting the probability density function (pdf) of the received ISNR as $f(x)$, the MGF can be computed by

$$\mathcal{M}(-y) = \int_0^\infty \exp(-yx) f(x)\, dx. \tag{2.11}$$

Based on the general expression in [3, Sections 5.1 and 8.1], the average SER has been computed for different modulation schemes. For example, the average SER in the case of $\mathcal{K}$-PSK modulation is given by

$$\mathrm{SER} = \frac{1}{\pi} \int_0^{(\mathcal{K}-1)\pi/\mathcal{K}} \mathcal{M}\left(-\frac{a^2}{\sin^2\theta}\right) d\theta, \tag{2.12}$$

where $a = \sin(\pi/\mathcal{K})$ is a constant.

In the high SNR regime, the diversity order, which is defined as the negative exponent d of the SNR in the asymptotic BER expression [20, 22]

$$\mathrm{BER} \simeq \frac{1}{G_c}\, \mathrm{SNR}^{-d}, \tag{2.13}$$

are generally used as a performance measure. The quantity G_c in (2.13) is commonly called the coding gain.

2.2.2 Channel Capacity

The notion of channel capacity was first introduced by Shannon in his original paper [77]. The channel capacity represents the ultimate limit on the rate of information that can be re-

liably transmitted over a fixed communication channel [78]. The channel capacity is defined as the mutual information maximized over all input distributions, where mutual information measures the reduction of uncertainty about the input due to the observation of the output of the communication system. In [79], the channel capacity of a point-to-point multiple-input and multiple-output (MIMO) Gaussian channel is computed. The capacity in fading scenario is considered for instance in [80] and [81].

In a fading channel, ergodic capacity and outage capacity are frequently used as performance measures. The ergodic capacity is the average of the channel capacity over the statistics of the channel. For long codewords, i.e., for coding along a large number of fading states, the ergodic capacity is a suitable measure of the achievable rate [6]. The k-percent outage capacity, on the other hand, is defined as the transmission rate achievable in k percent of the channel realizations. The k-percent outage capacity suitably represents the throughout performance if the codeword duration is significantly smaller than the channel coherence time τ_{coh} [6]. In the following chapters, we focus on the fading channel scenario and in the context of channel capacity, we implicitly assume that the codeword duration is much larger than τ_{coh}. Hence, we will adopt the ergodic channel capacity as the applied performance measure for data throughput.

Conditioned on a fixed complex channel gain h, the channel capacity of a point-to-point SISO discrete memoryless channel with AWGN is given by [2]

$$C_h = \log_2\left(1 + \frac{P|h|^2}{\sigma_n^2}\right) \text{ bps}, \tag{2.14}$$

where P is the transmitted power and σ_n^2 denotes the noise power. The ergodic capacity C, which is the average of C_h over the statistics of h, can then be computed as

$$C = \mathrm{E}_h\left\{\log_2\left(1 + \frac{P|h|^2}{\sigma_n^2}\right)\right\} \text{ bps}. \tag{2.15}$$

The channel capacity for point-to-point MISO, single-input and multiple-output (SIMO) and MIMO links can be found in [2] and [79]. In the case of a wireless network with multiple users, we refer to [2] and [78] for a comprehensive survey of the channel capacity.

2.3 Mathematical Background

In this section, we will briefly outline the important concepts from probability theory and statistical analysis that will be used in the later chapters.

2.3.1 Order Statistics

The theory of order statistics deals with the properties of the ordered random variables. If n random variables $X_1, \cdots, X_n$ are sorted in ascending order, then the kth order statistic of the sequence, denoted as $X_{(k)}$, is the kth-smallest value in the sequence [82]. The special cases of $X_{(1)} = \min\{X_1, \cdots, X_n\}$ and $X_{(n)} = \max\{X_1, \cdots, X_n\}$ are defined as the smallest and the largest order statistic, respectively. For notational simplicity, we will use $X_{[k]}$ to denote the kth largest value of $X_1, \cdots, X_n$.

Assume that $X_1, \cdots, X_n$ are continuous independent and identically distributed (i.i.d.) random variables, each with the cumulative distribution function (cdf) $F(x)$ and the pdf $f(x)$. Then, the cdf of the kth order statistic $X_{(k)}$, denoted as $F_{(k)}(x)$, is given by

$$F_{(k)}(x) = \sum_{i=k}^{n} \binom{n}{i} [F(x)]^i [1 - F(x)]^{n-i}, \tag{2.16}$$

where $F_{(k)}(x)$ represents the probability that at least k of the n random variables $X_1, \cdots, X_n$ are less than or equal to the value x. The pdf of $X_{(k)}$, denoted as $f_{(k)}(x)$, can be computed as

$$f_{(k)}(x) = \frac{1}{\beta(k, n-k+1)} [F(x)]^{k-1} [1 - F(x)]^{n-k} f(x). \tag{2.17}$$

A comprehensive survey of order statistics can be found in [82].

2.3.2 Extreme Value Theory

Extreme value theory focuses on the asymptotic behavior of the order statistics. In the special case of i.i.d. random variables, according to (2.16), the largest order statistic $X_{(n)} = \max\{X_1, \cdots, X_n\}$ has the cdf

$$F_{(n)}(x) = [F(x)]^n. \tag{2.18}$$

As $n \to \infty$, it is clear that for any fixed value of x

$$\lim_{n\to\infty} F_{(n)}(x) = \begin{cases} 1, & \text{if } F(x) = 1; \\ 0, & \text{if } F(x) < 1, \end{cases} \tag{2.19}$$

which is a degenerate distribution. To find the limiting distribution of interest, the random variables $X_{(n)}$ describing the largest order statistic must be transformed as $a_n X_{(n)} + b_n$, where a_n and b_n may depend on n but not on $X_{(n)}$. If there exist constants $a_n > 0$ and b_n and a non-degenerate cdf $G(x)$ such that

$$\lim_{n\to\infty} [F(a_n x + b_n)]^n = G(x) \tag{2.20}$$

at all continuity points of $G(x)$, then we say $F(x)$ is in the domain of maximal attraction of the limiting distribution $G(x)$ [82]. An important result on the limiting distribution $G(x)$ is given as follows [82] [83].

Result 1: For an arbitrary parent distribution $F(x)$, in general, even after suitable transformation, the largest order statistic $X_{(n)}$ does not necessarily possess a limiting distribution as $n \to \infty$. However, if a limiting distribution $G(x)$ exists, it must be one of the following three types, namely,

Fréchet-type distribution:

$$G_1(x) = \begin{cases} 0, & \text{for } x \le 0, \\ \exp\left(-x^{-\alpha}\right), & \text{for } x > 0; \end{cases} \tag{2.21}$$

Weibull-type distribution:

$$G_2(x) = \begin{cases} \exp\left(-(-x)^{\alpha}\right), & \text{for } x \le 0, \\ 1, & \text{for } x > 0; \end{cases} \tag{2.22}$$

Gumbel-type distribution:

$$G_3(x) = \exp\left(-e^{-x}\right), \text{ for } -\infty < x < \infty, \tag{2.23}$$

where $\alpha > 0$.

A result which we will frequently use in the following is that for the special case of the exponential distribution with pdf $f(x) = \exp(-x)$ $(x \ge 0)$, we have $a_n = 1$ and $b_n = \ln n$ and the random variable $X_{(n)} - \ln n$ has the limiting cdf $G_3(x)$.

2.3.3 Central Limit Theorem

We present the central limit theorem (CLT) for the case of n i.i.d. random variables $X_1, \cdots, X_n$. The CLT states that the sum of n i.i.d. random variables with finite mean and finite variance approaches a Gaussian random variable as $n \to \infty$.

Assuming that both the mean m_x and the variance σ_x^2 of X_i, $i = 1, \cdots, n$, are finite, we can define the normalized random variables as

$$Z_i = \frac{X_i - m_x}{\sigma_x}, \quad i = 1, \cdots, n. \tag{2.24}$$

Let

$$Y = \frac{1}{\sqrt{n}} \sum_{i=1}^{n} Z_i, \tag{2.25}$$

which has zero mean and unit variance. As $n \to \infty$, Y approaches a Gaussian random variable with zero mean and unit variance, namely, the distribution of Y converges with a Gaussian distribution with zero mean and unit variance, i.e., $Y \xrightarrow{d} \mathcal{N}(0, 1)$ [16], where "$\xrightarrow{d}$" denotes the convergence in distribution. In probability theory, a sequence of random variables $X_1, \cdots, X_n$ is called converge in distribution to a random variable X if $\lim_{n\to\infty} F_n(x) = F(x)$ for every $x \in R$ at which $F(x)$ is continuous. Convergence in distribution is a weak convergence measure [84].

Chapter 3

Transmit Diversity Techniques Based on Limited Feedback

Multiple antenna techniques can greatly enhance the system performance [2] [6] [12]. Although the link-level benefit has already been well quantified in terms of the channel capacity [79], the associated unrealistic assumptions such as perfect CSI at the transmitter depict heavy burdens on achieving the promised gain. Hence, research activities pursuing novel practical techniques to realize the predicted performance improvement never cease. In the scenarios such as FDD systems, where the uplink and downlink communications operate at different frequency bands and channel reciprocity does not hold, limited feedback has been well motivated due to its potential for providing precious CSI at the transmitter with acceptable communication overhead. This chapter focuses on the link-level performance where we assume that a single mobile user ($K = 1$) is scheduled by the base station as illustrated in Fig. 3.1. Several advanced techniques making use of transmit diversity and limited feedback are introduced in the sequel. The multiple antenna techniques studied in this chapter include a variety of combinations of antenna selection, space-time coding and power allocation techniques.

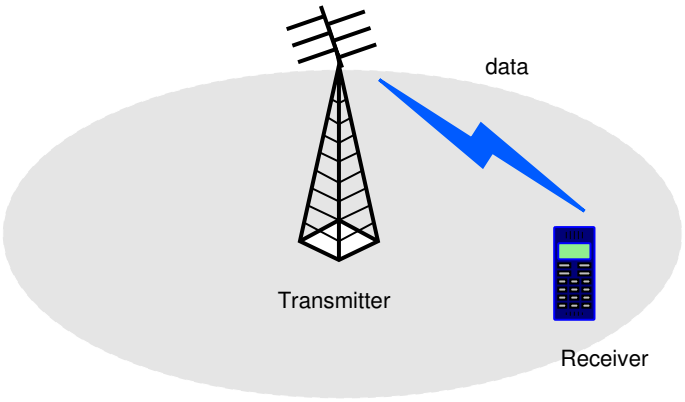

Figure 3.1: A MISO link

3.1 Transmit Antenna Selection

The simplest form of diversity techniques utilizing limited feedback is the transmit antenna selection (TAS) [22] [23]. One major obstacle in introducing multiple antenna system is the high hardware costs. The main advantage of TAS lies in fact that this technique can be simply and cost-efficiently implemented. While the issue of designing antenna selection algorithms to maximize the channel capacity has already been well addressed [34], the problem of analyzing and minimizing SER of TAS schemes under the existence of feedback error still depicts a heavy burden to clarify the performance of the TAS. In this section, by deriving exact BER expressions for the BPSK modulation[1], we provide powerful tools to depict the performance of TAS. Although the SER expressions presented in this and the subsequent sections of this chapter are derived for the BPSK modulation and Rayleigh fading case, SER expressions for other types of modulation and fading can be obtained in a similar manner following the steps of our derivations.

For a single communication link as depicted in Fig. 3.1, to select one transmit antenna from the existing M ones, a feedback message with $m = \lceil \log_2 M \rceil$ bits is required from the mobile user. Considering the existence of feedback errors, the BER of the considered mobile

[1]Note that for BPSK modulation, SER is equal to the BER.

user can be expressed as

$$\mathrm{BER}_{\mathrm{TAS}}(A, \mathcal{P}_e) = \mathcal{P}_{\mathrm{CF}}\, \mathrm{BER}_{\mathrm{CF}}(A) + \mathcal{P}_{\mathrm{EF}}\, \mathrm{BER}_{\mathrm{EF}}(A) \tag{3.1}$$

where A is defined as the average received SNR and $\mathcal{P}_e$ is the error probability of each feedback bit. For computational tractability, we assume in this chapter that the variance of each channel gain $h_{i,k}(t)$ in (2.1) with $1 \leq i \leq M$ and $k = 1$ is equal to one[2]. Hence, $A = P/\sigma_n^2$, where P is the transmitted power as defined in Section 2.2. In (3.1), $\mathcal{P}_{\mathrm{CF}}$ and $\mathcal{P}_{\mathrm{EF}}$ are the probabilities of the correct and erroneous feedback, respectively, and $\mathrm{BER}_{\mathrm{CF}}$ and $\mathrm{BER}_{\mathrm{EF}}$ are the BERs in the correct and erroneous feedback cases, respectively. If M is an integer so that $M = 2^m$, then $\mathcal{P}_{\mathrm{CF}} = (1 - \mathcal{P}_e)^m$ and $\mathcal{P}_{\mathrm{EF}} = 1 - (1 - \mathcal{P}_e)^m$. The received ISNR by using the ith ($i = 1, \cdots, M$) transmit antenna can be expressed as

$$\gamma_i = |h_i|^2 P/\sigma_n^2, \tag{3.2}$$

where the transmitted power P in any fading state is equal to an average value given by $\overline{P}$ since no power allocation is applied in this case. Without loss of generality, we let $\overline{P} = 1$ in this chapter. Following the assumptions that the channel gains are resulted by the Rayleigh fading and their variances are all equal to one, γ_i, $i = 1 \ldots, M$ can be found as centrally χ^2-distributed variables with two degrees of freedom.

From (2.17), the pdf of the nth largest ISNR $\gamma_{[n]}$ among all γ_i can be expressed as

$$f_{\gamma_{[n]}}(x) = \frac{M}{A} \binom{M-1}{n-1} \left[1 - \exp\left(-\frac{x}{A}\right)\right]^{M-n} \left[\exp\left(-\frac{x}{A}\right)\right]^{n}. \tag{3.3}$$

Inserting (3.3) in (2.11), the MGF can be expressed as

$$\mathcal{M}_{\gamma_{[n]}}(-y) = M \binom{M-1}{n-1} \sum_{k=0}^{M-n} \binom{M-n}{k} \frac{(-1)^k}{yA + n + k}. \tag{3.4}$$

Then, inserting (3.4) in (2.12), we can obtain the BER in the case of selecting the antenna with $\gamma_{[n]}$ as

$$\mathrm{BER}_{\gamma_{[n]}} = M \binom{M-1}{n-1} \sum_{k=0}^{M-n} \frac{(-1)^k \binom{M-n}{k}}{2(n+k)} \left(1 - \sqrt{\frac{A}{A+n+k}}\right). \tag{3.5}$$

[2]We will omit the time index t and subscript k in the remainder of this chapter for brevity.

The BER in the correct feedback case can be obtained from (3.5) by taking $n = 1$ as

$$\mathrm{BER}_{\mathrm{CF}} = M \sum_{k=0}^{M-1} \frac{(-1)^k \binom{M-1}{k}}{2(k+1)} \left(1 - \sqrt{\frac{A}{A+k+1}} \right). \tag{3.6}$$

The same expression as in (3.6) has been obtained in [85] where it has been shown that the asymptotic diversity order of M can be achieved in the correct feedback case. In the erroneous feedback case, where we assume that the errors are independently and uniformly distributed in the feedback message, any transmit antenna except the one corresponding to the strongest channel gain can erroneously be selected with the probability $1/(M-1)$. From (3.5), we obtain that

$$\mathrm{BER}_{\mathrm{EF}} = \frac{M}{M-1} \sum_{n=2}^{M} \sum_{k=0}^{M-n} \frac{(-1)^k \binom{M-1}{n-1} \binom{M-n}{k}}{2(n+k)} \left(1 - \sqrt{\frac{A}{A+n+k}} \right). \tag{3.7}$$

The final expression for $\mathrm{BER}_{\mathrm{TAS}}$ is given by substituting(3.6) and (3.7) in (3.1).

Fig. 3.2 shows the BER results of the TAS, denoted by $\mathrm{BER}_{\mathrm{TAS}}$, versus SNR for $M = 2, 4, 8$. The average SNR A is displayed in dB. It should be noted that in this and all subsequent figures in this chapter, the analytical and experimental curves coincide so well that they are indistinguishable. Therefore, the simulation curves in this chapter are hereafter omitted from the plots and only the analytical curves are displayed. From Fig. 3.2, it can be observed that in the case of error-free feedback, the performance can be substantially improved by increasing the number of transmit antennas M. However, in the erroneous feedback case this conclusion is no longer true, even for relatively low values of the feedback bit error probability. According to Fig. 3.2, increasing the number of transmit antennas M in the latter case may even negatively affect the link performance at high SNR values.

3.2 Antenna Selection Based OSTBC

Traditional OSTBCs do not rely on CSI at the transmitter side. This nice property makes the OSTBC a popular technique. Since its first appearance [24], a vast amount of research and standardization activities have been performed in this area [11] [12] [25]. In the case of more than two transmit antennas, however, there exists no full-rate OSTBC. To date, the only

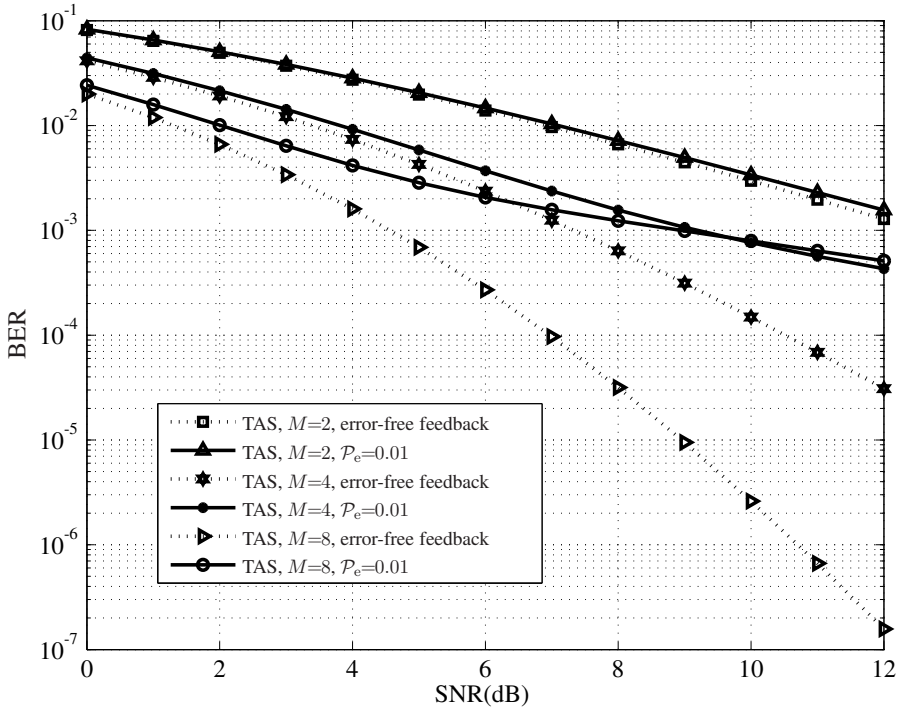

Figure 3.2: BERs versus SNR for TAS with correct and erroneous feedback.

OSTBC formally adopted by the LTE standard is the original AC which achieves full rate in the case of two transmit antennas [24]. In the communication scenarios where more than two transmit antennas exist, combinations of feedback-based antenna selection and OSTBC are proposed to further increase the efficiency of OSTBC [28]-[30]. In this section, we propose a group-based TAS scheme which can significantly increase the performance of the AC while keeps the signaling overhead due to the feedback signaling quite low.

Without loss of generality, let us assume that M is even. In the case that M is odd, in each transmission interval, a randomly selected antenna can be precluded from consideration such that the following proposed scheme can still be applied. Thus, the set of M transmit antennas can be randomly partitioned into $L = M/2$ non-overlapping antenna pairs. Then, in contrast to the TAS technique described in the previous section, a pair of two antennas can be selected[3] rather than a single antenna. Specifically, using the feedback of $m = \lceil \log_2 L \rceil$

[3]Note that another type of scheme has been proposed in [86], where the two antennas associated with the most strongest two channel gains are selected from the M transmit antennas to maximize the ISNR. However, the latter scheme requires $2\lceil \log_2 M \rceil$ bits of feedback (i.e., twice as many as the feedback bits required by the

bits, we can select one group of antennas and then transmit the signals through this group of two antennas using the AC. Similarly to the previous section, the system BER in such a case can be expressed as

$$\mathrm{BER}_{\mathrm{TAS-AC}}(A, \mathcal{P}_e) = \mathcal{P}_{\mathrm{CF}}\, \mathrm{BER}_{\mathrm{CF}}(A) + \mathcal{P}_{\mathrm{EF}}\, \mathrm{BER}_{\mathrm{EF}}(A), \tag{3.8}$$

where the subscript is modified accordingly. In the case that L is an integer such that $L = 2^m$, we have $\mathcal{P}_{\mathrm{CF}} = (1-\mathcal{P}_e)^m$ and $\mathcal{P}_{\mathrm{EF}} = 1-(1-\mathcal{P}_e)^m$. According to (2.8), the received ISNR by using the ith group of transmit antennas can be computed as

$$\gamma_i = \frac{|h_{i,\mathrm{a}}|^2 + |h_{i,\mathrm{b}}|^2}{2\sigma_n^2}, \tag{3.9}$$

where the subscripts "a" and "b" stand for the first and second transmit antennas, respectively. For each antenna, the average transmitted power in any fading state is equal to $\overline{P}/2 = 0.5$. Since γ_i is the sum of two independent identically and exponentially distributed random variables with mean $\frac{A}{2}$, it has a gamma distribution with scale parameter $\frac{A}{2}$ and a shape parameter 2. Thus, the pdf of γ_i is given by

$$f_{\gamma_i}(x) = \frac{4x}{A^2} \exp\left(-\frac{2x}{A}\right). \tag{3.10}$$

In the following, we denote the antenna group corresponding to the $(L-n+1)$th order statistic of γ_i with $i = 1, \cdots, L$ as the nth best antenna group. The pdf of the received ISNR of the nth best antenna group, $\gamma_{[n]}$, can be computed by inserting (3.10) in (2.17) as

$$f_{\gamma_{[n]}}(x) = \frac{4L\binom{L-1}{n-1}x}{A^2}\left[1-\left(\frac{2x}{A}+1\right)\exp\left(-\frac{2x}{A}\right)\right]^{L-n}\left[\left(\frac{2x}{A}+1\right)\exp\left(-\frac{2x}{A}\right)\right]^{n-1}\exp\left(-\frac{2x}{A}\right). \tag{3.11}$$

Using (3.11) along with (2.12) and (2.11), we obtain

$$\begin{aligned}\mathrm{BER}_{\gamma_{[n]}} = {} & L\binom{L-1}{n-1}\sum_{k=0}^{L-n}\sum_{i=0}^{n-1+k}\sum_{l=0}^{i+1}\binom{L-n}{k}\binom{n-1+k}{i}\frac{(-1)^k(i+1+l)!}{l!(n+k)^{i+2}2^{i+l+2}} \\ & \cdot\left(1-\sqrt{\frac{A}{A+2(n+k)}}\right)^{i+2}\left(1+\sqrt{\frac{A}{A+2(n+k)}}\right)^{l}.\end{aligned} \tag{3.12}$$

TAS scheme in Section 3.1) and, therefore, it is not considered here.

The expression for $\mathrm{BER}_{\mathrm{TAS-AC}}$ can be found in the way similar to $\mathrm{BER}_{\mathrm{TAS}}$ in (3.1), where $\mathrm{BER}_{\mathrm{CF}} = \mathrm{BER}_{\gamma_{[1]}}$ can be obtained from (3.12) with $n = 1$. Furthermore, $\mathrm{BER}_{\mathrm{EF}}$ is obtained from (3.12) as

$$\mathrm{BER}_{\mathrm{EF}} = \frac{1}{L-1} \sum_{n=2}^{L} \mathrm{BER}_{\gamma_{[n]}}, \tag{3.13}$$

where we have assumed that each antenna group corresponding to $\gamma_{[n]}$ with $n \geq 2$ has the same probability to be selected.

Fig. 3.3 shows the BERs versus SNR for $M = 4$. In this figure, $\mathrm{BER}_{\mathrm{TAS-AC}}$ in (3.8) is compared to $\mathrm{BER}_{\mathrm{TAS}}$ in (3.1) to see whether the combined TAS-AC transmission strategy can provide performance improvements relative to the single antenna TAS scheme. For both approaches, the total transmit power is assumed to be the identical. It can be observed from Fig. 3.3 that in the error-free feedback case, as it might be expected, the TAS technique shows improved performance as compared to the TAS-AC approach. However, as it follows from Fig. 3.3, the combined TAS-AC technique offers significantly improved robustness against CSI feedback errors as compared over the TAS approach. Therefore, in situations with significant feedback errors, the TAS-AC strategy should be preferred to the TAS approach. However, if the feedback probability of error is relatively small (for example, $\mathcal{P}_e = 0.01$ in Fig. 3.3), there is a turning point in SNR from which the simple TAS-AC strategy should be preferred. For any given value of $\mathcal{P}_e$, this point can be quantified by solving the equation $\mathrm{BER}_{\mathrm{TAS}}(A, \mathcal{P}_e) = \mathrm{BER}_{\mathrm{TAS-AC}}(A, \mathcal{P}_e)$ where $\mathrm{BER}_{\mathrm{TAS}}(A, \mathcal{P}_e)$ and $\mathrm{BER}_{\mathrm{TAS-AC}}(A, \mathcal{P}_e)$ are given by (3.1) and (3.8), respectively.

3.3 Limited-Feedback Based Power Allocation

Power allocation (PA) is a widely used and extensively studied scheme for combating the effects of multipath fading. In the field of information theory, the famous "water-filling" scheme sketches the optimal power allocation to achieve the channel capacity. In the context of limited feedback and SER minimization, however, the optimal power allocation scheme and its performance bound are not well known yet. Some works related to this topic can be found in [30] and [31]. The objective of this section is to propose novel limited-feedback

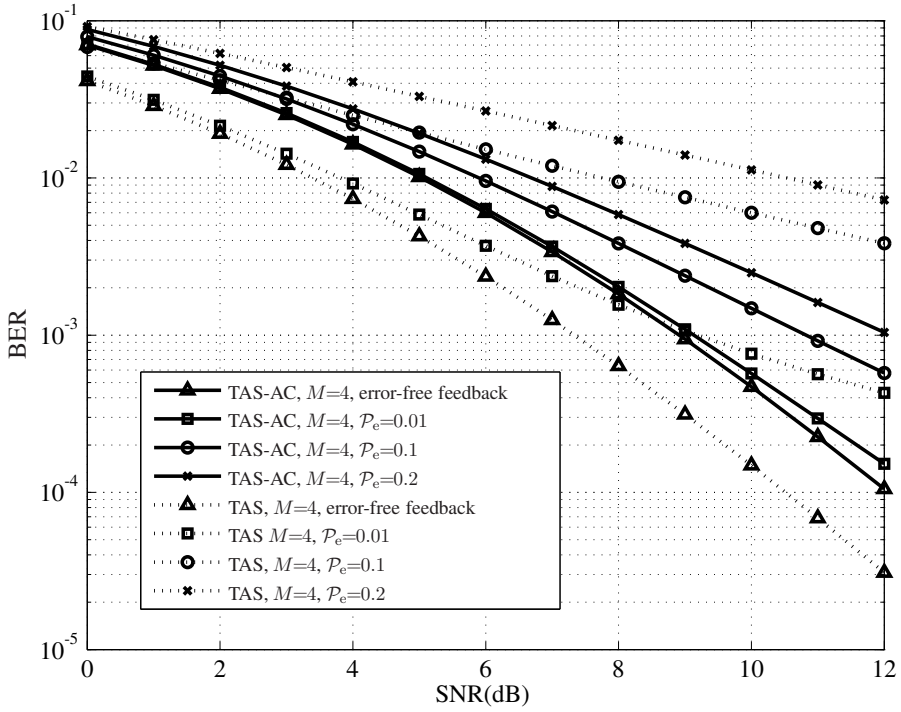

Figure 3.3: BERs versus SNR for TAS and TAS-AC with correct and erroneous feedback.

based power allocation schemes where antenna selection is applied to utilize the selection diversity in spatial domain. As in section 3.1, one antenna is selected in the combined TAS-PA scheme.

The combined TAS-PA scheme considered in this section requires $m = \lceil \log_2 M \rceil + 1$ feedback bits for each fading state, that is, the feedback rate is slightly higher than in the case of TAS. In the TAS-PA approach, $\lceil \log_2 M \rceil$ bits are used to select the transmit antenna with the strongest channel gain, while the remaining single bit is used for PA. Depending on the strongest channel gain, denoted as h_{best}, which corresponds to the largest order statistic of $|h_i|$ with $i = 1, \cdots, M$, a time-varying antenna weight w can be used that is equal to $\sqrt{\alpha}$ if $|h_{\text{best}}|^2 \leq \mu$ and $\sqrt{\beta}$ if $|h_{\text{best}}|^2 > \mu$, where μ is a certain preselected threshold value, and the parameters α and β determine two possible values for w [30]. Note that w in fact represents the power allocated to the antenna. The average transmitted power in a fading state is then equal to α and β for $|h_{\text{best}}|^2 \leq \mu$ and $|h_{\text{best}}|^2 > \mu$, respectively. Additionally, the time average of w is chosen to satisfy the constraint that the average transmitted power equals $\overline{P} = 1$. Denoting the peak transmitted power available at each antenna as $\widehat{P}$, the

values α and β of the time-varying weight w must satisfy $\alpha \leq \widehat{P}$ and $\beta \leq \widehat{P}$.

Case 1: Correct feedback case. In this case, the received ISNR, $\gamma_{\rm c1}$, is equal to $\gamma_{[1]}$ and can be written as

$$\gamma_{[1]} = \begin{cases} A\alpha|h_{\rm best}|^2, & |h_{\rm best}|^2 \leq \mu, \\ A\beta|h_{\rm best}|^2, & \text{otherwise.} \end{cases} \tag{3.14}$$

If the feedback is erroneous, the following three cases should be considered:

Case 2: Antenna selection is erroneous, but antenna weight selection is correct;

Case 3: Antenna selection is correct, but antenna weight selection is erroneous;

Case 4: Both antenna selection and weight selection are erroneous.

Denoting the system BERs in Case 1 to Case 4 as BER_1, BER_2, BER_3 and BER_4, respectively, we obtain

$$\mathrm{BER}_{\rm TAS-PA} = \sum_{i=1}^{4} \mathcal{P}_i \, \mathrm{BER}_i, \tag{3.15}$$

where $\mathcal{P}_i$ with $i = 1, \cdots, 4$ stand for the probabilities with which the corresponding Case 1-4 occur. If $M = 2^{m-1}$, then

$$\mathcal{P}_1 = (1 - \mathcal{P}_e)^m, \tag{3.16}$$

$$\mathcal{P}_2 = [1 - (1 - \mathcal{P}_e)^{m-1}](1 - \mathcal{P}_e), \tag{3.17}$$

$$\mathcal{P}_3 = (1 - \mathcal{P}_{\rm e})^{m-1}\mathcal{P}_e, \tag{3.18}$$

and

$$\mathcal{P}_4 = [1 - (1 - \mathcal{P}_e)^{m-1}]\mathcal{P}_e. \tag{3.19}$$

For the assumed Rayleigh fading channel, according to (2.17), the pdf of $|h_{\rm best}|^2$ is given by

$$f_{|h_{\rm best}|^2}(x) = M \left[1 - \exp\left(-x\right)\right]^{M-1} \exp\left(-x\right). \tag{3.20}$$

Then, calculating $\mathcal{M}_{\gamma_{[1]}}\left(-g\right)$ according to (2.11) and inserting it into (2.12), we have

$$\mathrm{BER}_1 = M \sum_{k=0}^{M-1} \frac{\binom{M-1}{k}}{(-1)^k} \left[\frac{1}{2(k+1)} \left(1 - \sqrt{\frac{A}{A + \frac{k+1}{\alpha}}} \right) - \rho(k+1, \alpha, 1, \mu) + \rho(k+1, \beta, 1, \mu) \right], \tag{3.21}$$

where

$$\rho(m, w, l, \tau) \triangleq \frac{1}{\pi} \int_0^{\frac{\pi}{2}} \frac{\exp\left(-\left(\frac{Aw}{\sin^2\theta} + m\right)\tau\right)}{\left(\frac{Aw}{\sin^2\theta} + m\right)^l} \, d\theta. \tag{3.22}$$

Note that for Case 3, the value of BER_3 can also be expressed by means of (3.21), however, with the interchanged parameters α and β.

Let use denote the channel gain, whose absolute value is the nth largest order statistic of $|h_i|$ with $i = 1, \cdots, M$, as the nth best channel $h_{\mathrm{n-best}}$. The transmit antenna corresponding to the nth best channel is denote as the nth best transmit antenna. In Case 2, the nth ($n \geq 2$) best transmit antenna is selected with the probability $1/(M-1)$. Provided that $|h_{\mathrm{n-best}}|^2 < |h_{\mathrm{best}}|^2 \leq \mu$, the pdf of the nth ($n \geq 2$) largest squared channel gain $|h_{\mathrm{n-best}}|^2$ can be written as

$$f_{|h_{\mathrm{n-best}}|^2}(x) = M \binom{M-1}{n-1} \left[1 - \exp\left(-x\right)\right]^{M-n} \left[\exp\left(-x\right) - \exp\left(-\mu\right)\right]^{n-1} \exp\left(-x\right). \tag{3.23}$$

If $|h_{\mathrm{n-best}}|^2 \leq \mu < |h_{\mathrm{best}}|^2$, then the pdf of $|h_{\mathrm{n-best}}|^2$ is given by

$$f_{|h_{\mathrm{n-best}}|^2}(x) = \frac{M! \exp\left(-x\right) \left[1 - \exp(-x)\right]^{M-n}}{(M-n)!\,(n-2)!} \int_{\mu}^{\infty} \exp(-t) \left[\int_{x}^{t} \exp\left(-y\right) dy\right]^{n-2} dt \tag{3.24}$$

and if $\mu < |h_{\mathrm{n-best}}|^2 < |h_{\mathrm{best}}|^2$, then this pdf can be expressed as

$$f_{|h_{\mathrm{n-best}}|^2}(x) = M \binom{M-1}{n-1} \left[1 - \exp\left(-x\right)\right]^{M-n} \left[\exp\left(-x\right)\right]^{n}. \tag{3.25}$$

Using (3.23)-(3.25) to compute the MGF in (2.11) in the case when the nth best antenna is used, and employing (2.12), after straightforward manipulations, we obtain

$$\begin{aligned}
\mathrm{BER}_2 = \frac{M}{M-1} \sum_{n=2}^{M} \Bigg\{ & \binom{M-1}{n-1} \sum_{k=0}^{n-1} \sum_{i=0}^{M-n} \binom{n-1}{k} \binom{M-n}{i} \exp\left(-\mu k\right) (-1)^{i+k} \\
& \cdot \left[\frac{1}{2(n+i-k)} \left(1 - \sqrt{\frac{A}{A + \frac{n+i-k}{\alpha}}} \right) - \rho(n+i-k, \alpha, 1, \mu) \right] \\
& + \binom{M-1}{n-1} (n-1) \sum_{k=0}^{n-2} \sum_{i=0}^{M-n} \frac{\binom{n-2}{k} \binom{M-n}{i} \exp\left(-\mu(k+1)\right) (-1)^{i+k}}{(k+1)} \\
& \cdot \left[\frac{1}{2(n+i-k-1)} \left(1 - \sqrt{\frac{A}{A + \frac{n+i-k-1}{\beta}}} \right) - \rho(n+i-k-1, \beta, 1, \mu) \right] \\
& + \binom{M-1}{n-1} \sum_{i=0}^{M-n} \binom{M-n}{i} (-1)^i \rho(n+i, \beta, 1, \mu) \Bigg\}.
\end{aligned} \tag{3.26}$$

Note that for Case 4 the value of BER_4 can be expressed by means of (3.26) with the interchanged values of α and β. The final expression for $\mathrm{BER}_{\mathrm{TAS-PA}}$ is then given by inserting the obtained expressions for $\mathrm{BER}_i,\ i = 1, \cdots, 4$ into (3.15).

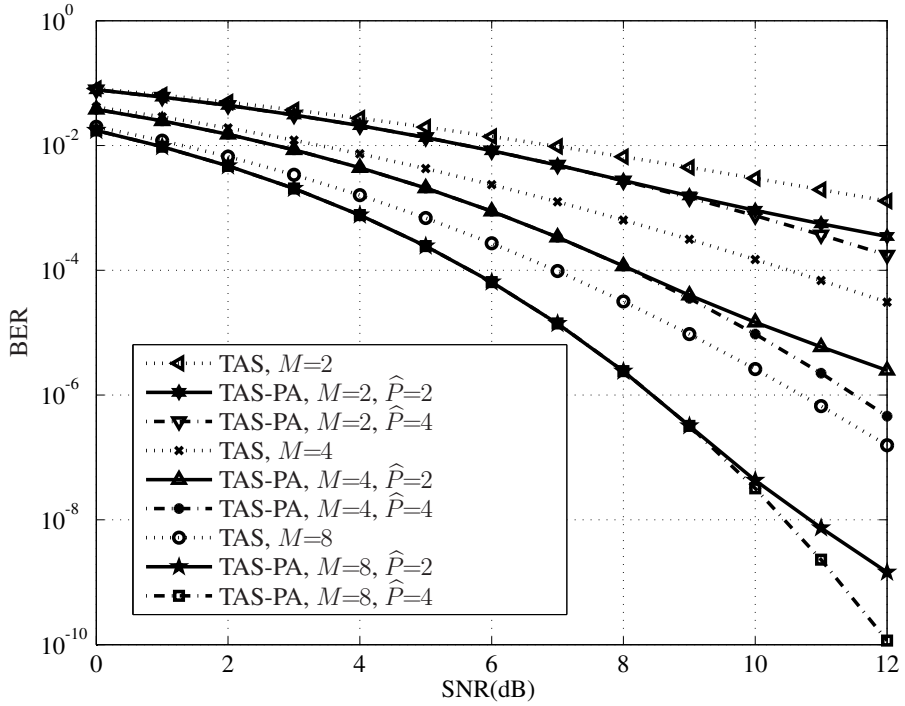

Figure 3.4: BERs versus SNR for TAS and TAS-PA with correct feedback.

The optimal values α_o, β_o and μ_o which minimize the system BER in the correct feedback case can be found by solving the following optimization problem:

$$\begin{aligned} \{\alpha_o, \beta_o, \mu_o\} = & \underset{\alpha,\beta,\mu}{\operatorname{argmin}} \operatorname{BER}_{\mathrm{TAS-PA}}(A, \alpha, \beta, \mu, \mathcal{P}_e = 0) \\ \text{s.t.} \quad & \int_0^{\mu} \alpha f_{|h_{\mathrm{best}}|^2}(x)\, dx + \int_{\mu}^{\infty} \beta f_{|h_{\mathrm{best}}|^2}(x)\, dx = 1, \\ & 0 \le \alpha \le \widehat{P}, \quad 0 \le \beta \le \widehat{P}, \end{aligned} \tag{3.27}$$

where the first constraint in (3.27) is the average power constraint, and the last two constraints are the peak power constraints. As the problem in (3.27) is non-convex, we can find an approximate solution numerically by quantizing the parameters α, β and μ; see also [31].

Fig. 3.4 displays the BERs of the TAS and TAS-PA strategies in the error-free feedback case. In this figure, the TAS-PA approach is tested for different values of the peak power. It follows from Fig. 3.4 that the TAS-PA approach provides significant improvements of the BER performance relative to the TAS technique at the price of one extra-bit of feedback. A part of optimal power allocation parameters for $M = 4$ are shown in Table 3.1.

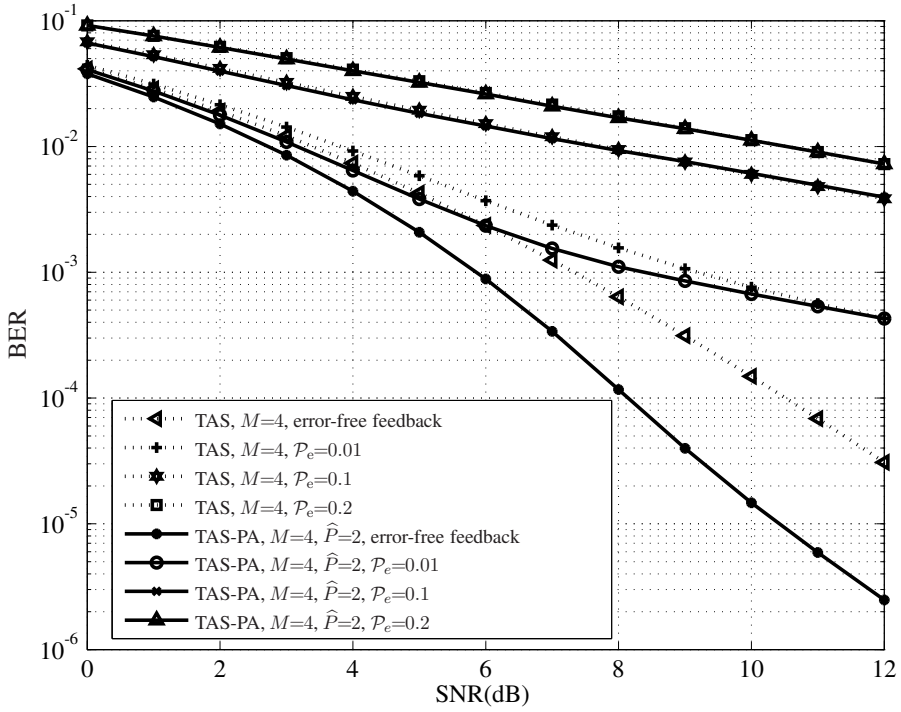

Figure 3.5: BERs versus SNR for TAS and TAS-PA with correct and erroneous feedback.

The BERs in the erroneous feedback case with $M = 4$ are shown in Fig. 3.5. The latter figure illustrates that the performance improvements due to combining the TAS and PA approaches tend to be less pronounced as the feedback BER increases. Note that the optimal parameters α_o, β_o, and μ_o are designed for the correct feedback case. In the case of erroneous feedback, the average power constraint may be slightly violated. However, as the value of $\mathcal{P}_e$ is small, this issue can be ignored in our SER analysis.

3.4 Combination of Limited-Feedback Based TAS, PA and OSTBC

The considered TAS, PA and OSTBC techniques in Sections 3.1-3.3 can be further merged into more reliable transmission techniques. In this section, we consider a combination of TAS, PA and AC techniques where a group of two antennas is selected and PA is performed.

Partitioning the M antennas randomly into $L = M/2$ antenna pairs similarly as in Sec-

$\widehat{P}=2$, SNR in dB	0	2	4	8	10	12
α_o	1.24	1.36	1.54	2.00	2.00	2.00
β_o	0.78	0.76	0.76	0.78	0.76	0.76
μ_o	1.781	1.586	1.366	1.055	1.089	1.089
$\widehat{P}=4$, SNR in dB	0	2	4	8	10	12
α_o	1.24	1.36	1.52	2.08	2.68	3.72
β_o	0.76	0.76	0.76	0.76	0.80	0.80
μ_o	1.838	1.586	1.385	1.058	0.847	0.717

Table 3.1: Optimal parameters of power allocation for $M = 4$.

tion 3.2, and quantizing the values of the channel gains into two levels, $m = \lceil \log_2 L \rceil + 1$ feedback bits are required for the proposed TAS-PA-AC technique. For an antenna pair i with $i = 1, \cdots, L$, in the sequel, we will denote the channel gains corresponding to its two antennas as $h_{i,a}$ and $h_{i,b}$. We will also denote the antenna pair corresponding to the largest order statistic of $|h_{i,a}|^2 + |h_{i,b}|^2$ as the best antenna pair and denote the channel gains of the two antennas in this pair as $h_{\mathrm{best,a}}$ and $h_{\mathrm{best,b}}$. Similarly, we will denote the antenna pair corresponding to the first order statistic of $|h_{i,a}|^2 + |h_{i,b}|^2$ as the worst antenna pair and the channel gains of the two antennas in the worst antenna pair will be denoted as $h_{\mathrm{worst,c}}$ and $h_{\mathrm{worst,d}}$. For a combined TAS-PA-AC scheme, the antenna weights can be expressed in matrix form as

$$\boldsymbol{W} = \begin{cases} \sqrt{\alpha}\boldsymbol{I}, & A(|h_{\mathrm{best,a}}|^2 + |h_{\mathrm{best,b}}|^2) \leq \mu; \\ \sqrt{\beta}\boldsymbol{I}, & \text{otherwise}, \end{cases} \tag{3.28}$$

where $h_{\mathrm{best,a}}$ and $h_{\mathrm{best,b}}$ are the channels between the two antennas (denoted as antennas "a" and "b") of the best transmit antenna pair and the receive antenna, and $\boldsymbol{I}$ is the 2×2 identity matrix. For the sake of simplicity, let us consider the case $M = 4$ in this section. The average transmitted power for each used antenna is equal to 0.5. Similarly to (3.27), the

optimal values α_o, β_o and μ_o, can be found by solving the following optimization problem

$$\{\alpha_o, \beta_o, \mu_o\} = \underset{\alpha,\beta,\mu}{\operatorname{argmin}} \, \mathrm{BER}_{\mathrm{TAS-PA-AC}}(A, \alpha, \beta, \mu, \mathcal{P}_e = 0) \tag{3.29}$$

$$\text{s.t.} \quad \int_0^{\mu} \alpha f_{\gamma_g}(x)\, dx + \int_{\mu}^{\infty} \beta f_{\gamma_g}(x)\, dx = 0.5, \tag{3.30}$$

$$0 \le \alpha \le \widehat{P}, \quad 0 \le \beta \le \widehat{P}, \tag{3.31}$$

where $f_{\gamma_g}(x)$ denotes the pdf

$$f_{\gamma_g}(x) = \frac{2x}{A^2} \exp\left(-\frac{x}{A}\right) \int_0^x \frac{t}{A^2} \exp\left(-\frac{t}{A}\right) dt \tag{3.32}$$

of $\gamma_g = A(|h_{\mathrm{best,a}}|^2 + |h_{\mathrm{best,b}}|^2)$. The constraint in (3.30) is the average power constraint, whereas the two constraints in (3.31) are the peak power constraints. Similar to (3.27), this problem is non-convex and numerical method can be used to find an approximated solution of it.

Let us derive an explicit expression for $\mathrm{BER}_{\mathrm{TAS-PA-AC}}$ by considering the follow cases.

Case 1: Error-free feedback. The received ISNR, denoted as $\gamma_{[1]}$, can be written as

$$\gamma_{[1]} = \begin{cases} \frac{\alpha\left(|h_{\mathrm{best,a}}|^2 + |h_{\mathrm{best,b}}|^2\right)}{\sigma_n^2} = \alpha\gamma_g, & \gamma_g \le \mu; \\ \frac{\beta\left(|h_{\mathrm{best,a}}|^2 + |h_{\mathrm{best,b}}|^2\right)}{\sigma_n^2} = \beta\gamma_g, & \gamma_g > \mu. \end{cases} \tag{3.33}$$

As it has been mentioned in the previous section, the selected antenna weights depend only on the best antenna pair (that is, on γ_g only).

Using (3.32) and (3.33) to compute the MGF in the case when the best antenna pair is used and employing (2.12), after straightforward manipulations, we obtain

$$\begin{aligned} \mathrm{BER}_1 = & -\frac{2\mu}{A}\left[\rho\left(1, \alpha, 1, \frac{\mu}{A}\right) - \rho\left(1, \beta, 1, \frac{\mu}{A}\right)\right] - 2\left[\rho\left(1, \alpha, 2, \frac{\mu}{A}\right) - \rho\left(1, \beta, 2, \frac{\mu}{A}\right)\right] \\ & + 2\left[\left(\frac{\mu}{A}\right)^2 + \frac{\mu}{A}\right]\left[\rho\left(2, \alpha, 1, \frac{\mu}{A}\right) - \rho\left(2, \beta, 1, \frac{\mu}{A}\right)\right] + 4\left[\rho\left(2, \alpha, 3, \frac{\mu}{A}\right) - \rho\left(2, \beta, 3, \frac{\mu}{A}\right)\right] \\ & + 2\left(2\frac{\mu}{A} + 1\right)\left[\rho\left(2, \alpha, 2, \frac{\mu}{A}\right) - \rho\left(2, \beta, 2, \frac{\mu}{A}\right)\right] + \frac{1}{2}\left(1 - \sqrt{\frac{A}{A + \frac{1}{\alpha}}}\right)^2 \left(2 + \sqrt{\frac{A}{A + \frac{1}{\alpha}}}\right) \\ & - \frac{1}{16}\left(1 - \sqrt{\frac{A}{A + \frac{2}{\alpha}}}\right)^3 \left[1 + \frac{3}{2}\left(1 + \sqrt{\frac{A}{A + \frac{2}{\alpha}}}\right) + \frac{3}{2}\left(1 + \sqrt{\frac{A}{A + \frac{2}{\alpha}}}\right)^2\right] \\ & - \frac{1}{8}\left(1 - \sqrt{\frac{A}{A + \frac{2}{\alpha}}}\right)^2 \left(2 + \sqrt{\frac{A}{A + \frac{2}{\alpha}}}\right). \end{aligned} \tag{3.34}$$

Case 2: Erroneous antenna selection, but correct antenna weight selection. The received ISNR $\gamma_{[2]}$ can be expressed as

$$\gamma_{[2]} = \begin{cases} \frac{\alpha\left(|h_{\mathrm{worst,c}}|^2+|h_{\mathrm{worst,d}}|^2\right)}{\sigma_n^2} = \alpha\gamma_w, & \gamma_g \leq \mu; \\ \frac{\beta\left(|h_{\mathrm{worst,c}}|^2+|h_{\mathrm{worst,d}}|^2\right)}{\sigma_n^2} = \beta\gamma_w, & \gamma_g > \mu, \end{cases} \tag{3.35}$$

where $\gamma_w = A(|h_{\mathrm{worst},c}|^2 + |h_{\mathrm{worst},d}|^2)$ denotes the received ISNR of the actually selected worst transmit antenna pair. For $\gamma_w \leq \gamma_g \leq \mu$, the pdf f_{γ_w} of γ_w can be expressed as

$$f_{\gamma_w}(x) = \frac{2x}{A^2}\exp\left(-\frac{x}{A}\right)\int_x^{\mu}\frac{t}{A^2}\exp\left(-\frac{t}{A}\right)dt. \tag{3.36}$$

To describe f_{γ_w} in the case $\gamma_w \leq \mu \leq \gamma_g$, the same expression can be used, but the lower and upper limits of the integral in (3.36) should be changed to μ and ∞, respectively. Similarly, (3.36) can also be used to describe f_{γ_w} in the case $\mu \leq \gamma_w \leq \gamma_g$, where the lower and upper limits of the integral in (3.36) is changed to x and ∞, respectively.

Using the latter results for f_{γ_w} and (2.11) to compute the MGF in the case when the worst antenna pair is used and employing (2.12), we have

$$\begin{aligned}
\mathrm{BER}_2 = {} & 2\left[\left(\frac{\mu}{A}\right)^2+\frac{\mu}{A}\right]\exp\left(-\frac{\mu}{A}\right)\left[\rho\left(1,\alpha,1,\frac{\mu}{A}\right)-\rho\left(1,\beta,1,\frac{\mu}{A}\right)\right] \\
& +2\left(\frac{\mu}{A}+1\right)\exp\left(-\frac{\mu}{A}\right)\left[\rho\left(1,\alpha,2,\frac{\mu}{A}\right)-\rho\left(1,\beta,2,\frac{\mu}{A}\right)\right] \\
& -2\left[\left(\frac{\mu}{A}\right)^2+\frac{\mu}{A}\right]\left[\rho\left(2,\alpha,1,\frac{\mu}{A}\right)-\rho\left(2,\beta,1,\frac{\mu}{A}\right)\right] \\
& -2\left(2\frac{\mu}{A}+1\right)\left[\rho\left(2,\alpha,2,\frac{\mu}{A}\right)-\rho\left(2,\beta,2,\frac{\mu}{A}\right)\right] \\
& -4\left[\rho\left(2,\alpha,3,\frac{\mu}{A}\right)-\rho\left(2,\beta,3,\frac{\mu}{A}\right)\right] \\
& -\frac{1}{2}\left(\frac{\mu}{A}+1\right)\exp\left(-\frac{\mu}{A}\right)\left[\left(1-\sqrt{\frac{A}{A+\frac{1}{\alpha}}}\right)^2\left(2+\sqrt{\frac{A}{A+\frac{1}{\alpha}}}\right)\right. \\
& \left.-\left(1-\sqrt{\frac{A}{A+\frac{1}{\beta}}}\right)^2\left(2+\sqrt{\frac{A}{A+\frac{1}{\beta}}}\right)\right] \\
& +\frac{1}{32}\left(1-\sqrt{\frac{A}{A+\frac{2}{\alpha}}}\right)^3\left[2+3\left(1+\sqrt{\frac{A}{A+\frac{2}{\alpha}}}\right)+3\left(1+\sqrt{\frac{A}{A+\frac{2}{\alpha}}}\right)^2\right] \\
& +\frac{1}{8}\left(1-\sqrt{\frac{A}{A+\frac{2}{\alpha}}}\right)^2\left(2+\sqrt{\frac{A}{A+\frac{2}{\alpha}}}\right).
\end{aligned} \tag{3.37}$$

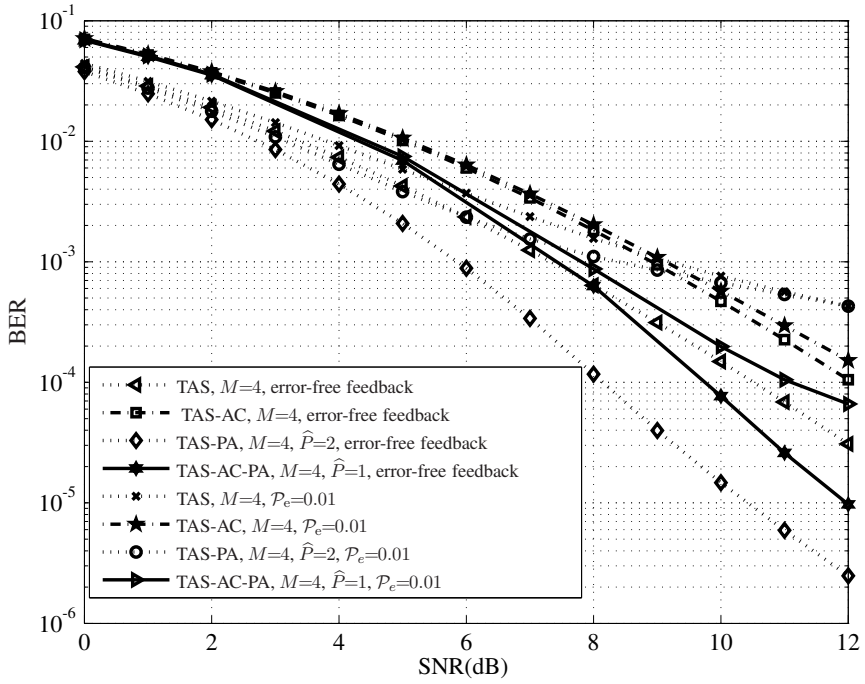

Figure 3.6: BERs versus SNR for TAS, TAS-AC, TAS-PA, and TAS-AC-PA with correct and erroneous feedback.

Case 3: Correct antenna selection, but erroneous antenna weight selection. The BER in this case, BER_3, can be expressed by (3.34) with interchanged α and β.

Case 4: Erroneous antenna and weight selection. The BER in this case, BER_4, is given by (3.37) with interchanged α and β.

The resulting BER of the combined TAS-PA-AC technique can be explicitly expressed as

$$\mathrm{BER}_{\mathrm{TAS-PA-AC}} = (1-\mathcal{P}_e)^2\,\mathrm{BER}_1 + \mathcal{P}_e\,(1-\mathcal{P}_e)\,\mathrm{BER}_2 + (1-\mathcal{P}_e)\,\mathcal{P}_e\mathrm{BER}_3 + \mathcal{P}_e^2\mathrm{BER}_4. \tag{3.38}$$

The BERs of different combinations of the discussed transmission strategies are displayed in Fig. 3.6 both in the cases of error-free and erroneous feedback. As can be observed from this figure, the TAS-PA-AC approach offers the best robustness against feedback imperfections, while the TAS-PA technique demonstrates the best performance in the error-free feedback case.

3.5 Chapter Summary

In this chapter, we have focused on the link-level performance and proposed several transmission techniques based on limited feedback. The performance of the proposed schemes has been analyzed and quantified in terms of the SER. Our results have shown that the TAS scheme based on correct feedback messages can, as the number of transmit antennas increases, greatly reduce the SER while inducing low hardware cost and implementation complexity. When the feedback channel can provide reliable feedback message, combining TAS with PA can further decrease the SER without increasing the number of antennas. In the scenario where the feedback messages can be erroneous, combination of TAS based scheme and OSTBCs can reduce the size of feedback message and provide more robustness against the feedback errors. Hence, proper selection of transmission techniques according to the feedback quality plays a significant role in wireless communication. Our study in this chapter has shown the potential benefits obtainable by embedding the proposed schemes into future mobile communication standards. Based on transmit antenna selection, better channel condition than in the SISO case can be achieved without significant addtional expense. Therefore, antenna selection based techniques can help us to achieve future high-rate wireless data services.

Chapter 4

Multiuser Diversity and Opportunistic Scheduling

In the previous chapter, we have introduced several transmit diversity techniques to enhance the link-level performance. In this chapter, we will consider the system-level performance and focus on the concept of multiuser scheduling. As pointed out in the Chapter 1, the scheduler is essential to achieve high spectrum efficiency and to a large extent determines the overall system performance. Channel-aware dynamic scheduling schemes that make use of multiuser diversity have already been enabled by the standards such as the LTE and LTE-Advanced [11] [12]. Although the throughput performances of different scheduling schemes such as opportunistic beamforming scheme have been intensively studied [42]-[47], less work has been done to analyze the system reliability in terms of the SER. In this chapter, we present a first approach to address this topic. In particular, we study the opportunistic downlink scheduling approach and analyze its performance in terms of the SER.

4.1 Scenario of Opportunistic Scheduling

We consider the downlink scenario as shown in Fig. 4.1, where one base station equipped with a single antenna ($M = 1$) schedules the data transmissions of multiple connected mobile users ($K > 1$). In each time block, the transmitter sends data only to the user with the

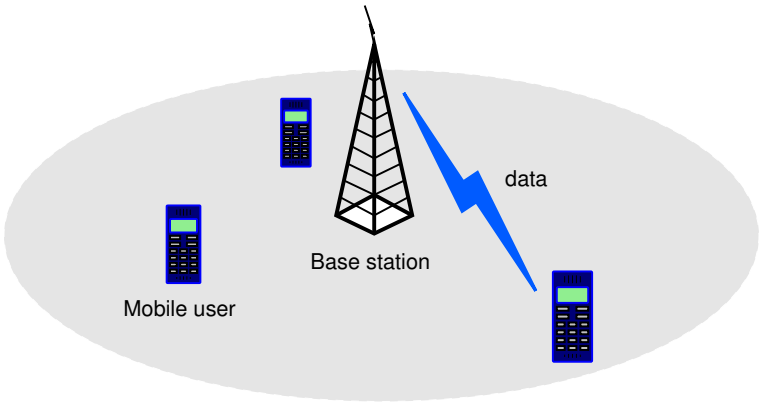

Figure 4.1: Downlink opportunistic scheduling

strongest instantaneous channel. The channel gains $h_{i,k}$ with $i = M = 1$ and $1 \leq k \leq K$ given in (2.1) are assumed to be constant within any single time block and the size of each block does not exceed the channel coherence time τ_{coh}. As we consider the case of single transmit antenna ($M = 1$), for notational simplicity, we will omit the subscript i in (2.1) and denote the channel gains and the transmitted signal at the time index t as $h_k(t)$ and $s(t)$, correspondingly. Note that signal $s(t)$ is dedicated to the *scheduled* user.

In this chapter, we study the case of a homogeneous network where the average SNR is the same for all users and each user enjoys the same average feedback quality. Similar to Chapter 3, the channel gains $h_k(t)$ are assumed to have variances all equal to one. The noise power received by each user is equal to σ_n^2, i.e., $\sigma_{n_1}^2 = \sigma_{n_2}^2 = \ldots = \sigma_{n_K}^2 = \sigma_n^2$. The power consumed to transmit a symbol $s(t)$ is assumed to be fixed at P in each time block, i.e., power allocation ability is not considered in this chapter. For the sake of compactness of our BER expressions, as in Chapter 3, we will use the notation A for the average received SNR. Under the assumption of a homogeneous network, we have $A = P/\sigma_n^2$ for each user and the average BER is the same for all users.

4.2 Performance Bounds with Full CSI Feedback

For any scheduling scheme based on limited feedback, the performance in the case of full CSI feedback can be used as a performance bound and a useful benchmark for comparison. This

section focuses on the SER performance of the opportunistic scheduling based on full CSI feedback. Similar to Chapter 3, we base our analysis on the example of BPSK modulation scheme. These results can however be generalized to higher modulation orders using similar derivations as presented here. In the full CSI feedback case, the feedback messages in each time block contain the values of the individual ISNRs of the users. Based on these messages, the transmitter schedules the user with the highest ISNR for data transmission.

4.2.1 General BER Analysis

The received ISNR of the kth user can be expressed as $\gamma_k = A|h_k|^2$. According to our assumptions, all γ_k ($k = 1, \ldots, K$) are centrally χ^2-distributed with two degrees of freedom. Let $\gamma_{[n]}$ denote the nth highest ISNR among all the user ISNRs γ_k ($k = 1, \ldots, K$). Following (2.17), the pdf of $\gamma_{[n]}$, denoted as $f_{\gamma_{[n]}}(x)$, can be expressed similarly as in (3.3) by substituting K for M.

When the feedback message is error-free, the user with the highest ISNR is selected and scheduled for the data transmission. In this case, the pdf of the received ISNR is given by $f_{\gamma_{[n]}}(x)$ with $n = 1$. According to (2.12), the BER for this user is given by

$$\mathrm{BER}_{\gamma_{[1]}} = \frac{1}{\pi} \int_0^{\pi/2} \mathcal{M}_{\gamma_{[1]}} \left(-\frac{1}{\sin^2 \theta} \right) d\theta \tag{4.1}$$

where $\mathcal{M}_{\gamma_{[1]}}$ is the MGF defined in (2.11), which can be computed as

$$\mathcal{M}_{\gamma_{[1]}}(-g) = \int_0^{\infty} \exp(-gx) f_{\gamma_{[1]}}(x)\, dx = M \sum_{k=0}^{M-1} \frac{\binom{M-1}{k}(-1)^k}{gA + k + 1}. \tag{4.2}$$

Inserting $f_{\gamma_{[n]}}(x)$ with $n = 1$ into (4.2) and then substituting the MGF into (4.1), the BER can be expressed as[1]

$$\mathrm{BER}_{\gamma_{[1]}} = K \sum_{j=0}^{K-1} \frac{(-1)^j \binom{K-1}{j}}{2(j+1)} \left(1 - \sqrt{\frac{A}{A + j + 1}} \right). \tag{4.3}$$

4.2.2 Asymptotic BER Analysis

The performance improvement provided by multiuser diversity increases as the number of users K increases. Hence, it is important to pursue the asymptotic performance bound for the

[1] Note that mathematically similar expressions have been obtained in [56] and [85] in different contexts.

case of $K \to \infty$. Moreover, in terms of BER, a traditional asymptotic performance measure is the diversity order in the case of $\mathrm{SNR} \to \infty$. We derive the asymptotic behavior of the BER for both cases. In the following we refer to the regime of $\mathrm{SNR} \to \infty$ as the high SNR regime and the regime of $K \to \infty$ as the large number of users regime.

In the high SNR regime, we will study the diversity order as defined in (2.13). In the second regime, we wish to determine how the BER scales when increasing the number of users K. To quantify the scaling law, let us define the multiuser diversity gain as the negative exponent g of the number of users K in the asymptotic BER expression

$$\mathrm{BER} \simeq \frac{1}{\tilde{G}_c} K^{-g} \tag{4.4}$$

where $\tilde{G}_c$ can be considered as the multiuser diversity coding gain.

It should be stressed that the multiuser diversity gain is commonly defined in terms of the sum capacity; see, for example, [2, p. 253]. In contrast to the capacity-based definition of [2], our definition in (4.4) characterizes the multiuser diversity gain in terms of the BER.

The asymptotic BER behavior can be specified by the following theorem.

Theorem 1. *If K is fixed and $A \to \infty$, then the opportunistic scheduling strategy in the case of full CSI feedback achieves the full diversity order of K. If the average SNR A is fixed and $K \to \infty$, then the opportunistic scheduling strategy in the case of full CSI feedback achieves the asymptotic multiuser diversity gain equal to A.*

Proof: As stated above, a similar expression as (4.3) has been obtained in [85] for a point-to-point MISO communication system with K transmit antennas, where the transmit antenna with the strongest channel gain is selected for data transmission. In [85], it has been shown that for any fixed K and $A \to \infty$, this expression can be further simplified as

$$\mathrm{BER}_{\gamma_{[1]}} \simeq \frac{(2K-1)!}{2^{2K}(K-1)!} A^{-K}. \tag{4.5}$$

Note that the approximation in (4.5) becomes exact as $A \to \infty$. Applying (4.5) to our opportunistic scheduling case, we conclude that the diversity order d defined in (2.13) is equal to K.

Let us now prove the second part of Theorem 1. According to our assumptions, $|h_k|^2$ has the exponential distribution with the pdf $f(x) = e^{-x}$ $(x \geq 0)$ and the cdf $F(x) = 1 - e^{-x}$

($x \geq 0$). According to definition of γ_k, we denote the largest order statistic of $|h_k|^2$ ($k = 1, \ldots, K$) as $\max_{k=1,\ldots,K} |h_k|^2 = \gamma_{[1]}/A$. From the extreme value theory in Section 2.3.2, for $K \to \infty$, the value of $\gamma_{[1]}/A - \ln K$ has the limiting cdf $G_3(x)$ in (2.23).

In [3], it has been shown that (4.1) can be equivalently expressed as

$$\mathrm{BER}_{\gamma_{[1]}} = \int_0^\infty Q(\sqrt{2x}) f_{\gamma_{[1]}}(x)\, dx \tag{4.6}$$

where $Q(x)$ is the Gaussian Q-function defined as [3]

$$Q(x) \triangleq \frac{1}{\pi} \int_0^{\pi/2} \exp\left(-\frac{x^2}{2\sin^2\theta}\right) d\theta. \tag{4.7}$$

Using (2.23) in the case of large K, (4.6) can be rewritten as

$$\mathrm{BER}_{\gamma_{[1]}} = \int_{-\ln K}^\infty Q(\sqrt{2A\,(x + \ln K)}) \exp\left(-e^{-x}\right) e^{-x}\, dx. \tag{4.8}$$

With the Chernoff bound, we have [3]

$$Q(x) \leq \frac{1}{2} \exp(-x^2/2). \tag{4.9}$$

Inserting (4.9) into (4.8), we obtain that for $K \to \infty$, $\mathrm{BER}_{\gamma_{[1]}}$ can be bounded as

$$\mathrm{BER}_{\gamma_{[1]}} \leq \frac{1}{2} \int_{-\infty}^\infty e^{-Ax - A\ln K} \exp(-e^{-x}) e^{-x} dx = \frac{1}{2}\Gamma(A+1) K^{-A}, \tag{4.10}$$

where the equality in (4.10) follows [98, (8.312.10)] . Hence, the multiuser diversity gain is lower bounded by A.

A lower bound on $Q(x)$ is given by [91, eqn. (11)]

$$Q(x) > \frac{1}{\sqrt{x^2+4}} \frac{1}{\sqrt{2\pi}} \exp(-x^2/2). \tag{4.11}$$

Inserting (4.11) into (4.8), we obtain a lower bound on $\mathrm{BER}_{\gamma_{[1]}}$ for $K \to \infty$ as

$$\mathrm{BER}_{\gamma_{[1]}} > \frac{1}{\sqrt{2\pi}} \int_{-\ln K}^{\infty} \frac{e^{-Ax - A\ln K} \exp(-e^{-x}) e^{-x}}{\sqrt{2A\,(x + \ln K) + 4}} dx \tag{4.12}$$

$$= \frac{1}{\sqrt{2\pi}} K^{-A} \int_{0}^{K} \frac{t^A e^{-t}\, dt}{\sqrt{2A\,(\ln K - \ln t) + 4}} \tag{4.13}$$

$$> \frac{1}{\sqrt{2\pi}} K^{-A} \int_{1}^{K} \frac{t^A e^{-t}\, dt}{\sqrt{2A\,(\ln K - \ln t) + 4}} \tag{4.14}$$

$$> \frac{K^{-A}}{\sqrt{4A\pi \ln K + 8\pi}} \int_{1}^{K} t^A e^{-t}\, dt \tag{4.15}$$

$$\simeq \frac{\Gamma(A+1,1)}{\sqrt{4A\pi}} \frac{K^{-A}}{\sqrt{\ln K}} \tag{4.16}$$

$$\geq \frac{\Gamma(A+1,1)}{\sqrt{4A\pi}} K^{-(A+\epsilon)} \text{ for any } \epsilon > 0, \tag{4.17}$$

where (4.14) holds because the integrand is nonnegative on the interval $t \in [0, K]$, (4.15) follows from the inequality $\ln t \geq 0$ for $1 \leq t \leq K$, (4.16) is true for $K \to \infty$, and $\Gamma(s, x) = \int_x^\infty t^{s-1} e^{-t}\, dt$ is the upper incomplete gamma function. In (4.17), for any $\epsilon > 0$, there exists K_0 such that for all $K > K_0$, we have $K^{2\epsilon} > \ln K$. Taking $\epsilon \to 0$ as $K \to \infty$, we have that the multiuser diversity gain is also upper bounded by A. This completes the proof of the second part, and hence the proof of the Theorem 1. □

4.3 Error-Free Quantized CSI Feedback

In practice, the rate of the feedback link is quite limited and it is generally infeasible to feed back the exact values of the ISNR. Hence, the values of the received ISNR are often quantized to a set of discrete values which can be expressed by a finite set of binary sequences of limited size. These binary sequences are then sent back to the transmitter. In this section, we study the performance of opportunistic scheduling schemes that are based on limited feedback. The feedback message is assumed to be received without error in this section. The impact of feedback errors will be considered in Section 4.4. First of all, let us consider an extreme case of one feedback bit per user. The case of higher-rate feedback will be studied in Section 4.3.3.

4.3.1 General BER Analysis with One-Bit Feedback

In the one-bit feedback per user case, the values of $|h_k|^2$ ($k = 1, \ldots, K$) can be quantized into two levels with a threshold μ. At the beginning of each time block, each user is assumed to report its current channel level to the transmitter using one binary symbol where "1" and "0" correspond to the higher and lower channel levels, respectively. Then the transmitter randomly schedules one of the users whose feedback message is "1". If none of the user has reported a feedback message "1", an arbitrary user is scheduled randomly from all the available users.

Let us consider the scheduled user with the received ISNR γ. If this user's feedback message is "1", then $\gamma > A\mu$; otherwise $\gamma \leq A\mu$. For any user k, denoting the probability of the event $|h_k|^2 \leq \mu$ as $\mathcal{P}_1$, we have that $\mathcal{P}_1 = 1 - e^{-\mu}$. Similarly, the probability of the event $|h_k|^2 > \mu$ can be expressed as $\mathcal{P}_2 = e^{-\mu}$. With γ_k, the distribution of γ is a mixture distribution [87] of two truncated distributions of γ_k, which are defined for $0 < \gamma_k \leq \mu A$ and $\gamma_k > \mu A$ correspondingly. Let

$$\tilde{\mathcal{P}}_1 = \left(1 - e^{-\mu}\right)^K, \quad \tilde{\mathcal{P}}_2 = 1 - \left(1 - e^{-\mu}\right)^K \tag{4.18}$$

denote the probabilities of the events that the channel gain of the scheduled user belongs to the lower and higher channel level, respectively. We can express the pdf of γ as

$$f_\gamma(x) = \begin{cases} \frac{\tilde{\mathcal{P}}_1}{\mathcal{P}_1 A} \exp\left(-\frac{x}{A}\right), & \text{for } 0 < x \leq \mu A \\ \frac{\tilde{\mathcal{P}}_2}{\mathcal{P}_2 A} \exp\left(-\frac{x}{A}\right), & \text{for } x > \mu A. \end{cases} \tag{4.19}$$

Inserting (4.19) in (4.2) instead of $f_{\gamma_{[1]}}(x)$ and using (4.1), the BER of the scheduled user can be computed as

$$\mathrm{BER}_\gamma = \frac{1}{\pi}\left(\frac{\tilde{\mathcal{P}}_2}{\mathcal{P}_2} - \frac{\tilde{\mathcal{P}}_1}{\mathcal{P}_1}\right) \int_0^{\pi/2} \frac{\exp\left(-\left(\frac{A}{\sin^2\theta} + 1\right)\mu\right)}{\frac{A}{\sin^2\theta} + 1}\, d\theta + \frac{\tilde{\mathcal{P}}_1}{2\mathcal{P}_1}\left(1 - \sqrt{\frac{A}{A+1}}\right). \tag{4.20}$$

To the best of our knowledge, there is no closed-form expression for the integral in (4.20).

However, we can use its upper bound

$$\begin{aligned} \mathrm{I} &\triangleq \int_0^{\pi/2} \frac{\exp\left(-\left(\frac{A}{\sin^2\theta}+1\right)\mu\right)}{\frac{A}{\sin^2\theta}+1}\,d\theta \\ &\leq \int_0^{\pi/2} \frac{\exp\left(-\left(\frac{A}{\sin^2\theta}+1\right)\mu\right)}{\frac{A}{\sin^2\theta}}\,d\theta \\ &= e^{-\mu}\left[\frac{\sqrt{\pi\mu}}{2\sqrt{A}}e^{-A\mu}+\left(\frac{\pi}{4A}-\frac{\pi\mu}{2}\right)\mathrm{erfc}(\sqrt{A\mu})\right] \end{aligned} \tag{4.21}$$

to simplify our analysis. Here, $\mathrm{erfc}(x)$ denotes the complementary error function. Inserting (4.21) in (4.20), we obtain

$$\begin{aligned} \mathrm{BER}_\gamma &\leq \frac{\tilde{\mathcal{P}}_1}{2\mathcal{P}_1}\left(1-\sqrt{\frac{A}{A+1}}\right)+e^{-\mu}\left(\frac{\tilde{\mathcal{P}}_2}{\mathcal{P}_2}-\frac{\tilde{\mathcal{P}}_1}{\mathcal{P}_1}\right)\left[\frac{\sqrt{\mu}}{2\sqrt{\pi A}}e^{-A\mu}+\left(\frac{1}{4A}-\frac{\mu}{2}\right)\mathrm{erfc}\left(\sqrt{A\mu}\right)\right] \\ &\triangleq \mathrm{BER}_{\gamma,\mathrm{up}}. \end{aligned} \tag{4.22}$$

The approximation in (4.21) is accurate for large values of A. Hence, the upper bound $\mathrm{BER}_{\gamma,\mathrm{up}}$ in (4.22) is expected to be tight at high SNRs.

Clearly, BER_γ depends on the value of the threshold μ. The optimal threshold μ_{opt} can be found by minimizing BER_γ as

$$\mu_{\mathrm{opt}} = \arg\min_{\mu} \mathrm{BER}_\gamma. \tag{4.23}$$

This problem can be solved numerically by a one-dimensional search over μ. In a practical system, the solution to (4.23) can be computed offline for different values of SNR A and number of users K. The so-obtained threshold values can then be stored in a look-up table for simple access in real time implementations.

4.3.2 Asymptotic BER Analysis with One-Bit Feedback

As next, we study the asymptotic performance of our opportunistic scheduling scheme with one-bit channel feedback per user. As in Section 4.2.2, we consider the high SNR ($A \to \infty$) and large number of users ($K \to \infty$) regimes. As μ_{opt} has no closed-form expression, we seek for threshold values that result in similar scaling laws as those determined by Theorem 1. If such threshold values exist, we can conclude that with the optimal threshold, the same

scaling laws can also be achieved, as, clearly, opportunistic scheduling with one-bit CSI feedback cannot overcome that with the full CSI feedback.

In the high SNR regime where K is fixed and $A \to \infty$, the inequality in (4.22) can be replaced by equality and we can use $\mathrm{BER}_{\gamma,\mathrm{up}}$ instead of BER_{γ}. It can be shown from the first order Taylor series expansion of the first summand in (4.22) that, to achieve the diversity order larger than one, the factor $\tilde{\mathcal{P}}_1/\mathcal{P}_1$ is required to decay to zero when $A \to \infty$. Using (4.18), we have that, equivalently, the choice of μ must approach zero ($\mu \to 0$) as A reaches infinity. At the same time, to achieve the diversity order higher than one, the factor $\frac{\sqrt{\mu}}{2\sqrt{\pi A}}e^{-A\mu} + \left(\frac{1}{4A} - \frac{\mu}{2}\right)\mathrm{erfc}(\sqrt{A\mu})$ has to decay faster than A^{-1}. This requires that $A\mu \to \infty$ when $A \to \infty$.

In [91], it has been shown that

$$Q(x) \simeq \frac{1}{\sqrt{2\pi}x}\exp\left(-\frac{x^2}{2}\right) \tag{4.24}$$

for $x \gg 0$. Inserting the values of $\mathcal{P}_1$, $\tilde{\mathcal{P}}_1$, $\mathcal{P}_2$ and $\tilde{\mathcal{P}}_2$ into (4.22) and using the identity $\mathrm{erfc}(x) = 2Q(\sqrt{2}x)$, we obtain that if $A\mu \gg 0$, then $\mathrm{BER}_{\gamma,\mathrm{up}}$ can be approximated as

$$\mathrm{BER}_{\gamma,\mathrm{up}} \simeq \frac{\left(1-e^{-\mu}\right)^{K-1}}{2}\left(1-\sqrt{\frac{A}{A+1}}\right) + \frac{1-\left(1-e^{-\mu}\right)^{K-1}}{4A\sqrt{\pi A\mu}}e^{-A\mu}. \tag{4.25}$$

To achieve the full diversity order of K, it is sufficient that both terms in (4.25) decrease with the rate A^{-K} for $A \to \infty$.

For the second summand in (4.25) to decrease with the rate A^{-K}, the following condition must hold:

$$\frac{1-\left(1-e^{-\mu}\right)^{K-1}}{4A\sqrt{\pi A\mu}}e^{-A\mu} \simeq CA^{-K} \text{ for } A \to \infty \tag{4.26}$$

where C is a constant independent of A. Taking the logarithm of both sides of (4.26), we obtain

$$\ln\left[1-\left(1-e^{-\mu}\right)^{K-1}\right] - A\mu - \frac{3}{2}\ln A - \frac{1}{2}\ln\mu - \ln\left(4\sqrt{\pi}\right) \simeq -K\ln A + \ln C. \tag{4.27}$$

As mentioned before, it is required that $\mu \to 0$ when $A \to \infty$. If $\mu \to 0$, then

$$\ln\left[1-\left(1-e^{-\mu}\right)^{K-1}\right] \to 0.$$

Moreover, for $A \to \infty$ the finite constant terms $\ln(4\sqrt{\pi})$ and $\ln C$ can be neglected in (4.27). Then, we obtain

$$\mu \simeq \frac{(K-1.5)\ln A - 0.5\ln\mu}{A}. \tag{4.28}$$

Taking the logarithm of both sides of (4.28), we observe that for $A \to \infty$ and $\ln\mu \simeq -\ln A$. Using this fact in (4.28), a suboptimal value of the threshold μ can be computed for large values of A as

$$\mu = \frac{(K-1)\ln A}{A}. \tag{4.29}$$

Substituting (4.29) into (4.25) and using the first-order Taylor approximation $e^{-x} \simeq 1-x$ ($x \ll 1$), we have

$$\lim_{A\to\infty} \frac{\mathrm{BER}_{\gamma,\mathrm{up}}}{A^{-K}} = \lim_{A\to\infty} \frac{(K-1)^{K-1}}{4}(\ln A)^{K-1} \to \infty. \tag{4.30}$$

At the same time, for any arbitrary small constant $\epsilon > 0$, the limit $\lim_{A\to\infty}(\ln A)^{K-1}/A^{\epsilon} = 0$ and, therefore,

$$\lim_{A\to\infty} \frac{\mathrm{BER}_{\gamma,\mathrm{up}}}{A^{-(K-\epsilon)}} = \lim_{A\to\infty} \frac{(K-1)^{K-1}}{4}\frac{(\ln A)^{K-1}}{A^{\epsilon}} = 0. \tag{4.31}$$

With (4.30) and (4.31), we can conclude that as $A \to \infty$, an asymptotic diversity order smaller than, but arbitrarily close to K can be achieved by using the suboptimal threshold (4.29). This implies that in the asymptotic case $A \to \infty$, the opportunistic scheduling scheme with the *optimal* threshold can also achieve a diversity order arbitrarily close to K. In Fig. 4.2, the suboptimal threshold of (4.29) is compared with the optimal threshold of (4.23) and the suboptimal threshold obtained from the same equation (4.23) but with BER_{γ} replaced by $\mathrm{BER}_{\gamma,\mathrm{up}}$:

$$\mu_{\mathrm{sopt}} = \arg\min_{\mu} \mathrm{BER}_{\gamma,\mathrm{up}}. \tag{4.32}$$

In this figure, $K = 4$ and all the thresholds are plotted versus SNR. As follows from Fig. 4.2, the two suboptimal thresholds are very close to the optimal one when the SNR is above 10 dB. This, in particular, shows that $\mathrm{BER}_{\gamma,\mathrm{up}}$ is an accurate approximation of BER_{γ} at moderate to large values of SNR.

Let us now consider the case when $K \to \infty$ and A is fixed. Intuitively, as K increases, the value of μ should increase correspondingly, to select a user with a high channel gain.

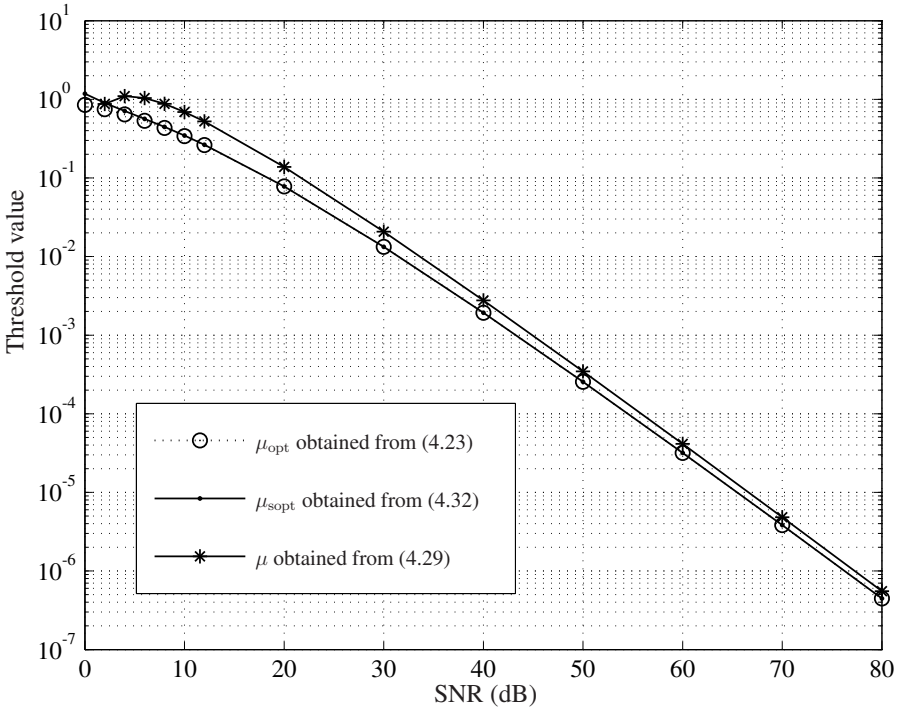

Figure 4.2: Optimal and suboptimal thresholds versus SNR.

Noting that the term

$$e^{-\mu}\left(\frac{\tilde{\mathcal{P}}_2}{\mathcal{P}_2}-\frac{\tilde{\mathcal{P}}_1}{\mathcal{P}_1}\right)=1-\left(1-e^{-\mu}\right)^{K-1} \tag{4.33}$$

in (4.22) vanishes with increasing K, we observe from (4.33) that μ indeed must approach infinity as $K\to\infty$. Otherwise, (4.33) approaches one as $K\to\infty$ and, correspondingly, (4.22) approaches some positive constant value larger than 0. As a result, no multiuser diversity gain is achieved in the latter case.

As $\mu\to\infty$, we have $A\mu\to\infty$ for any fixed A. Hence, (4.25) still holds in this case. Rewriting it as

$$\mathrm{BER}_{\gamma,\mathrm{up}}\simeq\frac{e^{-A\mu}}{4A\sqrt{\pi A\mu}}+\frac{\left(1-e^{-\mu}\right)^{K-1}}{2}\left(1-\sqrt{\frac{A}{A+1}}-\frac{e^{-A\mu}}{2A\sqrt{\pi A\mu}}\right) \tag{4.34}$$

we can see that if both terms in (4.34) decrease as K^{-A} for $K\to\infty$, then from $\mathrm{BER}_\gamma\le\mathrm{BER}_{\gamma,\mathrm{up}}$, we can conclude that BER_γ decreases at least as fast as K^{-A}. Let the second term in (4.34) decrease as K^{-A} for $K\to\infty$, that is,

$$\frac{\left(1-e^{-\mu}\right)^{K-1}}{2}\left(1-\sqrt{\frac{A}{A+1}}-\frac{e^{-A\mu}}{2A\sqrt{\pi A\mu}}\right)\simeq CK^{-A} \tag{4.35}$$

for $K \to \infty$, where C is a constant independent of K. Taking the logarithm on both sides of (4.35) and omitting all negligible constants, we obtain for $K \to \infty$ that

$$\ln\left(1 - e^{-\mu}\right) \simeq -\frac{A \ln K}{K-1}. \tag{4.36}$$

From the identity $\ln(1+x) = \sum_{k=1}^{\infty} (-1)^{k+1} x^k/k$ that is valid for $-1 < x \leq 1$ [98], we have

$$\ln(1-x) \simeq -x \tag{4.37}$$

for small x. Using the approximation $\ln(1-x) \simeq -x$ for small x [98], we can find the following suboptimal value of the threshold μ from (4.35)

$$\mu = \ln\left(\frac{K-1}{A \ln K}\right). \tag{4.38}$$

With this threshold value, we obtain from (4.34) that for any arbitrarily small positive ϵ,

$$\lim_{K\to\infty} \frac{\mathrm{BER}_{\gamma,\mathrm{up}}}{K^{-(A-\epsilon)}} = \lim_{K\to\infty} \frac{A^{A-1.5}}{4\sqrt{\pi}} \frac{(\ln K)^{A-1/2}}{K^{\epsilon}} = 0 \tag{4.39}$$

$$\lim_{K\to\infty} \frac{\mathrm{BER}_{\gamma,\mathrm{up}}}{K^{-A}} = \lim_{K\to\infty} \frac{A^{A-1.5}}{4\sqrt{\pi}} (\ln K)^{A-1/2} = \infty. \tag{4.40}$$

Therefore, we conclude that as $K \to \infty$, an asymptotic multiuser diversity gain arbitrarily close to A can be achieved by using the suboptimal threshold (4.38). This means that in the asymptotic case $K \to \infty$, the opportunistic scheduling scheme with the optimal threshold can also achieve a multiuser diversity gain arbitrarily close to A.

Fig. 4.3 compares the suboptimal threshold of (4.38) with the optimal threshold of (4.23) and the suboptimal threshold of (4.32). In this figure, the SNR $A = 10$ dB is assumed, and all the thresholds are displayed versus the number of users K. It can be observed from Fig. 4.3 that, as K increases, the threshold (4.38) closely approaches the other two thresholds (which coincide for all values of K).

The BER for n-bit CSI feedback is analyzed in the next subsection. We note that the BER for n-bit CSI feedback can be expected to show the same asymptotic behavior as in the one-bit and the full CSI feedback cases which represent the lower- and upper-bounds, respectively, for the n-bit case.

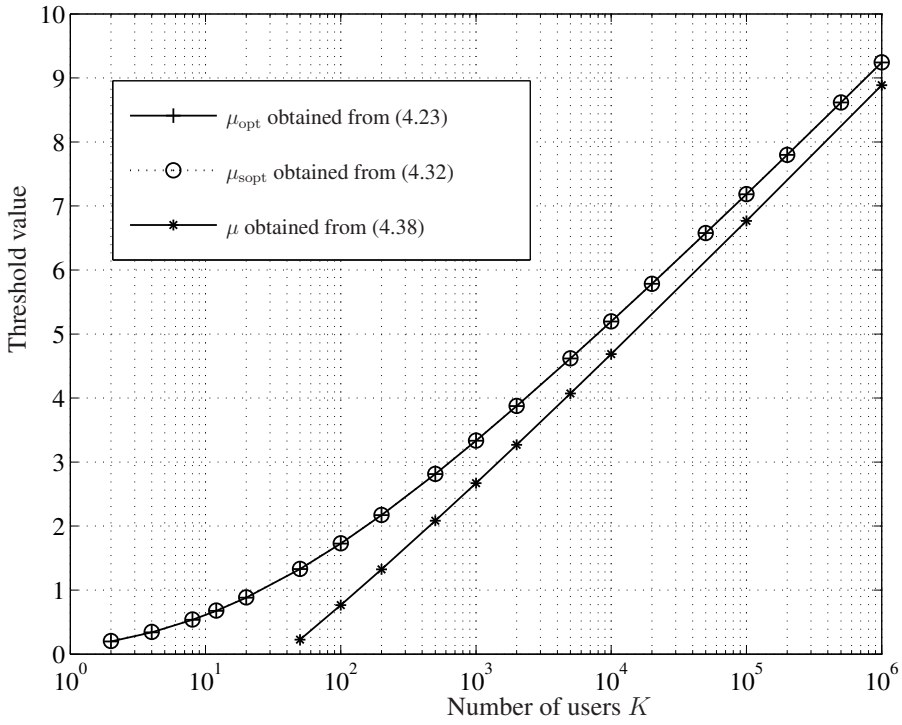

Figure 4.3: Optimal and suboptimal thresholds versus K.

4.3.3 General BER Analysis with Low-Rate Feedback

Let us consider the general case when the value of the channel gain $|h_k|^2$ is quantized into $m \geq 2$ levels with $m-1$ thresholds $\mu_1, \mu_2, \ldots, \mu_{m-1}$. For the sake of simplicity, we also define $\mu_0 = 0$ and $\mu_m \to \infty$. Then, each user reports its current channel state to the transmitter with $\lceil \log_2 m \rceil$ bits of feedback, where $\lceil x \rceil$ denotes the smallest integer larger than x. The transmitter schedules the user with the highest channel level for transmission. If there are more than one user with the highest channel level, then only one out of these users is selected randomly for data transmission.

The achieved BER as a function of m and $\mu_1, \ldots, \mu_{m-1}$ can be computed using the following steps:

- Step 1. For each $k = 1, \ldots, K$, compute the probability $\mathcal{P}_i$ of the channel gain $|h_k|^2$ to belong to the ith quantization level as

$$\mathcal{P}_i = \int_{\mu_{i-1}}^{\mu_i} \exp(-x)\, dx \tag{4.41}$$

where we use the fact that each $|h_k|^2$ is centrally χ^2-distributed with two degrees of freedom.

- Step 2. Compute the probability $\tilde{\mathcal{P}}_i$ of the channel gain of the *scheduled* user to belong to the ith channel level. In the error-free feedback case, $\tilde{\mathcal{P}}_i$ can be calculated as

$$\tilde{\mathcal{P}}_i = \left(\sum_{j=1}^{i} \mathcal{P}_j\right)^K - \left(\sum_{j=1}^{i-1} \mathcal{P}_j\right)^K. \tag{4.42}$$

- Step 3. Compute the pdf of the received ISNR γ as

$$f_\gamma(x) = \begin{cases} \frac{\tilde{\mathcal{P}}_1}{\mathcal{P}_1 A} \exp\left(-\frac{x}{A}\right), & \text{for } 0 < x \le \mu_1 A \\ \frac{\tilde{\mathcal{P}}_2}{\mathcal{P}_2 A} \exp\left(-\frac{x}{A}\right), & \text{for } \mu_1 A < x \le \mu_2 A \\ \cdots & \\ \frac{\tilde{\mathcal{P}}_m}{\mathcal{P}_m A} \exp\left(-\frac{x}{A}\right), & \text{for } x > \mu_{m-1} A \end{cases} \tag{4.43}$$

and then the MGF as

$$\begin{aligned} M_\gamma(-g) &= \int_0^\infty \exp(-gt) f_\gamma(t)\, dt \\ &= \sum_{i=1}^{m} \frac{\tilde{\mathcal{P}}_i \left[e^{(-(Ag+1)\mu_{i-1})} - e^{(-(Ag+1)\mu_i)}\right]}{\mathcal{P}_i (Ag+1)}. \end{aligned} \tag{4.44}$$

- Step 4. Using (4.44), compute the BER as

$$\mathrm{BER}_\gamma = \frac{1}{\pi} \int_0^{\frac{\pi}{2}} M_\gamma\left(-\frac{1}{\sin^2\theta}\right) d\theta. \tag{4.45}$$

Although we could not obtain any closed-form BER expression, it can be easily evaluated numerically using the above sequence of steps.

For any given value of m, a total of $m-1$ threshold values need to be determined to obtain the quantization levels. The optimal set of thresholds $\mu_{\mathrm{opt}} \triangleq \{\mu_{1,\mathrm{opt}}, \ldots, \mu_{m-1,\mathrm{opt}}\}$, can be obtained by solving the following optimization problem

$$\mu_{\mathrm{opt}} = \arg\min_{\mu} \mathrm{BER}_\gamma. \tag{4.46}$$

This problem can be solved numerically by means of $(m-1)$-dimensional search over $\mu_{1,\mathrm{opt}}$, …, $\mu_{m-1,\mathrm{opt}}$. Optimal threshold values can be computed offline and stored in a look-up table, as described after (4.23).

4.4 Erroneous Quantized Feedback

Feedback messages in practical systems are likely to be erroneous. In this section, we study the impact of CSI feedback errors on the proposed opportunistic scheduling scheme based on limited feedback. As before, in each time block only one user is scheduled for data transmission. Therefore, as long as no user resides at the channel levels larger than the level of the scheduled user, the user selection is proper even if there are feedback errors. However, if at least one user is at one of the channel levels larger than the scheduled user's level, then the user scheduling is improper.

Let us evaluate the BER of the opportunistic scheduling strategy under erroneous feedback. The procedure outlined in Section 4.3.3 can be adopted here, however, with a modified choice of $\tilde{\mathcal{P}}_i$. Obviously, in this case the probability $\tilde{\mathcal{P}}_i$ depends not only on $\mathcal{P}_i$ ($i = 1, \ldots, m$), but also on the bit error probability in the feedback message, $\mathcal{P}_e$. In the case of uncoded feedback, $\mathcal{P}_e$ denotes the error probability for each feedback bit. However, if channel coding is used to protect the feedback message, then $\mathcal{P}_e$ can be viewed as the error probability for each message bit after decoding.

Let us derive the probability $\tilde{\mathcal{P}}_i$ for the scheduled user. Let us assume that some arbitrary user actually belongs to the ith channel level, while the transmitter receives the jth channel level from the report of this user. If the feedback message is correct, then, clearly, $i = j$; otherwise $i \neq j$. For each user, let $Z_{i,j}$ ($i = 1, \ldots, m$; $j = 1, \ldots, m$) denote the probability of the event that the actual channel level is i, while the received at the transmitter level is j. Note that $Z_{i,j}$ depends on $\mathcal{P}_i$, $\mathcal{P}_e$ and the actual configuration of the feedback messages. For example, in the case of one-bit CSI feedback with $m = 2$ and the lower and higher channel levels being the first and second levels, respectively, we have

$$\begin{aligned} Z_{1,1} &= \mathcal{P}_1(1 - \mathcal{P}_e) \\ Z_{1,2} &= \mathcal{P}_1\mathcal{P}_e \\ Z_{2,1} &= \mathcal{P}_2\mathcal{P}_e \\ Z_{2,2} &= \mathcal{P}_2(1 - \mathcal{P}_e). \end{aligned} \tag{4.47}$$

In the general case, let $N_{i,j}$ out of K users have the actual channel level i while the

received level at the transmitter is j. Generally, if the pth channel level is the highest reported level, we have

$$\sum_{l=p+1}^{m}\sum_{i=1}^{m} N_{i,l} = 0, \quad \sum_{i=1}^{m} N_{i,p} > 0. \tag{4.48}$$

Using (4.48), after straightforward but tedious manipulations, we obtain

$$\tilde{\mathcal{P}}_i = \sum_{N_1=0}^{K}\sum_{N_2=0}^{K-N_1}\cdots\sum_{N_{m^2-1}=0}^{K-\sum_{l=1}^{m^2-2}N_l}\binom{K}{N_1}Z_1^{N_1}\binom{K-N_1}{N_2}Z_2^{N_2}\cdots\binom{K-\sum_{l=1}^{m^2-2}N_l}{N_{m^2-1}}Z_{m^2-1}^{N_{m^2-1}}Z_{m^2}^{N_{m^2}}F_i \tag{4.49}$$

where $F_i \triangleq \frac{N_{i,p}}{\sum_{l=1}^{m} N_{l,p}}$, $N_{m^2} = K - \sum_{k=1}^{m^2-1} N_k$, and, for the sake of notational simplicity, $Z_{i,j}$ and $N_{i,j}$ are translated to Z_k and N_k, respectively, with $k = (i-1)m+j$ for all $i = 1, \ldots, m$ and $j = 1, \ldots, m$. (4.49) can be simplified in the particular case of one-bit CSI feedback ($m = 2$). Using (4.47), we have that in this case, (4.49) can be rewritten as

$$\tilde{\mathcal{P}}_i = \sum_{N_1=0}^{K}\sum_{N_2=0}^{K-N_1}\sum_{N_3=0}^{K-N_1-N_2}\binom{K}{N_1}Z_1^{N_1}\binom{K-N_1}{N_2}Z_2^{N_2}\binom{K-N_1-N_2}{N_3}Z_3^{N_3}Z_4^{N_4}F_i \tag{4.50}$$

where $N_4 = K - \sum_{k=1}^{3} N_k$ and

$$F_1 = \begin{cases} \frac{N_1}{N_1+N_3}, & \text{if } N_2 = N_4 = 0, \\ \frac{N_2}{N_2+N_4}, & \text{otherwise;} \end{cases} \tag{4.51}$$

$$F_2 = \begin{cases} \frac{N_3}{N_1+N_3}, & \text{if } N_2 = N_4 = 0, \\ \frac{N_4}{N_2+N_4}, & \text{otherwise.} \end{cases} \tag{4.52}$$

Using (4.49) or (4.50) in (4.43) and (4.44), we obtain the pdf and MGF of γ in the erroneous feedback case. Using the so-obtained MGF, the resulting BER can be expressed as (4.45).

4.5 Numerical Results

In this section, the BER performances of the opportunistic scheduling approach is compared numerically for different types of feedback in scenarios with and without feedback errors.

In our first example, the BER performances of the opportunistic scheduling approach are compared in the cases of one-bit and full CSI. In this example, the feedback channel

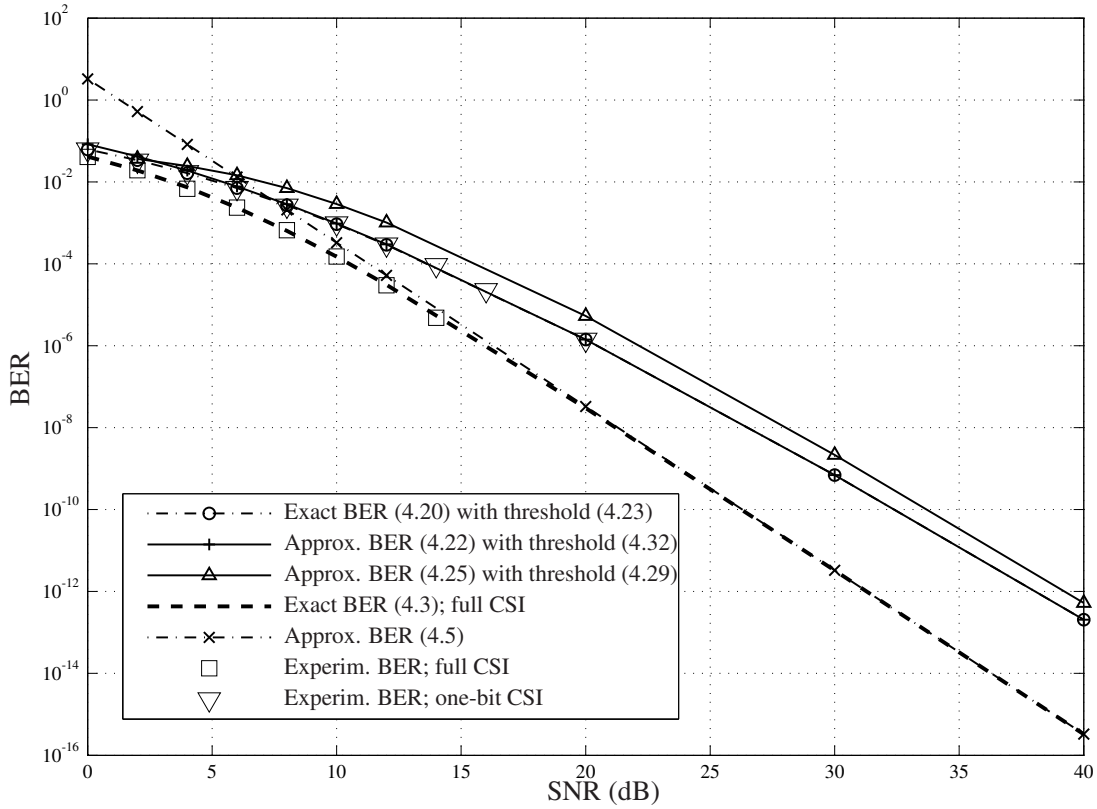

Figure 4.4: Theoretical and experimental BERs versus SNR; first example.

is assumed to be ideal, i.e., without errors. Fig. 4.4 shows BERs versus SNR in the case of $K = 4$. The following theoretical curves are compared: the exact BER in the one-bit CSI case given by (4.20), its approximations (4.22) and (4.25), as well as the exact BER in the full CSI case given by (4.3) and its approximation given by (4.5). For the exact BER expression in (4.20), we use the optimal threshold of (4.23). For the approximate BERs of (4.22) and (4.25), we use the thresholds obtained from (4.32) and (4.29), respectively. Also, the experimental BER points corresponding to the cases of one-bit and full CSI are displayed in Fig. 4.4. To limit the overall simulation runtime, the experimental points have been obtained only for relatively high BER values (not lower than 10^{-6}).

It can be observed from this figure that the experimental BER points match very well to the analytical results of (4.3) and (4.20). Moreover, the approximation quality of the exact

BER is quite high for both (4.22) and (4.25). All BER curves are nearly parallel to each other at high SNRs. This fact justifies our choices of suboptimal threshold values and supports our theoretical conclusion of Section 4.3.2 that an asymptotic diversity order arbitrarily close to K can be achieved by the one-bit feedback scheme.

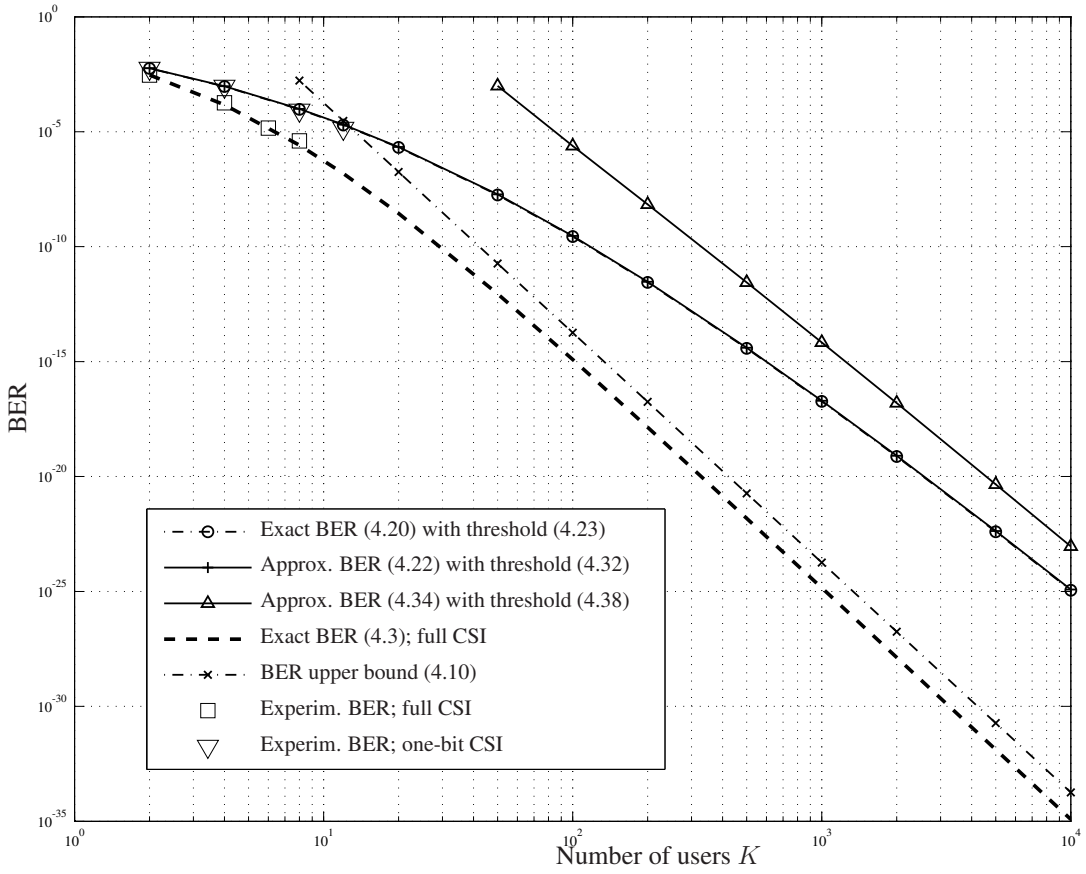

Figure 4.5: Theoretical and experimental BERs versus K; first example.

Fig. 4.5 displays BERs versus number of users K in the case of $\mathrm{SNR} = 10$ dB. In this figure, the following theoretical curves are compared: the exact BER in the one-bit CSI case given by (4.20); its approximations (4.22) and (4.34), as well as the exact BER in the full CSI case given by (4.3) and its upper bound given by (4.10). For the approximate BERs of (4.22) and (4.34), we use the thresholds obtained from (4.32) and (4.38), respectively. Similar to Fig. 4.4, the experimental BER points corresponding to the cases of one-bit and full CSI are

added to Fig. 4.5.

As follows from this figure, the experimental BER points again match very well to the analytical results of (4.3) and (4.20). Also, the exact BER of (4.20) is closely approximated by (4.22). The approximation of (4.20) provided by (4.34) is reasonably accurate in the asymptotic (large number of users) case. It can be also observed that all BER curves are nearly parallel to each other at large K. As in the high SNR case, this fact justifies our choices of suboptimal threshold values. Moreover, it validates our theoretical conclusion of Section 4.3.2 that a multiuser diversity gain arbitrarily close to SNR can be achieved by the one-bit feedback scheme.

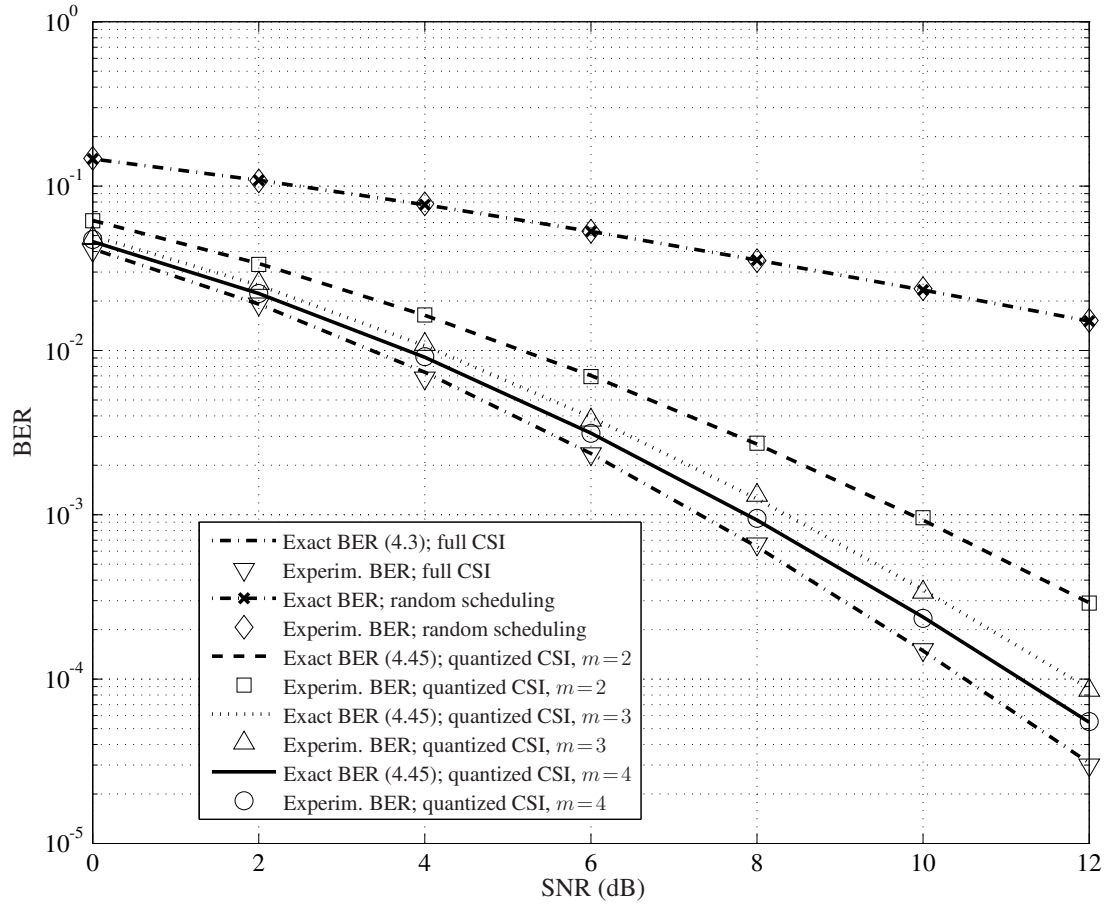

Figure 4.6: Theoretical and experimental BERs versus SNR in the error-free CSI feedback case; second example.

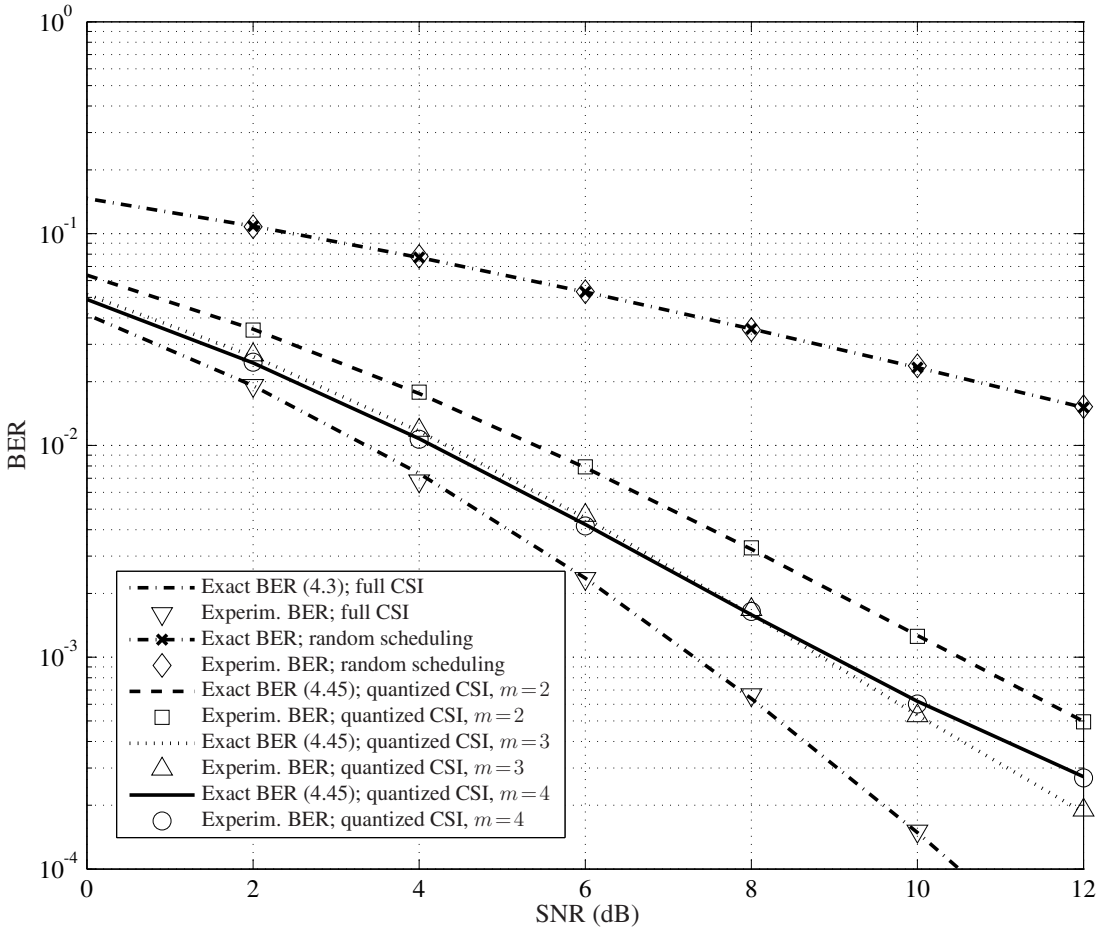

Figure 4.7: Theoretical and experimental BERs versus SNR in the erroneous CSI feedback case with $\mathcal{P}_e = 0.01$; second example.

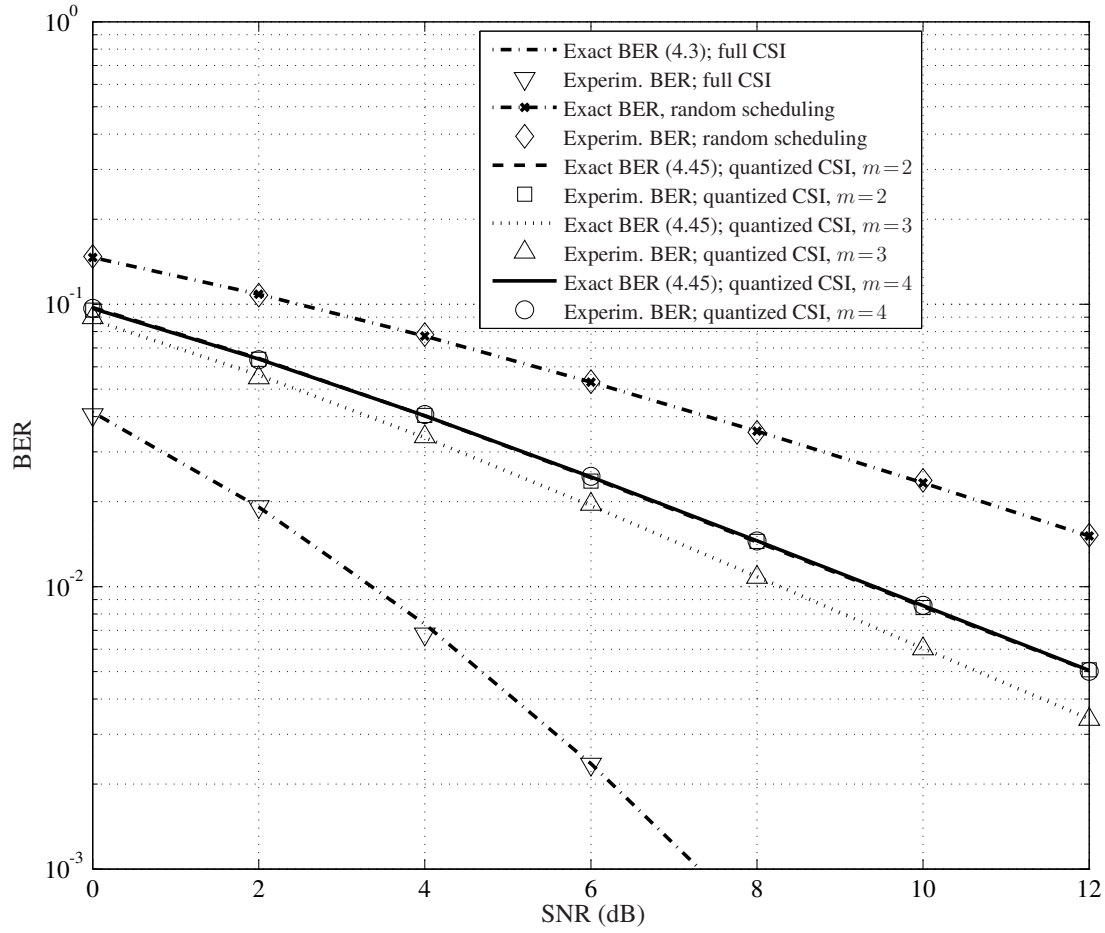

Figure 4.8: Theoretical and experimental BERs versus SNR in the erroneous CSI feedback case with $\mathcal{P}_e = 0.2$; second example.

In our second example, the BER performances of the opportunistic scheduling scheme are compared in the cases of more than one bit CSI and full CSI. In the quantized CSI case, both the situations with error-free and erroneous feedback channels have been considered. First, let us describe the configuration of feedback messages used in this example. In the one-bit feedback case, this configuration is the same as discussed in Section 4.3.1. In the case of two-bit feedback, the channel is quantized into $m = 4$ levels, and the feedback messages "00", "01", "11" and "10" are used to denote the levels 1, 2, 3 and 4, respectively. If the channel is quantized into $m = 3$ levels, the binary feedback messages "00", "01" and "11" are used to denote the lowest, middle and highest channel levels. If the message "10" is received because of feedback errors, then the channel level is selected randomly. The optimal thresholds in the cases of $m = 2$ and $m > 2$ are computed by solving (4.23) and (4.46), respectively.

Figs. 4.6-4.8 display the BERs versus SNR for $K = 4$. In each of these figures, the following theoretical curves are compared: the exact BER in the full CSI case given by (4.3), the exact BER in the case of quantized CSI feedback given by (4.45) for $m = 2, 3, 4$, as well as the exact BER of the random scheduling strategy (where no CSI feedback is required for scheduling). For the exact BER expression of (4.45), we use the thresholds obtained from (4.46). In Fig. 4.6, all the curves based on quantized CSI feedback are displayed in the error-free case ($\mathcal{P}_e = 0$). In Figs. 4.7 and 4.8, such curves are drawn for the erroneous feedback case with $\mathcal{P}_e = 0.01$ and $\mathcal{P}_e = 0.2$, respectively. From Figs. 4.6-4.8, we observe that all the analytical BER curves match very well to the experimental points. This validates our theoretical results for both the error-free and erroneous feedback cases.

From Fig. 4.6 it follows that in the error-free feedback case, the BER performance improves as the number of channel levels increases, and it approaches the exact BER (4.3) of the full CSI case. Compared with random scheduling, the opportunistic scheduling with even one-bit feedback greatly improves the BER performance. As follows from Fig. 4.7 and Fig. 4.8, the BER performance of the opportunistic scheduling approach with a quantized CSI feedback deteriorates in the erroneous feedback case as compared to the error-free feedback case. As m increases, the opportunistic scheduling scheme becomes more sensitive to

the feedback errors. In the case of extremely large $\mathcal{P}_e$ (Fig. 4.8), for example, the quantized CSI feedback with $m = 3$ is always substantially better in terms of BER than that with $m = 2$ and $m = 4$. This shows that in the case of erroneous CSI feedback, there is some value of m that depends on $\mathcal{P}_e$, and there is no benefit in increasing the number of channel quantization levels beyond this value. Moreover, the opportunistic scheduling scheme with a low-rate CSI feedback has a significantly better performance than the random scheduling approach even when $\mathcal{P}_e$ is large. This observation justifies the use of low-rate CSI feedback in multiuser systems with opportunistic scheduling.

4.6 Chapter Summary

In this chapter, the SER performance of the opportunistic scheduling scheme has been studied for the multiuser downlink channel. While channel-aware scheduling has been extensively studied in terms of the channel capacity, our study clearly shows its benefit to the overall system reliability. Our results in this chapter motivate the study of new aspects of scheduler design beyond the data throughput. As the number of users increases, the tail behavior of the distribution of the channel gains significantly affects the system performance. In this chapter, we have studied the asymptotic behavior of the SER under the assumption of i.i.d Rayleigh fading channels. Extensions to non-i.i.d. fading and other fading types formulate a part of the future work of this thesis.

Chapter 5

Multiuser Diversity in Cognitive Radio System I: Channel Capacity

As an emerging technology aimed at flexible and efficient spectrum usage, CR has recently attracted much attention in academia, industry, standards bodies and regulatory agencies. In the following two chapters, we will present some results from our timely research on this topic. In a communication system based on CR, the radio access is granted to the secondary users under the premise that no harmful interference will be caused at the existing primary users. Considering that a primary user in practice can tolerate a certain amount of noise and interference, the underlay CR model is strongly motivated and the primary users in this model are protected by some predefined thresholds of received interference. Certainly, in a network where primary and secondary users coexists, the scheduling scheme at the secondary network will not only affect the performance of the secondary users, but also the interference received at the PRs. In this chapter, we will study the opportunistic scheduling scheme in a secondary CR network and analyze its performance in terms of the channel capacity. The performance of opportunistic scheduling in terms of the SER will be investigated in Chapter 6.

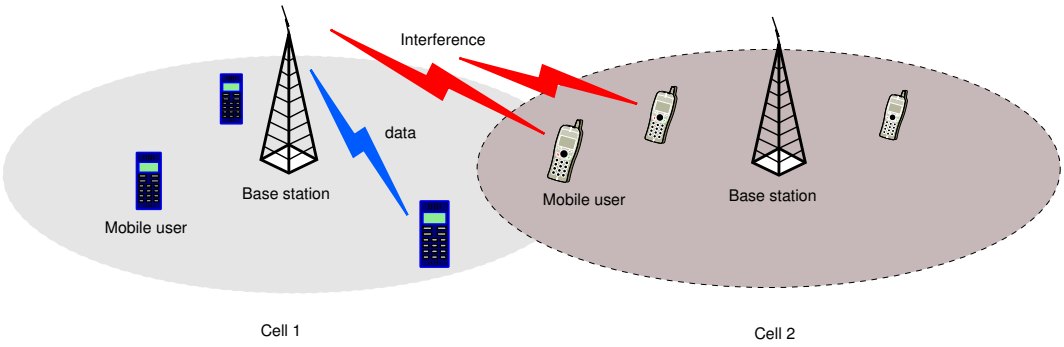

Figure 5.1: Underlay cognitive radio

5.1 Opportunistic Scheduling in Underlay Cognitive Radio

Let us consider the system model displayed in Fig. 5.1. In the context of CR considered in this chapter, Cell 1 in Fig. 5.1 represents a CR network where a cognitive base station coordinates the data transmission of several secondary mobile users. Cell 2 represents the existing primary network where there are U PRs. In this chapter, we assume the base station in Cell 1 is equipped with a single antenna ($M = 1$) and consider an opportunistic-scheduling based downlink scenario in Cell 1 similar to that considered in Chapter 4.

For notational convenience, we will omit the subscript $i = 1$ and time index t in (2.1) and (2.2) throughout this chapter. Instead, we will reserve the subscript i to denote the index of the fading states. To simplify the expressions, we will use $\underline{h}_k$ ($1 \leq k \leq K$) and $\underline{g}_m$ ($1 \leq m \leq U$) to denote power gains. This means that $\underline{h}_k = |h_{i,k}|^2$ and $\underline{g}_m = |g_{i,m}|^2$ with $h_{i,k}$ and $g_{i,m}$ defined as in (2.1) and (2.2). The realizations of $\underline{h}_k$ and $\underline{g}_m$ in a particular fading state i are denoted as $\underline{h}_{k,i}$ and $\underline{g}_{m,i}$, respectively. These realizations are assumed to be perfectly known at the CR base station[1].

Denoting the transmitted power per symbol at the ith fading state as P_i, we can compute the induced interference at the mth PR as $\underline{g}_{m,i}P_i$. Note that the interference only depends on the channel power gain of the mth PR $\underline{g}_{m,i}$ and the transmitted power P_i, but not on the scheduling policy of the secondary system. That is, fixing the value of P_i at the ith fading state, the instantaneous interference received at the mth PR does not depend on which SR is

[1] In the downlink scenario, the CR base station is the secondary transmitter.

actually scheduled. For the conventional BC fading channel without any PR's present, it has been shown in [44] that the capacity-maximizing user scheduling scheme is the opportunistic scheduling where the user with the largest instantaneous power gain is selected for data transmission. In the context of underlay CR, given a specific amount of transmitted power P_i, the capacity-achieving user selection scheme for the conventional (non-cognitive) BC channel is also capacity-achieving for the cognitive BC channel as different SR's scheduling schemes induce the same interference at each PR[2].

We study the channel capacity of the cognitive BC under the constraints that the consumed average transmitted power does not exceed the available power budget $\widetilde{P}$ and the average (or peak) interference temperature caused at the mth PR falls below some given interference temperature threshold, denoted by $\widetilde{Q}_m$ (or $\widehat{Q}_m$). We assume that the Gaussian codebook, which maximizes the sum capacity of the conventional BC fading channel, is used. Hence, the achievable sum capacity in the ith fading state can be expressed as $C_s(i) = \ln\left(1 + \frac{\hat{h}_i P_i}{\sigma_n^2}\right)$, where $\hat{\underline{h}}_i = \max_{1\leq k\leq K} \underline{h}_{k,i}$ denotes the instantaneous power gain of the scheduled SR[3].

5.2 Sum Capacity under Average IPC's

In the scenarios where the primary user's signal consists of long coded messages, the performance of the primary user is generally limited by the average interference it experiences. In this case, to protect the licensed primary users, average IPC's should be put on the secondary transmitters (STs). In this section, we study the sum capacity of the cognitive network under average IPC's.

[2]Based on the uplink-downlink duality [55], it has been shown in [54] that opportunistic scheduling is indeed capacity-maximizing.

[3]$\hat{\underline{h}}_i$ is used to denote the largest order statistic of $\underline{h}_{k,i}$ with respect to $k = 1, \cdots, K$ in this chapter to simplify the complicated notation $\underline{h}_{[1],i}$.

5.2.1 Sum Capacity Averaged over a Finite Number of Fading States

Given a sequence of $N < \infty$ fading states[4], the average sum capacity $\overline{C}_s$ can be expressed as

$$\overline{C}_s\left(P_1, \cdots, P_N\right) = \frac{1}{N}\sum_{i=1}^{N} C_s(i) = \frac{1}{N}\sum_{i=1}^{N} \ln\left(1 + \frac{\hat{h}_i P_i}{\sigma_n^2}\right). \tag{5.1}$$

In this subsection, we maximize $\overline{C}_s$ over P_i $(i = 1, \cdots, N)$ under an average TPC and U average IPC's. Defining $\mathbf{p} = \left[P_1, \cdots, P_N\right]^T$, the problem can be stated as

$$\max_{\mathbf{p}\in\mathbb{R}^N} \frac{1}{N}\sum_{i=1}^{N} \ln\left(1 + \frac{\hat{h}_i P_i}{\sigma_n^2}\right) \tag{5.2a}$$

$$\text{s. t. } \overline{P} \triangleq \frac{1}{N}\sum_{i=1}^{N} P_i \leq \widetilde{P}; \tag{5.2b}$$

$$\overline{Q}_m \triangleq \frac{1}{N}\sum_{i=1}^{N} \underline{g}_{m,i} P_i \leq \widetilde{Q}_m,\ m = 1, \cdots, U; \tag{5.2c}$$

$$P_i \geq 0,\ i = 1, \cdots, N, \tag{5.2d}$$

where $\mathbb{R}^N$ denotes the N-dimensional Euclidean space, (5.2b) and (5.2c) are the average TPC and average IPC's, respectively, $\overline{P}$ in (5.2b) denotes the consumed average transmitted power, and $\overline{Q}_m$ in (5.2c) is the induced average interference temperature at the mth PR. The existence of a unique solution to (5.2) is assured by the following proposition.

Proposition 1. *The optimization problem in (5.2) has a unique global maximum* $\mathbf{p}^\star$.

Proof: Problem in (5.2) can be formulated as an equivalent minimization problem with a convex objective function. The feasible set of the problem in (5.2), given by the constraints (5.2b)-(5.2d), is a polyhedral set which is closed and convex [93, p. 700]. Furthermore, it immediately follows from (5.2b) and (5.2d) that the feasible set of problem in (5.2) is bounded as $0 \leq P_i \leq N\widetilde{P}$ for all $i = 1, \cdots, N$, hence it is also compact. This feasible set is non-empty since $\mathbf{p} = \mathbf{0}_{N\times 1}$ is a feasible solution. Then, following the Weierstrass' Theorem [93, Proposition A.8], there exists a maximum $\mathbf{p}^\star$ of the objective function (5.2a). Moreover, the objective function (5.2a) is strictly concave since its Hessian is negative definite for all

[4]In this chapter, we are interested in the case of $N \gg \max\{K, U\}$ since in fading environments, the data transmission generally undergoes a large number of fading states.

feasible values of $\mathbf{p}$. Also, the objective function (5.2a) is proper since $-\infty < \overline{C}_s < \infty$ for all feasible values of $\mathbf{p}$ [92, p. 25]. Then, from Proposition 2.1.2 in [92, p. 87], it follows that $\mathbf{p}^\star$ is the unique global maximum of $\overline{C}_s$ over the feasible set defined by (5.2b)-(5.2d). □

The problem in (5.2) is a convex optimization problem with linear inequality constraints which can be efficiently solved using interior point methods [94]. Inserting the optimal power allocation $\mathbf{p}^\star$ in (5.1), the sum capacity $\overline{C}_s$ can be obtained. In the following, we derive an alternative procedure for computing the optimal power allocation, known as the constrained water-filling algorithm. Towards this aim, we write the Lagrangian function of (5.2) as [93]

$$\begin{aligned}\mathcal{L}\left(\mathbf{p},\boldsymbol{\mu}\right) = &-\frac{1}{N}\sum_{i=1}^{N}\ln\left(1+\frac{\hat{\underline{h}}_i P_i}{\sigma_n^2}\right)+\mu_0\left(\frac{1}{N}\sum_{i=1}^{N}P_i-\widetilde{P}\right)\\ &+\sum_{m=1}^{U}\mu_m\left(\frac{1}{N}\sum_{i=1}^{N}\underline{g}_{m,i}P_i-\widetilde{Q}_m\right)-\sum_{j=U+1}^{U+N}\mu_j P_{j-U},\end{aligned} \tag{5.3}$$

where μ_j $(j = 0, 1, \cdots, U+N)$ are the Lagrange multipliers. Let us define the vector of Lagrange multipliers as $\boldsymbol{\mu} = \left[\mu_0, \mu_1, \cdots, \mu_{U+N}\right]^T$. Since all constraints in (5.2) are linear, from [93, Propositions 3.3.6 and 3.3.7], there exists a vector of optimal Lagrange multipliers $\boldsymbol{\mu}^\star$ satisfying the following KKT necessary conditions [93, Proposition 3.3.1]

$$\nabla_{\mathbf{p}}\mathcal{L}\left(\mathbf{p}^\star,\boldsymbol{\mu}^\star\right) = \mathbf{0}_{N\times 1}, \tag{5.4a}$$

$$\boldsymbol{\mu}^\star \geq \mathbf{0}_{(U+1+N)\times 1}, \tag{5.4b}$$

$$\mu_0^\star\left(\tfrac{1}{N}\textstyle\sum_{i=1}^{N}P_i^\star-\widetilde{P}\right)=0, \tag{5.4c}$$

$$\mu_m^\star\left(\tfrac{1}{N}\textstyle\sum_{i=1}^{N}\underline{g}_{m,i}P_i^\star-\widetilde{Q}_m\right)=0;\ m=1,\cdots,U, \tag{5.4d}$$

$$-\mu_j^\star P_{j-U}^\star = 0;\ j=U+1,\cdots,U+N, \tag{5.4e}$$

where (5.4c)-(5.4e) are commonly referred to as the CS conditions. Reformulating the KKT conditions (5.4a), (5.4b), and (5.4e), the optimal solution $\mathbf{p}^\star$ can be expressed as

$$P_i^\star = \left[\frac{1}{\sum_{m=1}^{U}\mu_m^\star\underline{g}_{m,i}+\mu_0^\star}-\frac{\sigma_n^2}{\hat{\underline{h}}_i}\right]^+ \text{for } i=1,\cdots,N, \tag{5.5}$$

where the Lagrange multipliers $\mu_m^\star$ for $m = 0, \cdots, U$ must be chosen such that the CS conditions (5.4c), and (5.4d) are satisfied. A related constrained water-filling solution as

in (5.5) has been previously derived in [54] for the ergodic capacity of the cognitive BC channel.

Note that in a practical situation and for N given fading states, the knowledge of all the channel power gains $\underline{g}_{m,i}$ and $\hat{\underline{h}}_i$ ($m = 1, \cdots, U$, $i = 1, \cdots, N$) is required at the ST to compute the optimal power allocation $\mathbf{p}^\star$. In a time-selective fading scenario, this power allocation scheme would require non-causal CSI.

5.2.2 Ergodic Sum Capacity under Average IPC's

As pointed out in Chapter 2, ergodic sum capacity is defined as the statistical expectation of the sum capacity with respect to the random channel power gains $\underline{g}_m$ and $\underline{h}_k$, $m = 1, \cdots, U$ and $k = 1, \cdots, K$. As in this chapter we assume stationary ergodic channels, the ergodic sum capacity is equivalent to the average sum capacity in problem (5.2) for the limiting case of $N \to \infty$. The problem in (5.2) for $N \to \infty$ can be reformulated as

$$C = \max_{P \geq 0} \mathrm{E}\left\{ \ln\left(1 + \frac{\hat{\underline{h}} P}{\sigma_n^2}\right)\right\} \tag{5.6a}$$

$$\text{s. t. } \overline{P} \triangleq \mathrm{E}\left\{P\right\} \leq \widetilde{P}; \tag{5.6b}$$

$$\overline{Q}_m \triangleq \mathrm{E}\left\{\underline{g}_m P\right\} \leq \widetilde{Q}_m,\ m = 1, \cdots, U, \tag{5.6c}$$

where $\hat{\underline{h}}$ is the largest order statistic of $\underline{h}_k$ with $m = 1, \cdots, U$, the transmitted power P is a random variable which, according to (5.6), depends on the random channel power gains $\underline{g}_m$ and $\hat{\underline{h}}$.

Note that Proposition 1 and the KKT conditions (5.4a)-(5.4e) presented in the last subsection hold true for arbitrary values of N. Therefore, also in the limiting case of $N \to \infty$, the optimal power allocation in each fading state is given by (5.5). Hence, replacing in (5.5) the channel realizations $\underline{g}_{m,i}$ and $\hat{\underline{h}}_i$ by their corresponding random variables $\underline{g}_m$ and $\hat{\underline{h}}$, the optimal power allocation rule can be expressed as

$$P^\star = \left[\frac{1}{\sum_{m=1}^{U} \mu_m^\star \underline{g}_m + \mu_0^\star} - \frac{\sigma_n^2}{\hat{\underline{h}}}\right]^+, \tag{5.7}$$

where $\mu_m^\star \geq 0$ with $m = 0, \cdots, U$ are the optimal Lagrange multipliers satisfying the CS

conditions for $N \to \infty$. The latter conditions are given by

$$\mu_0^\star \left(\mathrm{E}\left\{P^\star\right\} - \widetilde{P} \right) = 0; \tag{5.8}$$

$$\mu_m^\star \left(\mathrm{E}\left\{ \underline{g}_m P^\star \right\} - \widetilde{Q}_m \right) = 0, \quad m = 1, \cdots, U. \tag{5.9}$$

Next, we extend the discussion on the optimal power allocation in the cognitive BC channel and investigate the uniqueness conditions for the optimal Lagrange multipliers $\mu_0^\star$, $\cdots$, $\mu_{U+N}^\star$. In fact, it can be shown [93, p.279] that the optimal solution $\boldsymbol{\mu}^\star$ is unique if $\mathbf{p}^\star$ is regular, that is, if the gradients of all active inequality constraints are linearly independent at $\mathbf{p}^\star$. If $\mathbf{p}^\star$ is not regular, there may exist an infinite number of solutions for $\boldsymbol{\mu}^\star$. However, according to Proposition 1, these solutions must all yield the same optimal power allocation $\mathbf{p}^\star$. Specifically, we will show that for the asymptotic case $N \to \infty$, the unique solution $\mathbf{p}^\star$ becomes regular so that there exists a *unique* solution $\boldsymbol{\mu}^\star$ satisfying the KKT conditions in (5.4). The gradients of the $U+N+1$ inequality constraints in problem (5.2) can be computed as

$$\nabla \overline{P}(\mathbf{p}) = \frac{1}{N} \mathbf{1}_{N\times 1};\ \nabla \overline{Q}_m(\mathbf{p}) = \frac{1}{N} \left[\underline{g}_{m,1}, \cdots, \underline{g}_{m,N} \right]^T;\ \nabla(-P_i) = -\mathbf{e}_i, \tag{5.10}$$

where $m = 1, \cdots, U$, $i = 1, \cdots, N$. Obviously, to achieve a non-zero capacity, at least one $P_i^\star$ must be strictly positive. If we define the number of strictly positive P_i's as k, then, the number of active constraints in problem (5.2) is less than or equal to $N - k + U + 1$. In the limiting case of $N \to \infty$, the number of strictly positive P_i's obtained from (5.5) becomes much larger than $U + 1$, i.e.,

$$k \gg U + 1, \tag{5.11}$$

since all power gains $\underline{g}_{m,i}$ are assumed to be generated by stationary ergodic random processes. Note that the dimension of each gradient vector in (5.10) is equal to the number of fading states, N. Thus, from (5.11), we have that

$$N - k + U + 1 < N \tag{5.12}$$

for large N, and the gradients of all active constraints are almost surely linearly independent at $\mathbf{p}^\star$ since $\nabla \overline{Q}_m(\mathbf{p})$ are statistically independent random vectors. This means that $\mathbf{p}^\star$ becomes regular as $N \to \infty$.

From the previous discussion, we see that the solution of $\mu_m^\star$ $(m = 0, \cdots, U)$ is unique as $N \to \infty$. In contrast to the case of a finite number of fading states, problem (5.6) cannot be directly solved using interior point methods due to the statistical expectation involved in (5.6a)-(5.6c).

In the following, we derive a general procedure to efficiently compute the optimal Lagrange multipliers. The first idea is to identify the inactive TPC and IPC's and discard them from the optimization problem. Given a particular budget $\widetilde{P}$ at the transmitter and the average interference thresholds $\widetilde{Q}_m$ $(i = 1, \cdots, U)$ for all U PR's, we identify PR's which undergo an interference temperature strictly lower than their thresholds. Similarly, we investigate if the entire transmitted power budget is consumed by the optimal power allocation scheme. The following proposition provides a useful insight into this issue.

Proposition 2. *With the optimal power allocation $P^\star$ given in (5.7), for any two PR's k and j with $\overline{Q}_k = \widetilde{Q}_k$ and $\overline{Q}_j < \widetilde{Q}_j$, we have*

$$\frac{\overline{Q}_k}{\mathrm{E}\{\underline{g}_k\}} \leq \overline{P} = \frac{\overline{Q}_j}{\mathrm{E}\{\underline{g}_j\}}. \tag{5.13}$$

Proof: For any PR j with $\overline{Q}_j < \widetilde{Q}_j$, we have $\mu_j^\star = 0$ from the CS condition (5.9). In this case, $P^\star$ in (5.7) becomes independent of $\underline{g}_j$. Substituting $P = P^\star$ and $\mu_j^\star = 0$ in (5.6b) and (5.6c), we obtain

$$\overline{Q}_j = \mathrm{E}\left\{\underline{g}_j P^\star\right\} = \mathrm{E}\left\{\underline{g}_j\right\} \mathrm{E}\left\{P^\star\right\} = \overline{P}\mathrm{E}\left\{\underline{g}_j\right\}. \tag{5.14}$$

Thus, $\overline{P} = \frac{\overline{Q}_j}{\mathrm{E}\left\{\underline{g}_j\right\}}$ holds for any $\overline{Q}_j < \widetilde{Q}_j$.

For any PR k with $\overline{Q}_k = \widetilde{Q}_k$, inserting (5.7) in (5.6b) yields

$$\overline{P} = \mathrm{E}\left\{\left[\frac{1}{\left(\sum_{j=1}^{M} \mu_j^\star \underline{g}_j + \mu_0^\star\right)} - \frac{\sigma_n^2}{\underline{\hat{h}}}\right]^+\right\} = \mathrm{E}\left\{\left[\frac{1}{\left(\mu_k^\star \underline{g}_k + \alpha\right)} - \frac{\sigma_n^2}{\underline{\hat{h}}}\right]^+\right\} \tag{5.15}$$

where $\alpha = \sum_{j=1, j\neq k}^{M} \mu_j^\star \underline{g}_j + \mu_0^\star$ denotes a new random variable. Inserting $P = P^\star$ in (5.6c) for the PR k, we obtain

$$\overline{Q}_k = \mathrm{E}\left\{\underline{g}_k\left[\frac{1}{\left(\mu_k^\star \underline{g}_k + \alpha\right)} - \frac{\sigma_n^2}{\underline{\hat{h}}}\right]^+\right\}. \tag{5.16}$$

If $\mu_k^\star = 0$, then it can be readily shown that $\overline{P} = \frac{\overline{Q}_k}{\mathrm{E}\{\underline{g}_k\}}$. In the case of $\mu_k^\star > 0$, given α and $\hat{\underline{h}}$ such that $\frac{\hat{\underline{h}}}{\sigma_n^2} \geq \alpha \geq 0$, it can be easily shown that the function

$$y_1(x) = \frac{1}{\mu_k^\star x + \alpha} - \frac{\sigma_n^2}{\hat{\underline{h}}} \tag{5.17}$$

defined on the interval $\left[0, \frac{1}{\mu_k^\star}\left(\frac{\hat{\underline{h}}}{\sigma_n^2} - \alpha\right)\right]$ is convex in x and the function

$$y_2(x) = x\left(\frac{1}{\mu_k^\star x + \alpha} - \frac{\sigma_n^2}{\hat{\underline{h}}}\right) \tag{5.18}$$

is concave in x on the same interval. Let us define the pdf's of $\underline{g}_k$, α and $\hat{\underline{h}}$ as $f_{\underline{g}_k}(x)$, $f_\alpha(y)$ and $f_{\hat{\underline{h}}}(z)$, respectively. As the power gains are all jointly independent, $\overline{Q}_k$ in (5.16) can be rewritten and bounded as

$$\begin{aligned}
\overline{Q}_k &= \int_0^\infty \int_0^\infty \int_0^\infty x\left[\frac{1}{\mu_k^\star x + y} - \frac{\sigma_n^2}{z}\right]^+ f_{\underline{g}_k}(x) f_\alpha(y) f_{\hat{\underline{h}}}(z)\, dx\, dy\, dz \qquad (5.19)\\
&= \int_0^\infty \int_0^{\frac{z}{\sigma_n^2}} \int_0^{\frac{1}{\mu_k^\star}\left(\frac{z}{\sigma_n^2} - y\right)} x\left(\frac{1}{\mu_k^\star x + y} - \frac{\sigma_n^2}{z}\right) f_{\underline{g}_k}(x) f_\alpha(y) f_{\hat{\underline{h}}}(z)\, dx\, dy\, dz\\
&\overset{a}{=} \int_0^\infty \int_0^{\frac{z}{\sigma_n^2}} F_{\underline{g}_k}\left(\frac{z}{\mu_k^\star \sigma_n^2} - \frac{y}{\mu_k^\star}\right) \int_0^{\frac{1}{\mu_k^\star}\left(\frac{z}{\sigma_n^2} - y\right)} x\left(\frac{1}{\mu_k^\star x + y} - \frac{\sigma_n^2}{z}\right) f_{\tilde{\underline{g}}_k}(x)\, dx f_\alpha(y) f_{\hat{\underline{h}}}(z)\, dy\, dz\\
&\overset{b}{\leq} \int_0^\infty \int_0^{\frac{z}{\sigma_n^2}} F_{\underline{g}_k}\left(\frac{z}{\mu_k^\star \sigma_n^2} - \frac{y}{\mu_k^\star}\right) \mathrm{E}\left\{\tilde{\underline{g}}_k\right\} \left(\frac{1}{\mu_k^\star \mathrm{E}\left\{\tilde{\underline{g}}_k\right\} + y} - \frac{\sigma_n^2}{z}\right) f_\alpha(y) f_{\hat{\underline{h}}}(z)\, dy\, dz\\
&\overset{c}{\leq} \int_0^\infty \int_0^{\frac{z}{\sigma_n^2}} F_{\underline{g}_k}\left(\frac{z}{\mu_k^\star \sigma_n^2} - \frac{y}{\mu_k^\star}\right) \mathrm{E}\left\{\underline{g}_k\right\} \left(\frac{1}{\mu_k^\star \mathrm{E}\left\{\tilde{\underline{g}}_k\right\} + y} - \frac{\sigma_n^2}{z}\right) f_\alpha(y) f_{\hat{\underline{h}}}(z)\, dy\, dz\\
&\overset{d}{\leq} \mathrm{E}\{\underline{g}_k\} \int_0^\infty \int_0^{\frac{z}{\sigma_n^2}} F_{\underline{g}_k}\left(\frac{z}{\mu_k^\star \sigma_n^2} - \frac{y}{\mu_k^\star}\right)\\
&\quad \cdot \int_0^{\frac{1}{\mu_k^\star}\left(\frac{z}{\sigma_n^2} - y\right)} \left(\frac{1}{\mu_k^\star x + y} - \frac{\sigma_n^2}{z}\right) f_{\tilde{\underline{g}}_k}(x)\, dx f_\alpha(y) f_{\hat{\underline{h}}}(z)\, dy\, dz\\
&= \mathrm{E}\{\underline{g}_k\} \mathrm{E}\left\{\left[\frac{1}{\left(\mu_k^\star \underline{g}_k + \alpha\right)} - \frac{\sigma_n^2}{\hat{\underline{h}}}\right]^+\right\} = \overline{P} \mathrm{E}\{\underline{g}_k\},
\end{aligned}$$

where in (a) of (5.19), we define $f_{\tilde{\underline{g}}_k}(x) = \frac{f_{\underline{g}_k}(x)}{F_{\underline{g}_k}\left(\frac{z}{\mu_k^\star \sigma_n^2} - \frac{y}{\mu_k^\star}\right)}$ as the pdf of the truncated distribution of $\underline{g}_k$ on the interval $\left[0, \frac{1}{\mu_k^\star}\left(\frac{z}{\sigma_n^2} - y\right)\right]$ and denote the variable of the truncated distribution as $\tilde{\underline{g}}_k$. The Note that in this equation, $y \leq \frac{z}{\sigma_n^2}$. The inequality (b) follows from the Jensen's

inequality due to the concavity of $y_2(x)$, where the expectation of the truncated $\underline{g}_k$ is given by

$$\mathrm{E}\left\{\tilde{\underline{g}}_k\right\} \triangleq \frac{1}{F_{\underline{g}_k}\left(\frac{z}{\mu_k^\star \sigma_n^2} - \frac{y}{\mu_k^\star}\right)} \int_0^{\frac{1}{\mu_k^\star}\left(\frac{z}{\sigma_n^2}-y\right)} x f_{\underline{g}_k}(x)\, dx. \tag{5.20}$$

The inequality (c) comes from

$$\mathrm{E}\left\{\tilde{\underline{g}}_k\right\} = \frac{\int_0^{\frac{1}{\mu_k^\star}\left(\frac{z}{\sigma_n^2}-y\right)} x f_{\underline{g}_k}(x)\, dx}{\int_0^{\frac{1}{\mu_k^\star}\left(\frac{z}{\sigma_n^2}-y\right)} f_{\underline{g}_k}(x)\, dx} \leq \frac{\int_0^{\frac{1}{\mu_k^\star}\left(\frac{z}{\sigma_n^2}-y\right)} x f_{\underline{g}_k}(x)\, dx + \int_{\frac{1}{\mu_k^\star}\left(\frac{z}{\sigma_n^2}-y\right)}^{\infty} x f_{\underline{g}_k}(x)\, dx}{\int_0^{\frac{1}{\mu_k^\star}\left(\frac{z}{\sigma_n^2}-y\right)} f_{\underline{g}_k}(x)\, dx + \int_{\frac{1}{\mu_k^\star}\left(\frac{z}{\sigma_n^2}-y\right)}^{\infty} f_{\underline{g}_k}(x)\, dx} = \mathrm{E}\left\{\underline{g}_k\right\}, \tag{5.21}$$

since for any $\omega \geq 0$, $\frac{\int_0^\omega x f_{\underline{g}_k}(x)\, dx}{\int_0^\omega f_{\underline{g}_k}(x)\, dx} \leq \omega \leq \frac{\int_\omega^\infty x f_{\underline{g}_k}(x)\, dx}{\int_\omega^\infty f_{\underline{g}_k}(x)\, dx}$. The inequality (d) holds true due to the Jensen's inequality and the convexity of $y_1(x)$ on the interval $\left[0, \frac{1}{\mu_k^\star}\left(\frac{\hat{h}}{\sigma_n^2} - \alpha\right)\right]$. From (5.19), we obtain $\overline{P} \geq \frac{\overline{Q}_k}{\mathrm{E}\{\underline{g}_k\}}$ for any PR k with $\overline{Q}_k = \widetilde{Q}_k$. This completes the proof of Proposition 2. □

Proposition 2 shows that any PR with an inactive IPC receives an average interference power equal to its expected channel power gain multiplied by the average transmitted power. This is due to the fact that the optimal power allocation is independent of the channel power gain of that particular PR in this case. Similarly, for any PR with an active IPC, the optimal power allocation usually depends on its power gain. In this case, the average interference at that particular PR is less than or equal to its expected channel power gain multiplied by the average transmitted power.

Without loss of generality, let us order the U PR's so that

$$\frac{\widetilde{Q}_1}{\mathrm{E}\{\underline{g}_1\}} \leq \cdots \leq \frac{\widetilde{Q}_r}{\mathrm{E}\{\underline{g}_r\}} \leq \widetilde{P} < \frac{\widetilde{Q}_{r+1}}{\mathrm{E}\{\underline{g}_{r+1}\}} \leq \cdots \leq \frac{\widetilde{Q}_U}{\mathrm{E}\{\underline{g}_U\}}, \tag{5.22}$$

where $0 \leq r \leq U$. The following corollary follows directly from Proposition 2.

Corollary 1. *Ordering the U PR's as in (5.22) and using the power allocation scheme $P^\star$ of (5.7), we have that the IPC's in (5.6c) are inactive for all $r+1 \leq m \leq U$. Additionally, if the entire transmitted power budget is consumed, i.e. $\overline{P} = \widetilde{P}$, then the IPC's in (5.6c) are active for all $1 \leq m \leq r$, otherwise only a part of the IPC's with $1 \leq m \leq r$ are active.*

Corollary 1 shows that the PR's $r+1, \cdots, U$ have inactive IPC's and suffer interference temperatures strictly below their thresholds. According to the CS conditions (5.9), their corresponding optimal Lagrange multipliers are all equal to zero. The optimal power allocation scheme $P^\star$ in (5.7) then becomes

$$P^\star = \left[\frac{1}{\sum_{m=1}^{r} \mu_m^\star \underline{g}_m + \mu_0^\star} - \frac{\sigma_n^2}{\underline{\hat{h}}}\right]^+, \tag{5.23}$$

which is independent of $\underline{g}_m$ for $r+1 \leq m \leq U$. Inserting (5.23) in (5.6a), we can conclude that the ergodic sum capacity is also independent of $\underline{g}_m$ for $r+1 \leq m \leq U$. Thus, the PR's $r+1, \cdots, U$ do not affect the ergodic sum capacity of the CR network.

Corollary 1 provides us with the means to identify and eliminate $U-r$ IPC's in problem (5.6) that are guaranteed to be inactive. The remaining Lagrange multipliers can then be computed as described below. Ordering the U PR's as in (5.22), the optimal power allocation $P^\star$ is given by the water-filling solution (5.23), where $\mu_m^\star$ with $m = 0, \cdots, r$ satisfy the CS conditions (5.8) and (5.9).

The uniqueness of $\boldsymbol{\mu}^\star$ and $\mathbf{p}^\star$, together with the CS conditions (5.8) and (5.9), reveal a simple step-by-step procedure to find the optimal Lagrange multipliers. The detailed procedure is outlined as follows: *Procedure 1:* Compute $\mu_j^\star$ for $j = 0, \cdots, r$ as follows.

- Initialization: Set $\mu_l^\star = 0$ for $l = 0, \cdots, U$ and $j = 1$.

- Step j for $j = 1, \cdots, r$: Compute μ_m for $m = 1, \cdots, j$ by solving the following set of equations

$$\mathrm{E}\left\{\underline{g}_i \left[\frac{1}{\sum_{m=1}^{j} \mu_m \underline{g}_m} - \frac{\sigma_n^2}{\underline{\hat{h}}}\right]^+\right\} = \widetilde{Q}_i, \; i = 1, \cdots, j. \tag{5.24}$$

  If the so-obtained water-filling solution

$$P^{(j)} = \left[\frac{1}{\sum_{m=1}^{j} \mu_m \underline{g}_m} - \frac{\sigma_n^2}{\underline{\hat{h}}}\right]^+ \tag{5.25}$$

  is feasible, i.e., if $P^{(j)}$ satisfies the TPC (5.6b) and the IPC's (5.6c), then set $\mu_m^\star = \mu_m$ for $m = 1, \cdots, j$ and end the procedure. Otherwise go to the next step with $j = j+1$.

- Step $j = r+1$: Calculate $\mu_m^\star$ for $m = 0, \cdots, r$ by solving the following system of equations

$$\mathrm{E}\left\{\left[\frac{1}{\sum_{m=1}^{r}\mu_m^\star \underline{g}_m + \mu_0^\star} - \frac{\sigma_n^2}{\underline{\hat{h}}}\right]^+\right\} = \widetilde{P},$$
$$\mathrm{E}\left\{\underline{g}_i\left[\frac{1}{\sum_{m=1}^{r}\mu_m^\star \underline{g}_m + \mu_0^\star} - \frac{\sigma_n^2}{\underline{\hat{h}}}\right]^+\right\} = \widetilde{Q}_i,\ i = 1, \cdots, r.$$

  End the procedure.

Inserting the obtained $\mu_m^\star$ with $m = 0, \cdots, r$ in (5.23), we get the optimal power allocation scheme $P^\star$. Substituting $P^\star$ for P in (5.6a), the ergodic sum capacity can be expressed as

$$C = \mathrm{E}\left\{\ln\left(1 + \frac{\underline{\hat{h}}}{\sigma_n^2}\left[\frac{1}{\sum_{m=1}^{r}\mu_m^\star \underline{g}_m + \mu_0^\star} - \frac{\sigma_n^2}{\underline{\hat{h}}}\right]^+\right)\right\}. \tag{5.26}$$

Given the pdf's of $\underline{\hat{h}}$ and $\underline{g}_m$ $(m = 1, \cdots, r)$, the ergodic sum capacity C in the above equation can be straightforwardly computed numerically.

Note that all the Lagrange multipliers $\mu_m^\star$ $(m = 0, \cdots, r)$ in (5.26) are computed by using the statistical characteristics of the channel power gains. With the assumption that the ST knows the distributions of all $\underline{h}_k$ $(k = 1, \cdots, K)$ and $\underline{g}_m$ $(m = 1, \cdots, U)$, these Lagrange multipliers can be predetermined at the ST. Thus, in each particular fading state, the ST can adjust its transmitted power according to (5.23) solely based on the current channel state. In time-selective fading scenarios, this means that the power allocation mechanism requires only causal channel state information to achieve the ergodic sum capacity.

5.3 Sum Capacity under Peak IPC's

In the scenarios where the primary user's signal consists of very short messages such as feedback messages, pilot symbols, etc., the performance of the primary user is limited by the peak interference it may receive. In this case, to protect the licensed primary users, peak IPC's should be put on the STs. In this section, we study the sum capacity of the cognitive network under peak IPC's.

5.3.1 Sum Capacity Averaged over a Finite Number of Fading States

In this section, we maximize $\overline{C}_s$ over P_i $(i = 1, \cdots, N)$ under an average TPC and U peak IPC's. The capacity maximization problem can be formulated similarly to problem (5.2) as

$$\max_{\mathbf{p}\in\mathbb{R}^N} \frac{1}{N}\sum_{i=1}^{N} \ln\left(1+\frac{\hat{\underline{h}}_i P_i}{\sigma_n^2}\right) \tag{5.27a}$$

$$\text{s. t. } \overline{P} \triangleq \frac{1}{N}\sum_{i=1}^{N} P_i \le \widetilde{P}; \tag{5.27b}$$

$$Q_m \triangleq \max_{i=1,\cdots,N}\left\{\underline{g}_{m,i} P_i\right\} \le \widehat{Q}_m,\ m = 1, \cdots, U; \tag{5.27c}$$

$$P_i \ge 0,\ i = 1, \cdots, N, \tag{5.27d}$$

where (5.27b) and (5.27c) are the average TPC and peak IPC's, respectively. $\overline{P}$ in (5.27b) denotes the actually consumed average transmitted power as defined in (5.2b) and Q_m is the induced peak interference temperature at the mth PR given by (5.27c).

Let us define

$$G_i \triangleq \max_{1\le m\le U} \frac{\underline{g}_{m,i}}{\widehat{Q}_m} \tag{5.28}$$

for $i = 1, \cdots, N$. Then the peak IPC's in (5.27c) can be equivalently expressed as

$$G_i P_i \le 1 \text{ for } i = 1, \cdots, N. \tag{5.29}$$

Proposition 3. *The optimization problem (5.27) has a unique global maximum* $\mathbf{p}^\star$.

Proof: This proposition can be proven similarly to Proposition 1. The proof is, therefore, omitted for brevity. □

Similar to (5.2), the problem (5.27) is also convex and can be solved numerically using interior point methods [94]. The Lagrangian function of problem (5.27) can be written as

$$\begin{aligned}\mathcal{L}(\mathbf{p}, \boldsymbol{\mu}) = &-\frac{1}{N}\sum_{i=1}^{N} \ln\left(1+\frac{\hat{\underline{h}}_i P_i}{\sigma_n^2}\right) + \mu_0\left(\frac{1}{N}\sum_{i=1}^{N} P_i - \widetilde{P}\right)\\ &+ \sum_{i=1}^{N} \mu_i\left(G_i P_i - 1\right) - \sum_{i=1}^{N} \mu_{(i+N)} P_i,\end{aligned} \tag{5.30}$$

where $\boldsymbol{\mu} = \left[\mu_0, \mu_1, \cdots, \mu_{2N}\right]^T$ is the associated vector of Lagrange multipliers. As all inequality constraints in (5.27) are linear, from [93, Propositions. 3.3.6 and 3.3.7], it follows

that there exist the optimal vector $\boldsymbol{\mu}^\star = \left[\mu_0^\star, \mu_1^\star, \cdots, \mu_{2N}^\star\right]^T$ satisfying the corresponding KKT necessary conditions

$$\nabla_{\mathbf{p}} \mathcal{L}\left(\mathbf{p}^\star, \boldsymbol{\mu}^\star\right) = \mathbf{0}_{N\times 1}, \tag{5.31}$$

$$\boldsymbol{\mu}^\star \geq \mathbf{0}_{(2N+1)\times 1}, \tag{5.32}$$

$$\mu_0^\star \left(\tfrac{1}{N}\textstyle\sum_{i=1}^N P_i^\star - \widetilde{P}\right) = 0, \tag{5.33}$$

$$\mu_i^\star \left(G_i P_i^\star - 1\right) = 0,\ i = 1, \cdots, N, \tag{5.34}$$

$$-\mu_{(i+N)}^\star P_i^\star = 0, i = 1, \cdots, N. \tag{5.35}$$

From the KKT conditions (5.31)-(5.35), the optimal power allocation $\mathbf{p}^\star$ can be expressed using the optimal Lagrange multipliers as

$$P_i^\star = \frac{1}{NG_i\mu_i^\star - N\mu_{(i+N)}^\star + \mu_0^\star} - \frac{\sigma_n^2}{\underline{\hat{h}}_i},\ i = 1, \cdots, N. \tag{5.36}$$

With (5.32) and the CS conditions in (5.34) and (5.35), we have $\mu_{(i+N)}^\star = 0$ if $P_i^\star > 0$; and $\mu_i^\star = 0$ if $G_i P_i^\star < 1$, for $i = 1, \cdots, N$. Hence, (5.36) can be compactly written as the following water-filling-type solution

$$P_i^\star = \min\left\{\frac{1}{G_i}, \left[\frac{1}{\mu_0^\star} - \frac{\sigma_n^2}{\underline{\hat{h}}_i}\right]^+\right\}. \tag{5.37}$$

The power allocation in (5.37) can also be derived from the Lagrange dual problem [54]. Using (5.37), we can distinguish two cases which facilitate the computation of the optimal power allocations.

First, assume the case when $\frac{1}{N}\sum_{i=1}^N \frac{1}{G_i} > \widetilde{P}$ for which we can prove by contradiction that $\overline{P} = \widetilde{P}$. Indeed, if $\overline{P} < \widetilde{P}$, the CS condition (5.33) leads to $\mu_0^\star = 0$ and we have $P_i^\star = \frac{1}{G_i}$ in (5.37). Hence, $\overline{P} = \frac{1}{N}\sum_{i=1}^N P_i^\star = \frac{1}{N}\sum_{i=1}^N \frac{1}{G_i} > \widetilde{P}$ violates the average TPC $\overline{P} \leq \widetilde{P}$. Hence, $\overline{P} = \widetilde{P}$. Using this fact and the CS conditions (5.33)-(5.35), we can compute a unique solution for $\boldsymbol{\mu}^\star$.

Next, assume that $\frac{1}{N}\sum_{i=1}^N \frac{1}{G_i} \leq \widetilde{P}$. Then from (5.37) and from the fact that the sum capacity increases with $P_i^\star$, we can conclude that the optimal power allocation is given by $P_i^\star = \frac{1}{G_i}$. The last observation outlines a simple procedure for computing the optimal power allocation for the case when $\frac{1}{N}\sum_{i=1}^N \frac{1}{G_i} \leq \widetilde{P}$.

Similar to Section 5.2.1, the optimal power allocation $\mathbf{p}^\star$ is computed based on the knowledge of all $\underline{\hat{h}}_i$ and $\underline{g}_{m,i}$ with $i = 1, \cdots, N$ and $m = 1, \cdots, U$. However, if the power allocation is performed in time domain, the proposed procedure requires non-causal channel state information.

5.3.2 Ergodic Sum Capacity under Peak IPC's

As stated in Section 5.2.2, the mean value of the samples generated by a stationary ergodic random process approaches the statistical expectation of this random process as $N \to \infty$. In the sequel, we use G to denote the largest order statistic of $\underline{g}_m/\widehat{Q}_m$ for $m = 1, \cdots, U$, i.e.,

$$G = \max_{1 \le m \le U} \frac{\underline{g}_m}{\widehat{Q}_m}. \tag{5.38}$$

We denote the cdf and pdf of G by $F_G(x)$ and $f_G(x)$, respectively. Following the discussion presented in Subsection 5.3.1, the optimal power allocation scheme in (5.37) defines a random variable given by

$$P^\star = \begin{cases} \frac{1}{G}, & \text{if } \mathrm{E}\left\{\frac{1}{G}\right\} \le \widetilde{P}; \\ \min\left\{\frac{1}{G}, \left[\frac{1}{\mu_0^\star} - \frac{\sigma_n^2}{\underline{\hat{h}}}\right]^+\right\}, & \text{otherwise.} \end{cases} \tag{5.39}$$

From (5.38) and (5.39), we observe that in the interference limited case $\mathrm{E}\left\{\frac{1}{G}\right\} \le \widetilde{P}$, the ergodic sum capacity-achieving strategy is to transmit to the SR with the strongest channel gain with the transmitted power assigned according to the inverse of the strongest normalized PR's channel gain. Thus, in the case of $\overline{P} = \mathrm{E}\left\{\frac{1}{G}\right\} \le \widetilde{P}$, the ergodic sum capacity is given by

$$C = \mathrm{E}\left\{\ln\left(1 + \frac{\underline{\hat{h}}}{\sigma_n^2}\frac{1}{G}\right)\right\}. \tag{5.40}$$

If $\mathrm{E}\left\{\frac{1}{G}\right\} > \widetilde{P}$, the ergodic sum capacity can be expressed as

$$C = \mathrm{E}\left\{\ln\left(1 + \frac{\underline{\hat{h}}}{\sigma_n^2}\min\left\{\frac{1}{G}, \left[\frac{1}{\mu_0^\star} - \frac{\sigma_n^2}{\underline{\hat{h}}}\right]^+\right\}\right)\right\}, \tag{5.41}$$

where the Lagrange multiplier $\mu_0^\star > 0$ in (5.41) can be computed by solving the following equation

$$\mathrm{E}\left\{\min\left\{\frac{1}{G}, \left[\frac{1}{\mu_0^\star} - \frac{\sigma_n^2}{\underline{\hat{h}}}\right]^+\right\}\right\} = \widetilde{P}. \tag{5.42}$$

5.4 Asymptotic Performance Analysis in Rayleigh Fading Channels

The results presented in Section 5.2 and 5.3 are valid for any particular fading distribution. In this section, we consider the special case of Rayleigh fading channels. In the Rayleigh fading case, we are interested in the asymptotic behavior of the ergodic sum capacity, both for large numbers of SR's and PR's. In the first asymptotic regime, we fix the number of PR's and let the number of SR's K increase to infinity, while in the second regime we fix K and let U increase to infinity. For the sake of simplicity, we assume a Rayleigh faded homogeneous system similar to that in Chapter 4, in which:

- (A1) The channel power gains of all PR's and SR's are i.i.d. variables.
- (A2) The pdf of each of the channel power gains $\underline{g}_m$ and $\underline{h}_k$ ($m = 1, \cdots, U$; $k = 1, \cdots, K$) is given by $f(x) = \exp(-x)$.
- (A3) The PR's interference thresholds are identical and equal to $\widetilde{Q}$ and $\widehat{Q}$ in the cases of average and peak IPC's, respectively.

Note that the particular choice of pdf in (A2) corresponds to the Rayleigh fading channel with unit variance. Further, the pdf of the largest order statistic $\hat{\underline{h}}$ of $\underline{h}_k$ is given by $f_{\hat{\underline{h}}}(y) = K(1-e^{-y})^{K-1}e^{-y}$ [82].

5.4.1 Asymptotic Capacity for a Large Number of SR's

It is well known that in the conventional BC channel with a fixed transmitted power $P_0 < \infty$ and without PR's, the ergodic sum capacity increases as $\ln \ln K$ for $K \to \infty$ [46] [52]. This capacity increase is due to the multiuser diversity, which takes advantage of the opportunistic user scheduling. Since the multiuser diversity advantage also applies to the underlay cognitive BC channel, we can expect a capacity increase with the number of SR's. In particular, we are interested in the scaling order of the ergodic sum capacity as a function of the number of SR's K. In our analysis, we distinguish between the cases of average and peak IPC's.

Average IPC's

To investigate the asymptotic behavior of C, let us derive upper and lower bounds for the ergodic sum capacity C of (5.26). Note first that the ergodic sum capacity is a monotonically non-increasing function of the number of PR's U. Thus, the ergodic sum capacity in the case of $U = 1$ (which we will denote as $C|_{U=1}$) marks an upper bound for the case of any $U \geq 1$. A lower bound can be obtained from a feasible but suboptimal constant power allocation scheme $P = P_0$, where the constant transmitted power is characterized by $P_0 = \min\left\{\widetilde{P}, \frac{\widetilde{Q}_m}{\mathrm{E}\{\underline{g}_m\}}\right\}$ for $m = 1, \cdots, U$. We denote this lower bound as $C|_{P=P_0}$. Then, we have

$$C|_{P=P_0} \leq C \leq C|_{U=1}. \tag{5.43}$$

Before we show that both the upper and lower bounds (and, hence, also C) increase with $\ln\ln K$ as $K \to \infty$, let us first present some results for the upper bound $C|_{U=1}$.

Proposition 4. *Given the threshold $\widetilde{Q}$ for the average interference temperature and a single PR ($U = 1$), for any fixed value of transmitted power budget $\widetilde{P} < \infty$, the optimal power allocation scheme is given by $P^\star = \left[\frac{1}{\mu_1^\star \underline{g}_1 + \mu_0^\star} - \frac{\sigma_n^2}{\underline{\hat{h}}}\right]^+$ with $\mu_0^\star > 0$ and we have that $\overline{P} = \widetilde{P}$. If $\widetilde{P} < \widetilde{Q}$, we have that $\mu_1^\star = 0$, and $P^\star$ becomes the conventional water-filling solution.*

Proof: With the assumption (A2) made in the beginning of this section, we have that $\mathrm{E}\{\underline{g}_1\} = 1$. If $\widetilde{P} < \widetilde{Q}$, we obtain from Corollary 1 that $\mu_1^\star = 0$. In this case, $P^\star$ in (5.23) reduces to the traditional water-filling solution with an average TPC $\widetilde{P}$. Thus, it can be readily shown that $\overline{P} = \widetilde{P}$ and $\mu_0^\star > 0$.

In the case of $\widetilde{P} \geq \widetilde{Q}$, we follow Procedure 1 of Section 5.2.2 to compute the optimal power allocation. Inserting the pdf's $f(x)$ and $f_{\underline{\hat{h}}}(y)$ into (5.24), Step 1 of Procedure 1 yields the following equality

$$\begin{aligned}\widetilde{Q} &= \int_0^\infty \int_0^\infty \left[\frac{1}{\mu_1} - \frac{\sigma_n^2 x}{y}\right]^+ e^{-x} K\left(1 - e^{-y}\right)^{K-1} e^{-y}\, dx\, dy \\ &= \sum_{j=1}^{K} \binom{K}{j} (-1)^{j+1} \left[\frac{1}{\mu_1} - \sigma_n^2 j \ln\left(1 + \frac{1}{\mu_1 \sigma_n^2 j}\right)\right].\end{aligned} \tag{5.44}$$

By solving (5.44) numerically, we can find the value of μ_1. The corresponding power allocation is given by (5.25) as $P^{(1)} = \left[\frac{1}{\mu_1 \underline{g}_1} - \frac{\sigma_n^2}{\underline{\hat{h}}}\right]^+$. Then, the average transmitted power can

be computed as

$$\begin{aligned}\overline{P} &= \mathrm{E}\left\{\left[\frac{1}{\mu_1 \underline{g}_1} - \frac{\sigma_n^2}{\underline{\hat{h}}}\right]^+\right\} \\ &= \lim_{\epsilon\to 0^+} \int_{\epsilon}^{\infty}\int_{\mu_1\sigma_n^2 x}^{\infty}\left[\frac{1}{\mu_1 x} - \frac{\sigma_n^2}{y}\right] f_{\underline{\hat{h}}}(y) e^{-x}\, dy\, dx \\ &= \lim_{\epsilon\to 0^+} \frac{-\mathrm{Ei}(-\epsilon)}{\mu_1} - \sigma_n^2 \sum_{j=1}^{K} \binom{K}{j} (-1)^{j+1} j \ln\left(1+\frac{1}{\mu_1\sigma_n^2 j}\right),\end{aligned} \tag{5.45}$$

where the outer integral is computed in terms of the Cauchy principal value due to the singularity at the point $x = 0$, $\mathrm{Ei}\,(x) = \int_{-\infty}^{x} \frac{e^t}{t}\, dt$ is the exponential integral. As

$$\lim_{\epsilon\to 0^+} -\mathrm{Ei}(-\epsilon) = +\infty,$$

we observe that the average transmitted power $\overline{P}$ becomes infinite for $\mu_1 > 0$ and the power allocation $P^{(1)}$ is infeasible for finite $\widetilde{P}$.

Then, proceeding according to the next step in Procedure 1, we choose

$$P^\star = \left[\frac{1}{\mu_1^\star \underline{g}_1 + \mu_0^\star} - \frac{\sigma_n^2}{\underline{\hat{h}}}\right]^+$$

for $\mu_0^\star > 0$. From the CS conditions, we obtain that in this case all the transmitted power budget is consumed by the power allocation $P^\star$, i.e. $\overline{P} = \widetilde{P}$. □

In contrast to Proposition 4, if the transmitted power budget $\widetilde{P}$ is infinitely large, then the TPC can be omitted in problems (5.2) and (5.6). The power allocation is hence given by

$$P^\star = \left[\frac{1}{\mu_1^\star \underline{g}_1} - \frac{\sigma_n^2}{\underline{\hat{h}}}\right]^+, \tag{5.46}$$

where $\mu_1^\star > 0$ is obtained from the numerical solution of (5.44).

We stress that the capacity in the special case of a single SR and without transmitted power constraint has been investigated in [74]. Our result for $K = 1$ coincides with the former result; see [74, Sec. III-C].

Equipped with Proposition 4, let us now study the asymptotic performance of C. We summarize our results in the following theorem.

Theorem 2. *Given a Rayleigh faded homogeneous system satisfying assumptions (A1)-(A3) and a fixed interference temperature threshold $\widetilde{Q} > 0$, the ergodic sum capacity C scales as $\ln\ln K$ for a large number of SR's K. This result holds even if the transmitted power budget $\widetilde{P}$ is infinitely large.*

Proof: The fact that $C|_{P=P_0}$ scales as $\ln\ln K$ for $K \to \infty$ can be straightforwardly deduced from the results of [46] [52] and [53], where it has been shown that in the case of a constant transmitted power, the sum capacity asymptotically scales as $\ln\ln K$. For the upper bound $C|_{U=1}$, which marks the ergodic sum capacity in the single PR case, we distinguish two cases. In the first one, we consider $\widetilde{P} < \infty$, i.e., the transmitted power budget is limited. In the second case, we assume infinitely large $\widetilde{P}$, such that TPC is always met with strict inequality. In the first case, the optimal power allocation scheme to achieve $C|_{U=1}$ is given by $P^\star = \left[\frac{1}{\mu_1^\star \underline{g}_1 + \mu_0^\star} - \frac{\sigma_n^2}{\underline{\hat{h}}}\right]^+$ with $\mu_0^\star > 0$ as shown in Proposition 4. We can further bound $C|_{U=1}$ from above by the ergodic sum capacity of the conventional BC channel with no PR present and fixed transmitted power $\widetilde{P}_0 = \frac{1}{\mu_0^\star} > P^\star$, given by $C|_{U=0,P=\widetilde{P}_0} = \mathrm{E}\left\{\ln\left(1 + \frac{\hat{h}}{\mu_0^\star \sigma_n^2}\right)\right\}$. Adopting the results of [46] [52] and [53], we can conclude that $C|_{U=0,P=\widetilde{P}_0}$ also increases as $\ln\ln K$ for $K \to \infty$. Hence, we have proven that for any fixed $\widetilde{P} < \infty$, the ergodic capacity C with $C|_{P=P_0} \leq C \leq C|_{U=0,P=\widetilde{P}_0}$ increases as $\ln\ln K$ for $K \to \infty$.

In the case of infinitely large $\widetilde{P}$, the results of [46] [52] and [53] cannot be used directly. In this case, we apply $P^\star$ in (5.46) to show that $C|_{U=1}$ asymptotically grows as $\ln\ln K + b$, where b is a constant independent of K. Note that, given the distribution $f_{\underline{h}_k}(x) = e^{-x}$, with $K \to \infty$, the limiting cdf of the random variable $\underline{\hat{h}} - \ln(K)$ exists and is given by [82]

$$F_{\underline{\hat{h}}-\ln(K)}(y) = \exp\left(-e^{-y}\right), \quad -\infty < y < \infty. \tag{5.47}$$

For any fixed $\widetilde{Q} > 0$, we can see from (5.44) that for large K, the Lagrange multiplier $\mu_1^\star$ asymptotically increases with K as the term $K(1 - e^{-y})^{K-1}$ decreases with K. In the

asymptotic case, the sum capacity $C|_{U=1}$ becomes

$$C|_{U=1} = \mathrm{E}\left\{\ln\left(1+\frac{\hat{\underline{h}}}{\sigma_n^2}\left[\frac{1}{\mu_1^\star \underline{g}_1}-\frac{\sigma_n^2}{\hat{\underline{h}}}\right]^+\right)\right\} \tag{5.48}$$

$$= \int_0^\infty\int_\eta^\infty \ln\left(y+\ln K\right)e^{-x-y}\exp\left(-e^{-y}\right)\,dy\,dx \tag{5.49}$$

$$- \int_0^\infty\int_\eta^\infty \ln\left(\mu_1^\star\sigma_n^2 x\right)e^{-x-y}\exp\left(-e^{-y}\right)\,dy\,dx,$$

where $\eta = \mu_1^\star\sigma_n^2 x - \ln K$. Let us define the two integrals in the above equation as

$$\mathcal{T}_I \triangleq \int_0^\infty\int_\eta^\infty \ln\left(y+\ln K\right)e^{-x-y}\exp\left(-e^{-y}\right)\,dy\,dx \tag{5.50}$$

$$\mathcal{T}_{II} \triangleq \int_0^\infty\int_\eta^\infty \ln\left(\mu_1^\star\sigma_n^2 x\right)e^{-x-y}\exp\left(-e^{-y}\right)\,dy\,dx. \tag{5.51}$$

Substituting $t = e^{-y}$ in (5.50) and letting $K \to \infty$, we find an upper bound on $\mathcal{T}_I$ as

$$\mathcal{T}_I = \int_0^\infty e^{-x}\int_0^{Ke^{-\mu_1^\star\sigma_n^2 x}} \ln\left(\ln K - \ln t\right)e^{-t}\,dt\;dx$$

$$\le \int_0^\infty e^{-x}\,dx\int_0^{Ke^{-1}} \ln\left(\ln K - \ln t\right)e^{-t}\,dt$$

$$\le \ln\left(\int_0^{Ke^{-1}}\left(\ln K - \ln t\right)e^{-t}\,dt\right) \simeq \ln\left(\ln K + \gamma_e\right), \tag{5.52}$$

where γ_e is the Euler's constant [98]. The first inequality in (5.52) follows from the fact that the integrand is positive for $0 < t \le Ke^{-1}$, and the second inequality in (5.52) is due to the Jensen's inequality

$$\mathrm{E}\left\{\ln\left(\ln(K)-\ln(t)\right)\right\} \le \ln\left(\mathrm{E}\left\{\ln(K)-\ln(t)\right\}\right) \tag{5.53}$$

for large K. The integral $\mathcal{T}_{II}$ defined in (5.51) can be bounded from below as

$$\mathcal{T}_{II} = \int_0^\infty \ln\left(\mu_1^\star\sigma_n^2 x\right)e^{-x}\left[1-\frac{1}{K}\exp\left(-e^{-\mu_1^\star\sigma_n^2 x}\right)\right]\,dx$$

$$\ge \int_0^{\frac{1}{\mu_1^\star\sigma_n^2}} \ln\left(\mu_1^\star\sigma_n^2 x\right)e^{-x}\left[1-\frac{1}{K}\exp\left(-e^{-\mu_1^\star\sigma_n^2 x}\right)\right]\,dx$$

$$\ge \int_0^{\frac{1}{\mu_1^\star\sigma_n^2}} \ln\left(\mu_1^\star\sigma_n^2 x\right)e^{-x}\,dx$$

$$\ge \int_0^{\frac{1}{c_0\sigma_n^2}} \ln\left(c_0\sigma_n^2 x\right)e^{-x}\,dx = -\left(\gamma_e + \ln\frac{1}{c_0\sigma_n^2}\right) + \mathrm{Ei}\left(-\frac{1}{c_0\sigma_n^2}\right), \tag{5.54}$$

where the first inequality in (5.54) follows from the fact that $\ln(\mu_1^\star\sigma_n^2 x) \geq 0$ for $x \geq 1/(\mu_1^\star\sigma_n^2)$. The second inequality stems from the inequalities $\left[1 - \frac{1}{K}\exp\left(-e^{-\mu_1^\star\sigma_n^2 x}\right)\right] \leq 1$ and $\ln(\mu_1^\star\sigma_n^2 x) \leq 0$, which hold for $0 \leq x \leq 1/(\mu_1^\star\sigma_n^2)$. Recall from (5.44) that the Lagrange multiplier $\mu_1^\star$ asymptotically increases with K. In the third inequality of (5.54), we use c_0 to denote the value of $\mu_1^\star$ for a fixed number of $K = K_0$. Then the third inequality holds for all $K \geq K_0$ since the last integral in (5.54) is an increasing function of c_0. Thus, we have

$$C|_{U=1} \;=\; \mathcal{T}_I - \mathcal{T}_{II} \leq \ln(\ln K + \gamma_e) + b, \tag{5.55}$$

where $b = \left(\gamma_e + \ln(\frac{1}{c_0\sigma_n^2})\right) - \mathrm{Ei}\left(-\frac{1}{c_0\sigma_n^2}\right)$ is a constant. Ignoring the Euler's constant γ_e, which in the limiting case is small compared to $\ln K$, we can conclude that C grows asymptotically as $\ln\ln K$ also in the case of infinitely large $\widetilde{P}$. □

Peak IPC's

Similar to the case of average IPC's, we derive upper and lower bounds to show the asymptotic behavior of the ergodic sum capacity C under the peak IPC's. With the assumptions (A1)-(A3), the pdf of $\underline{g}_m/\widehat{Q}$ for $m = 1, \cdots, U$ is given by $f_{\underline{g}_m/\widehat{Q}}(x) = \widehat{Q}\exp(-\widehat{Q}x)$. The pdf of G in (5.38) can then be derived as [82]

$$f_G(x) = U\widehat{Q}\left(1 - e^{-\widehat{Q}x}\right)^{U-1} e^{-\widehat{Q}x}$$

so that $\mathrm{E}\{G\} = \frac{U}{\widehat{Q}}\sum_{k=0}^{U-1}\binom{U-1}{k}\frac{(-1)^k}{(k+1)^2}$. Due to the singularity at $G = 0$, the expectation of $\frac{1}{G}$ in the Rayleigh fading case can be expressed in terms of the Cauchy principal value as

$$\mathrm{E}\left\{\frac{1}{G}\right\} = \lim_{\epsilon\to 0^+}\int_\epsilon^\infty \frac{1}{x} f_G(x)\,dx \tag{5.56}$$

$$= \lim_{\epsilon\to 0^+} U\widehat{Q}\sum_{k=0}^{U-1}\binom{U-1}{k}(-1)^{k+1}\mathrm{Ei}\left[-\widehat{Q}(k+1)\epsilon\right] \tag{5.57}$$

$$= \begin{cases} \lim_{\epsilon\to 0^+} -\widehat{Q}\mathrm{Ei}\left(-\widehat{Q}\epsilon\right) = \infty, & U = 1; \\ \widehat{Q}U\sum_{k=1}^{U-1}\binom{U-1}{k}(-1)^{k+1}\ln(k+1), & U \geq 2. \end{cases}$$

Let us first consider the case of $U \geq 2$. If the power budget is sufficiently large such that $\mathrm{E}\left\{\frac{1}{G}\right\} \leq \widetilde{P}$, then C is given by (5.40). Making use of Jensen's inequality, we find the

following upper and lower bounds

$$C \leq \mathrm{E}_{\underline{\hat{h}}}\left\{\ln\left(1+\frac{\underline{\hat{h}}}{\sigma_n^2}\mathrm{E}\left\{\frac{1}{G}\right\}\right)\right\} \tag{5.58}$$

$$C \geq \mathrm{E}_{\underline{\hat{h}}}\left\{\ln\left(1+\frac{\underline{\hat{h}}}{\sigma_n^2}\frac{1}{\mathrm{E}\{G\}}\right)\right\}, \tag{5.59}$$

where $\mathrm{E}\left\{\frac{1}{G}\right\}$ and $\frac{1}{\mathrm{E}\{G\}}$ are both positive constants. Applying the result of [46, eqn. (9)], where it has been shown that

$$\mathrm{E}_{\underline{\hat{h}}}\left\{\ln\left(1+\rho\underline{\hat{h}}\right)\right\}$$

with some constant $\rho > 0$ asymptotically grows as $\ln\ln K$, we can conclude that both the upper and lower bounds (and, hence, C) increase as $\ln\ln K$ at large K.

In the case of $U \geq 2$ and small power budget $\widetilde{P} < \mathrm{E}\left\{\frac{1}{G}\right\}$, the ergodic sum capacity C given in (5.41) has the same upper bound as in (5.58) since $P^\star = \min\left\{\frac{1}{G}, \left[\frac{1}{\mu_0^\star} - \frac{\sigma_n^2}{\underline{\hat{h}}}\right]^+\right\} \leq \frac{1}{G}$. A lower bound for C can be found by using a feasible but suboptimal power allocation scheme $P = \min\left\{\widetilde{P}, \frac{1}{G}\right\}$, for which the corresponding ergodic sum capacity C can be lower bounded as

$$\begin{aligned} C &\geq \mathrm{E}\left\{\ln\left(1+\frac{\underline{\hat{h}}}{\sigma_n^2}\min\left\{\widetilde{P}, \frac{1}{G}\right\}\right)\right\} && (5.60)\\ &\geq F_G\left(1/\widetilde{P}\right)\int_0^\infty \ln\left(1+\frac{x}{\sigma_n^2}\widetilde{P}\right) f_{\underline{\hat{h}}}(x)\,dx \\ &\quad + \left[1-F_G\left(1/\widetilde{P}\right)\right]\int_0^\infty \ln\left(1+\frac{x}{\sigma_n^2\mathrm{E}\left\{\widetilde{G}\right\}}\right) f_{\underline{\hat{h}}}(x)\,dx, && (5.61)\end{aligned}$$

where $F_G(x)$ is the cdf of G, the second inequality follows from the Jensen's inequality, and

$$\mathrm{E}\left\{\widetilde{G}\right\} = \int_{1/\widetilde{P}}^\infty \frac{x f_G(x)}{1-F_G\left(1/\widetilde{P}\right)}\,dx$$

describes the statistical expectation of the truncated distribution of G defined on the interval $\left[1/\widetilde{P}, \infty\right]$. As both integrals in (5.61) asymptotically grow with $\ln\ln K$ [52]-[46], this lower bound and, hence, C also increase as $\ln\ln K$ for large K.

Next, let us consider the case of $U = 1$. The ergodic sum capacity C is given by (5.41) for any fixed $\widetilde{P} < \infty$, since $\mathrm{E}\left\{\frac{1}{G}\right\} \to \infty$, and we have $\widetilde{P} < \mathrm{E}\left\{\frac{1}{G}\right\}$. In this case, the lower

bound defined in (5.60) still applies. For fixed $\widetilde{P}$, an upper bound of C is given by

$$C \leq \mathrm{E}\left\{\ln\left(1+\frac{\hat{\underline{h}}}{\sigma_n^2\mu_0^\star}\right)\right\} \tag{5.62}$$

as the optimally power allocation can be bounded from above as

$$P^\star = \min\left\{\frac{1}{G}, \left[\frac{1}{\mu_0^\star} - \frac{\sigma_n^2}{\hat{\underline{h}}}\right]^+\right\} \leq \frac{1}{\mu_0^\star}$$

for any $\mu_0^\star > 0$. This upper bound on the capacity increases as $\ln\ln K$ according to [46, eqn. (9)]. Hence, C asymptotically grows as $\ln\ln K$ for any fixed $\widetilde{P} < \infty$.

If the transmitted power budget $\widetilde{P}$ is infinitely large such that the TPC can be omitted, we have $P^\star = \frac{1}{G}$ and the lower bound (5.59) still applies. However, the upper bound (5.58) is not valid here since $\mathrm{E}\left\{\frac{1}{G}\right\} \to \infty$ for $U = 1$. A valid upper bound for C, which asymptotically grows as $\ln\ln K$, can be derived as

$$\begin{aligned} C &= \mathrm{E}\left\{\ln\left(\sigma_n^2 G + \hat{\underline{h}}\right) - \ln\left(\sigma_n^2 G\right)\right\} \\ &\leq \mathrm{E}_{\hat{\underline{h}}}\left\{\ln\left(\sigma_n^2 \mathrm{E}\left\{G\right\} + \hat{\underline{h}}\right)\right\} + \gamma_e + \ln\left(\frac{\widehat{Q}}{\sigma_n^2}\right), \end{aligned} \tag{5.63}$$

where the inequality in the last line of (5.63) follows from the Jensen's inequality. Applying the upper and lower bounds obtained in this subsection, we can finally conclude that C under the peak IPC also scales as $\ln\ln K$ for $K \to \infty$, even if $\widetilde{P}$ is infinitely large.

5.4.2 Asymptotic Capacity for a Large Number of PR's

Note that the number of IPC's increases with U while the objective functions in the capacity maximization problems (5.2), (5.6) and (5.27) are independent of U. Thus, the ergodic sum capacity is expected to be a non-increasing function of U in this asymptotic regime. We are interested in the asymptotic limits of C as $U \to \infty$.

Average IPC's

In the assumed homogeneous system, the U IPC's in problem (5.6) are symmetric, which means that all U IPC's are identical up to the ordering of the i.i.d. random channel power

gains $\underline{g}_m$ for $m = 1, \cdots, U$. Hence, in the sequel, we use $\mathrm{E}\{\underline{g}\}$ to denote their expectations. If $\widetilde{P} < \frac{\widetilde{Q}}{\mathrm{E}\{\underline{g}\}}$, then it follows from Corollary 1 that all PR's can be omitted in the capacity analysis and the optimal power allocation scheme is given by the conventional water-filling solution. In this case, the ergodic sum capacity is given by

$$C = \int_0^\infty \ln\left(1 + \frac{y}{\sigma_n^2}\left[\frac{1}{\lambda_0} - \frac{\sigma_n^2}{y}\right]^+\right) f_{\underline{\hat{h}}}(y)\, dy, \tag{5.64}$$

where λ_0 solves the equation $\widetilde{P} = \int_0^\infty \left[\frac{1}{\lambda_0} - \frac{\sigma_n^2}{y}\right]^+ f_{\underline{\hat{h}}}(y)\, dy$. Obviously, C in (5.64) remains constant as U increases. In the case of $\widetilde{P} \geq \frac{\widetilde{Q}}{\mathrm{E}\{\underline{g}\}}$, the optimal power allocation scheme $P^\star$ becomes

$$P^\star = \left[\frac{1}{\mu^\star \sum_{m=1}^U \underline{g}_m + \mu_0^\star} - \frac{\sigma_n^2}{\underline{\hat{h}}}\right]^+, \tag{5.65}$$

where $\mu_m^\star = \mu^\star$ for all $m = 1, \cdots, U$ due to the symmetry of the homogeneous system. Defining a new random variable as $S = \sum_{m=1}^U \underline{g}_m$ and summing up the IPC's in (5.6c) for $m = 1, \cdots, U$, we obtain an equivalent IPC which depends on the new random variable S

$$U\overline{Q} \triangleq \int_0^\infty \int_0^\infty x\left[\frac{1}{\mu^\star x + \mu_0^\star} - \frac{\sigma_n^2}{y}\right]^+ f_S(x) f_{\underline{\hat{h}}}(y)\, dx\, dy = U\widetilde{Q}, \tag{5.66}$$

where $\overline{Q}$ is the induced interference temperature at each PR and $f_S(x)$ is the pdf corresponding to S. Note that in this case ($\widetilde{P} \geq \widetilde{Q}/\mathrm{E}\{\underline{g}\}$) the equality $\overline{Q} = \widetilde{Q}$ holds according to Corollary 1. With (5.65), the ergodic sum capacity and the average TPC are given by

$$C = \mathrm{E}\left\{\ln\left(1 + \frac{\underline{\hat{h}}}{\sigma_n^2}\left[\frac{1}{\mu^\star S + \mu_0^\star} - \frac{\sigma_n^2}{\underline{\hat{h}}}\right]^+\right)\right\} \tag{5.67}$$

and

$$\overline{P} \triangleq \int_0^\infty \int_0^\infty \left[\frac{1}{\mu^\star x + \mu_0^\star} - \frac{\sigma_n^2}{y}\right]^+ f_S(x) f_{\underline{\hat{h}}}(y)\, dx\, dy \leq \widetilde{P}, \tag{5.68}$$

respectively. From the CLT, the distribution of $(S - U\mathrm{E}\{\underline{g}\})/(\sqrt{U}\sigma_g)$ approaches the standard normal distribution for large U, i.e.,

$$X = \frac{S - U\mathrm{E}\{\underline{g}\}}{\sqrt{U}\sigma_{\underline{g}}} \xrightarrow{d} \mathcal{N}(0, 1), \tag{5.69}$$

where $\sigma_{\underline{g}}$ is the standard deviation of $\underline{g}_m$ $(m = 1, \cdots, U)$. With (5.69), the equivalent IPC in (5.66) can be rewritten as

$$\begin{aligned}\frac{\widetilde{Q}}{\mathrm{E}\{\underline{g}\}} &= \int_0^{\infty}\int_{-\frac{\mathrm{E}\{\underline{g}\}\sqrt{U}}{\sigma_{\underline{g}}}}^{\infty}\left[\frac{1}{U\mu^{\star}\mathrm{E}\{\underline{g}\}+\frac{\mu_0^{\star}}{\frac{\sigma_{\underline{g}}x}{\mathrm{E}\{\underline{g}\}\sqrt{U}}+1}}-\frac{\sigma_n^2\left(\frac{\sigma_{\underline{g}}x}{\mathrm{E}\{\underline{g}\}\sqrt{U}}+1\right)}{y}\right]^{+}\phi(x)\,dx\,f_{\underline{\hat{h}}}(y)\,dy,\\ &\simeq \mathrm{E}_{\underline{\hat{h}}}\left\{\int_{-U^{\frac{1}{3}}}^{U^{\frac{1}{3}}}\left[\frac{1}{U\mu^{\star}\mathrm{E}\{\underline{g}\}+\mu_0^{\star}}-\frac{\sigma_n^2}{\underline{\hat{h}}}\right]^{+}\phi(x)\,dx\right\}\\ &\simeq \mathrm{E}_{\underline{\hat{h}}}\left\{\left[\frac{1}{U\mu^{\star}\mathrm{E}\{\underline{g}\}+\mu_0^{\star}}-\frac{\sigma_n^2}{\underline{\hat{h}}}\right]^{+}\right\}, \end{aligned} \tag{5.70}$$

where $\phi(x)$ is the pdf of the standard Gaussian distribution. The approximations hold for large values of U since $\phi(x) \simeq 0$ for $x < -U^{\frac{1}{3}}$ or $x > U^{\frac{1}{3}}$ and $\frac{\sigma_{\underline{g}}x}{\mathrm{E}\{\underline{g}\}\sqrt{U}} + 1 \simeq 1$ for $-U^{\frac{1}{3}} \leq x \leq U^{\frac{1}{3}}$. The approximation errors in (5.70) approach 0 as $U \to \infty$. Defining $\lambda_0^{\star} = U\mu^{\star}\mathrm{E}\{\underline{g}\} + \mu_0^{\star}$, we can rewrite the equivalent IPC in (5.66) as

$$\frac{\widetilde{Q}}{\mathrm{E}\{\underline{g}\}} \simeq \int_0^{\infty}\left[\frac{1}{\lambda_0^{\star}}-\frac{\sigma_n^2}{y}\right]^{+} f_{\underline{\hat{h}}}(y)\,dy, \tag{5.71}$$

where the value of $\lambda_0^{\star}$ can be obtained by solving (5.71) numerically. Similarly, for $U \to \infty$, the TPC (5.68) can be rewritten as

$$\begin{aligned}\overline{P} &= \mathrm{E}\left\{\left[\frac{1}{\mu^{\star}\left(\sqrt{U}\sigma_{\underline{g}}X + U\mathrm{E}\left\{\underline{g}\right\}\right)+\mu_0^{\star}}-\frac{\sigma_n^2}{\underline{\hat{h}}}\right]^{+}\right\}\\ &\simeq \int_0^{\infty}\left[\frac{1}{\lambda_0^{\star}}-\frac{\sigma_n^2}{y}\right]^{+} f_{\underline{\hat{h}}}(y)\,dy \leq \widetilde{P}. \end{aligned} \tag{5.72}$$

The ergodic sum capacity becomes

$$C \simeq \int_0^{\infty}\ln\left(1+\frac{y}{\sigma_n^2}\left[\frac{1}{\lambda_0^{\star}}-\frac{\sigma_n^2}{y}\right]^{+}\right) f_{\underline{\hat{h}}}(y)\,dy, \tag{5.73}$$

for $U \to \infty$. From (5.71)-(5.73), we can see that for $\widetilde{P} \geq \frac{\widetilde{Q}}{\mathrm{E}\{\underline{g}\}}$ and $U \to \infty$, the ergodic sum capacity approaches that of the conventional BC channel with the average transmitted power $\frac{\widetilde{Q}}{\mathrm{E}\{\underline{g}\}}$. The optimal power allocation scheme asymptotically becomes $P^{\star} = \left[\frac{1}{\lambda_0^{\star}} - \frac{\sigma_n^2}{\underline{\hat{h}}}\right]^{+}$, where $\lambda_0^{\star}$ solves the equation (5.71). It should be noted that the analysis in this subsection is based on the homogeneity assumptions (A1) and (A3). The Rayleigh fading assumption (A2) is not needed to derive the asymptotic capacity limits. Hence, the above asymptotic analysis is also valid for other types of fading.

Peak IPC's

Let us now consider the asymptotic behavior of the ergodic sum capacity under the assumptions (A1)-(A3). Using Jensen's inequality, an upper bound on (5.40) can be obtained similar to (5.58) as

$$C \leq \mathrm{E}_{\hat{\underline{g}}} \left\{ \ln \left(1 + \frac{a}{\hat{\underline{g}}} \right) \right\} \tag{5.74}$$

where $a = \widehat{Q}\mathrm{E}\{\hat{\underline{h}}\}/\sigma_n^2$ is a constant and $\hat{\underline{g}} = \max_{m=1,\cdots,U} \underline{g}_m$. As U increases, $X = \hat{\underline{g}} - \ln U$ has a limiting distribution whose cdf is given by $F_X(x) = \exp\left(-e^{-x}\right)$ for $-\infty < x < \infty$. The probability that $|X| < (\ln U)^{\frac{1}{2}}$ for a large value of U can be expressed as

$$\begin{aligned} & \Pr\left(|X| \leq (\ln U)^{\frac{1}{2}} \right) \\ = \; & F_X\left((\ln U)^{\frac{1}{2}} \right) - F_X\left(-(\ln U)^{\frac{1}{2}} \right) \\ \simeq \; & 1 \text{ for } U \to \infty. \end{aligned} \tag{5.75}$$

(5.75) states that $\ln U - (\ln U)^{\frac{1}{2}} \leq \hat{\underline{g}} \leq \ln U + (\ln U)^{\frac{1}{2}}$ almost sure as $U \to \infty$. Since $(\ln U)^{\frac{1}{2}} \ll \ln U$ for $U \to \infty$, the upper bound (5.74) asymptotically scales as

$$\tilde{C} = \ln\left(1 + \frac{a}{\ln U} \right). \tag{5.76}$$

Thus, both $\tilde{C}$ and C asymptotically converge to 0 as $U \to \infty$.

5.5 Numerical Results

In this section, we provide numerical results on the sum capacity. For the sake of computational simplicity, we consider only the homogeneous Rayleigh fading case of Section 5.4.

5.5.1 Comparison of Average and Ergodic Sum Capacity

The sum capacity $\overline{C}_s$ averaged over a finite number of N fading states has been investigated in Sections 5.2.1 and 5.3.1 under the average and peak IPC's, respectively. In Figs. 5.2-5.5, $\overline{C}_s$ in the case of $N = 100$ and $N = 1000$ is compared with the ergodic sum capacity C.

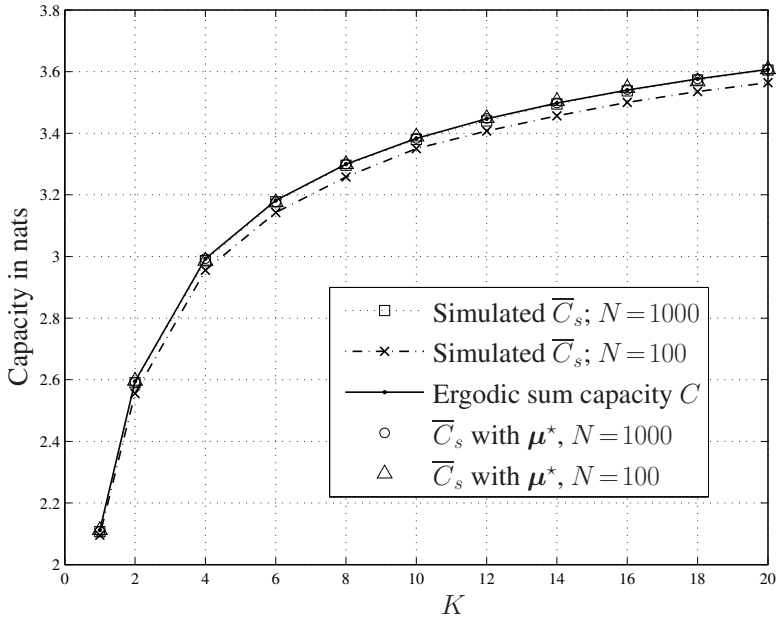

Figure 5.2: $\overline{C}_s$ and C vs. K with average IPC's, $U = 10$, $\widetilde{P} = 20$ dB and $\widetilde{Q} = 10$ dB.

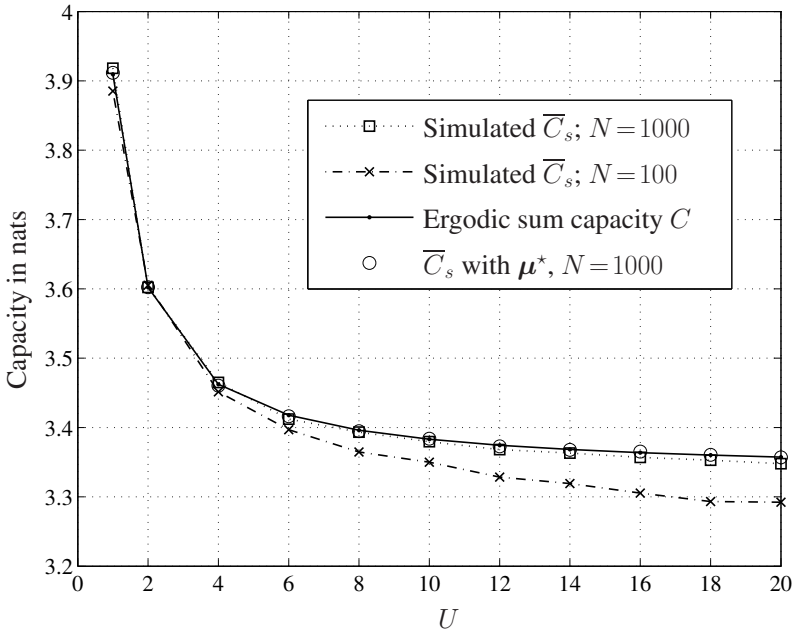

Figure 5.3: $\overline{C}_s$ and C vs. U with average IPC's, where $K = 10$, $\widetilde{P} = 20$ dB and $\widetilde{Q} = 10$ dB.

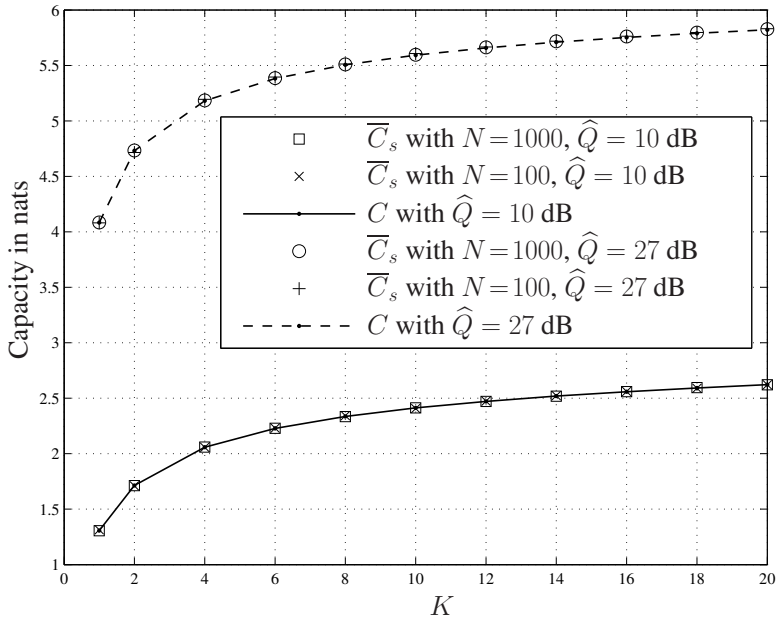

Figure 5.4: $\overline{C}_s$ and C vs. K with peak IPC's, $U = 10$ and $\widetilde{P} = 20$ dB.

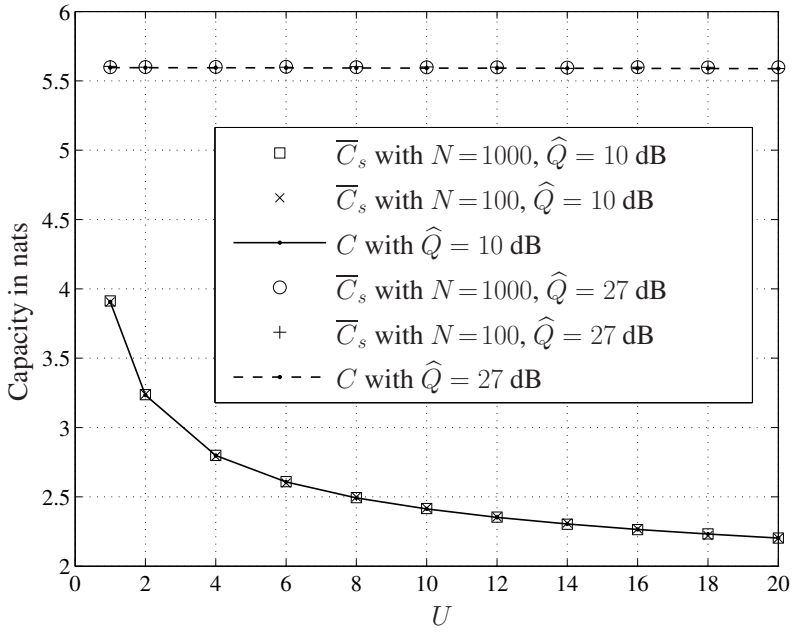

Figure 5.5: $\overline{C}_s$ and C vs. U with peak IPC's, $K = 10$ and $\widetilde{P} = 20$ dB.

A total of 100 Monte Carlo simulations are carried out and the average values of $\overline{C}_s$ are plotted. In each Monte Carlo simulation, the power gains $\underline{h}_{k,i}$ and $\underline{g}_{m,i}$ for $k = 1, \cdots, K$, $m = 1, \cdots, U$ and $i = 1, \cdots, N$ are randomly generated and the value of $\overline{C}_s$ is computed by solving problems (5.2) and (5.27) using CVX [95].

Figs. 5.2 and 5.3 demonstrate the sum capacity under the average IPC's, where the capacity values are displayed versus K and U, respectively. It can be seen from these figures that, as N increases, the values of simulated $\overline{C}_s$ approach that of C. In the case of $N = 1000$, the value of the simulated average sum capacity $\overline{C}_s$ nearly coincides with C. This observation confirms that $\overline{C}_s$ asymptotically converges to C as $N \to \infty$. To simplify the comparison, we have also computed the values of $\overline{C}_s$ using the power allocation scheme $P^\star$ given by (5.5), where the Lagrange multipliers are predetermined as in Section 5.2.2 to maximize the ergodic sum capacity C. The curves corresponding to the so-obtained $\overline{C}_s$ are labeled as "$\overline{C}_s$ with $\boldsymbol{\mu}^\star$". In both figures, the values of $\overline{C}_s$ with predetermined $\boldsymbol{\mu}^\star$ are very close to the computed ergodic capacity C. It should be also noted that, given the Lagrange multipliers, the power allocation $P^\star$ in (5.5) depends solely on the current channel gains. Hence, using the predetermined $\boldsymbol{\mu}^\star$, we can achieve the ergodic sum capacity C avoiding the requirement of non-causal channel state information in the time domain. At last, it can be readily verified from the Figs. 5.2 and 5.3 that the sum capacity increases with K and decreases with U, as intuitively expected.

The sum capacity under peak IPC's is illustrated in Figs. 5.4 and 5.5 versus K and U, respectively. In both figures, the average sum capacity $\overline{C}_s$ corresponds very well to the computed ergodic sum capacity C. We consider two cases with $\widehat{Q} = 10$ dB and $\widehat{Q} = 27$ dB. In the first case, we have $\mathrm{E}\left\{\frac{1}{G}\right\} < \widetilde{P} = 20$ dB for $2 \leq U \leq 20$ and $\mathrm{E}\left\{\frac{1}{G}\right\} > \widetilde{P}$ dB for $U = 1$. The ergodic sum capacity is, therefore, given by (5.40) for $2 \leq U \leq 20$ and (5.41) for $U = 1$. As follows from Fig. 5.4 and 5.5, the sum capacity increases with K and decreases with U in this case. In the second case, we have $\mathrm{E}\left\{\frac{1}{G}\right\} > \widetilde{P} = 20$ dB for $1 \leq U \leq 20$ and the ergodic sum capacity is given by (5.41) for all $U = 1, \cdots, 20$. As can be observed from in Fig. 5.4, C still increases with K in this case. In Fig. 5.5, however, C becomes nearly constant with increasing U. This effect can be explained by the fact that in

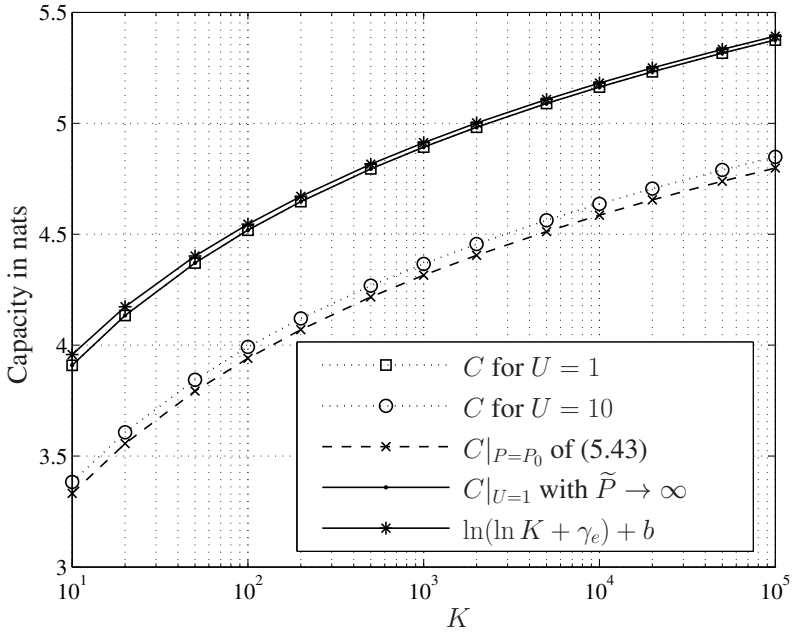

Figure 5.6: Asymptotic behavior of C with average IPC's and $\widetilde{Q} = 10$ dB.

this case the capacity C is limited mainly by the transmitted power $\overline{P} = \widetilde{P}$ and it decreases rather slowly with increasing U. In the next subsection, we will present more numerical results on the asymptotic behavior of C.

5.5.2 Asymptotic Performance of Ergodic Sum Capacity

Fig. 5.6 shows the asymptotic behavior of C under the average IPC's, where $K \to \infty$ and U is fixed. C is numerically computed with $\widetilde{P} = 20$ dB for $U = 1$ and $U = 10$, respectively. The upper bound $C|_{U=1}$ in (5.43) is derived for $\widetilde{P} \to \infty$. The function $\ln(\ln K + \gamma_e) + b$ in (5.55) is also depicted in the figure where b is computed with $K_0 = 100$. As K increases, all curves demonstrate the same asymptotic increasing rate. This observation confirms our theoretical result that C scales as $\ln \ln K$ with $K \to \infty$.

The asymptotic behavior of C under the peak IPC's is plotted in Fig. 5.7, where $K \to \infty$ and U is fixed. As can be seen from in Fig. 5.7, the ergodic sum capacity C and all its upper and lower bounds scale as $\ln \ln K$ for large values of K.

Figs. 5.8 and 5.9 correspond to the asymptotic regime of fixed K and $U \to \infty$. In

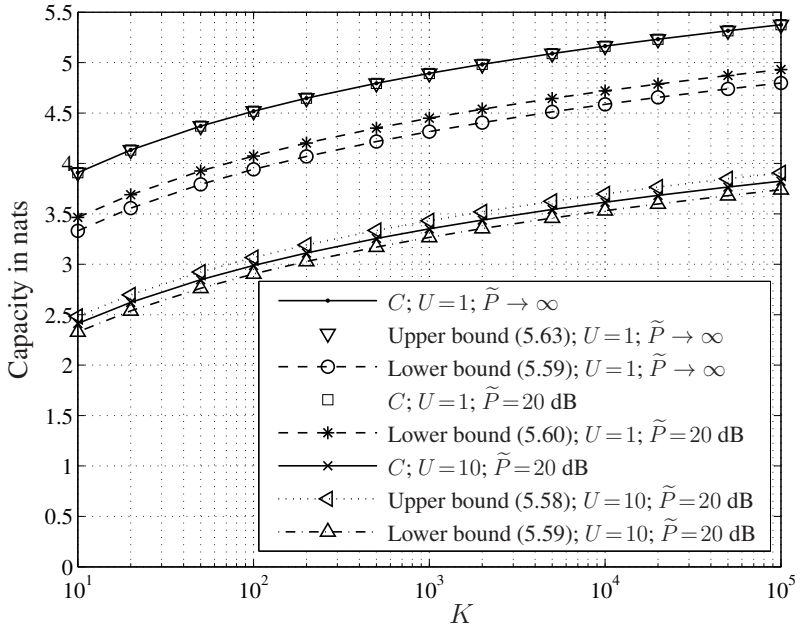

Figure 5.7: Asymptotic behavior of C with peak IPC's and $\widehat{Q} = 10$ dB.

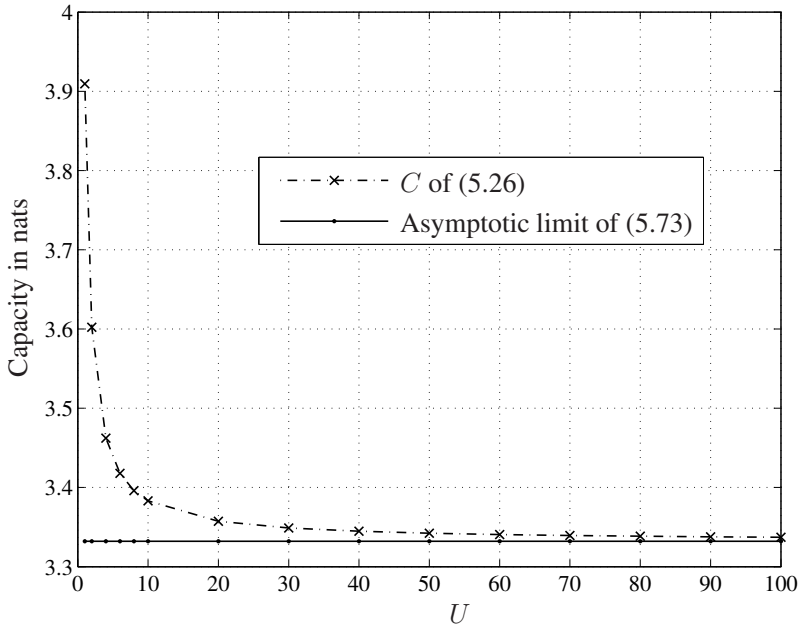

Figure 5.8: Asymptotic behavior of C with average IPC's, $K = 10$, $\widetilde{P} = 20$ dB and $\widetilde{Q} = 10$ dB.

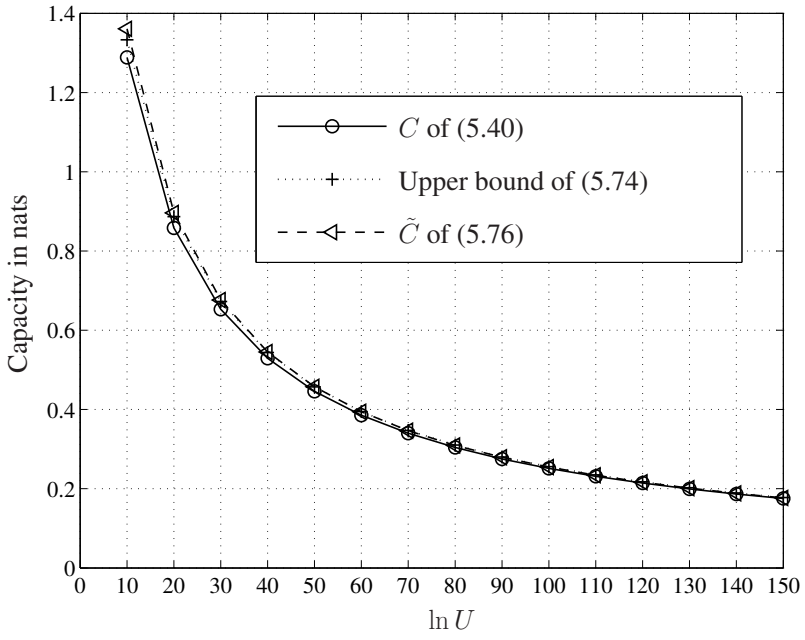

Figure 5.9: Asymptotic behavior of C with peak IPC's, $K = 10$, $\widetilde{P} = 20$ dB and $\widehat{Q} = 10$ dB.

Fig. 5.8, the ergodic sum capacity C under the average IPC's is depicted. It follows from this figure that, as U increases, C asymptotically approaches the limiting value given by (5.73). In Fig. 5.9, the capacity C under the peak IPC's is plotted versus $\ln U$. The upper bound of (5.74) and $\tilde{C}$ given by (5.76) are also shown in this figure. As can be observed from Fig. 5.9, all three curves coincide and approach 0 as $\ln U$ increases. This confirms our theoretical result that C decreases to 0 as fast as $\tilde{C} = \ln\left(1 + \frac{a}{\ln U}\right)$ for $U \to \infty$ and fixed K.

5.6 Chapter Summary

In an underlay CR BC channel, we have investigated the fundamental performance limits of the opportunistic scheduling in terms of the channel capacity. Our study in this chapter shows the potential gain obtainable by applying opportunistic scheduling in CR. The asymptotic performance of the channel capacity has illustrated the gain from multiuser diversity and provided the comparable benchmarks for the future work. In particular, we have shown that

the same asymptotic gain provided by multiuser diversity, $\ln \ln K$, can be achieved in a CR network where extra IPCs apply to the STs.

Chapter 6

Multiuser Diversity in Cognitive Radio System II: SER Performance

While the performance of CR has been extensively studied in terms of its spectral efficiency, less work has been done to quantify its link reliability performance. The objective of this chapter is to further analyze the underlay CR network considered in Chapter 5 in terms of its SER performance, where an opportunistic scheduler exploiting multiuser diversity is responsible for user selection. As an extension of the study presented in Chapter 4, we will derive analytical SER expressions for a cognitive network with K secondary users. For simplicity, we consider the case of single primary user ($U = 1$) in this chapter.

6.1 Analysis of SER Performance

In the considered downlink scenario with opportunistic scheduling, the ST exclusively transmits signals to the SR with the highest instantaneous channel gain. We assume a homogeneous system similar to that considered in Chapter 4, namely, the noise n_k has zero mean and variances σ_n^2 for all $k = 1, \ldots, K$ and the channel coefficients $h_k (k = 1, \ldots, K)$ are assumed to be i.i.d. circular complex Gaussian random variables with zero mean and unit variance.

In the considered underlay CR system, the PR is protected by the mandatory requirement

that the interference power caused by the ST is below a given threshold value $\widehat{Q}$ for all fading states. According to (2.1) and (2.2), we have

$$P|g|^2 \leq \widehat{Q}, \tag{6.1}$$

where P denotes the transmitted power in a fading state and we have omitted the subscripts i, l and the time index t as $i = l = 1$ in this chapter. Further, it is assumed that P is limited by a predefined power threshold $\widehat{P}$, i.e., the following peak TPC

$$P \leq \widehat{P}. \tag{6.2}$$

Given a fixed value of P, the SER of the signal modulated by the $\mathcal{K}$-PSK can be computed by (2.11) and (2.12). The received ISNR of the scheduled receiver is given by[1] $\gamma_{[1]}$, where $\gamma_{[1]}$ and its pdf $f_{\gamma_{[1]}}(x)$ are defined as in Section 4.2.1. Inserting $f_{\gamma_{[1]}}(x)$ into (2.11) and substituting the obtained MGF into (2.12), the average SER for $\mathcal{K}$-PSK modulation can be computed as

$$\mathrm{SER}(P) = K\sum_{k=0}^{K-1}\frac{(-1)^k\binom{K-1}{k}}{k+1}\left[\frac{(\mathcal{K}-1)}{\mathcal{K}} - \frac{1}{\pi}\sqrt{\frac{a^2P}{\sigma_n^2(k+1)+a^2P}}\left(\frac{\pi}{2}+\tan^{-1}(b)\right)\right], \tag{6.3}$$

where a is defined as in (2.12) and $b = \sqrt{\frac{a^2P}{\sigma_n^2(k+1)+a^2P}}\cot\frac{\pi}{\mathcal{K}}$.

In an underlay CR system, the ST needs to adjust the transmitted power P to meet the constraints (6.1) and (6.2). Depending on the instantaneous channel realizations, the ST must adjust its transmitted power P to minimize the average SER while fulfilling the power constraints (6.1) and (6.2). This can be expressed as the following optimization problem

$$\overline{\mathrm{SER}} = \min_{P\geq 0}\int_0^\infty \mathrm{SER}\,(P)\; f_{|g|^2}(x)dx \tag{6.4}$$

$$\text{s.t.}\quad P|g|^2 \leq \widehat{Q};\; P \leq \widehat{P}, \tag{6.5}$$

where $\overline{\mathrm{SER}}$ denotes the SER averaged over all fading states and the function $f_{|g|^2}(x) = \sigma_g^2\exp\left(-\sigma_g^2 x\right)$ is the pdf of the power gain $|g|^2$ with σ_g^2 representing the variance of $|g|$. It can be easily shown that the $\mathrm{SER}\,(P)$ in (6.3) are a monotonically decreasing function of P.

[1] Subscript i and time index t in (2.1) will be omitted in the sequel.

This means that the SER is reduced if we increase the transmitted power P. From constraints (6.1) and (6.2), the maximal allowed transmitted power at a given time instance is given by

$$P^* = \min\left\{\widehat{P}, \frac{\widehat{Q}}{|g|^2}\right\}. \tag{6.6}$$

Substituting (6.6) for P in (6.3) and then inserting (6.3) in (6.4), the resulting average SER can be expressed as

$$\begin{aligned}
\overline{\mathrm{SER}} &= \int_0^{\frac{\widehat{Q}}{\widehat{P}}} \mathrm{SER}\left(\widehat{P}\right) f_{|g|^2}(x)dx + \int_{\frac{\widehat{Q}}{\widehat{P}}}^{\infty} \mathrm{SER}\left(\frac{\widehat{Q}}{x}\right) f_{|g|^2}(x)dx \\
&= K\sum_{k=0}^{K-1} \frac{(-1)^k \binom{K-1}{k}}{k+1} \left\{\left(1-e^{-\frac{\sigma_g^2\widehat{Q}}{\widehat{P}}}\right)\right. \\
&\quad \cdot \left[\frac{\mathcal{K}-1}{\mathcal{K}} - \frac{1}{\pi}\sqrt{\frac{a^2\widehat{P}}{\sigma_n^2(k+1)+a^2\widehat{P}}}\left(\frac{\pi}{2}+\tan^{-1}\left(\sqrt{\frac{a^2\widehat{P}}{\sigma_n^2(k+1)+a^2\widehat{P}}}\cot\frac{\pi}{\mathcal{K}}\right)\right)\right] \\
&\quad + \int_{\frac{\widehat{Q}}{\widehat{P}}}^{\infty} \sigma_g^2 e^{-\sigma_g^2 x}\left[\frac{\mathcal{K}-1}{\mathcal{K}} - \frac{1}{\pi}\sqrt{\frac{a^2\widehat{Q}}{\sigma_n^2 x(k+1)+a^2\widehat{Q}}}\right. \\
&\quad \left.\left.\cdot\left(\frac{\pi}{2}+\tan^{-1}\left(\sqrt{\frac{a^2\widehat{Q}}{\sigma_n^2 x(k+1)+a^2\widehat{Q}}}\cot\frac{\pi}{\mathcal{K}}\right)\right)\right] dx\right\}.
\end{aligned} \tag{6.7}$$

In the specific case of BPSK and QPSK modulations, we can simplify the expression of $\overline{\mathrm{SER}}$ by inserting $\mathcal{K}=2$ and $\mathcal{K}=4$ into (6.7), respectively. In the following two subsections, we present the obtained SER expressions for these specific modulation types.

6.1.1 The Case of BPSK Modulation

For $\mathcal{K}=2$, the integral in (6.7) can be expressed as

$$I = \int_{\widehat{Q}/\widehat{P}}^{\infty} \sigma_g^2 e^{-\sigma_g^2 x}\, dx - \int_{\widehat{Q}/\widehat{P}}^{\infty} \sigma_g^2 e^{-\sigma_g^2 x}\sqrt{\frac{\widehat{Q}}{\widehat{Q}+\sigma_n^2 x(k+1)}}\, dx. \tag{6.8}$$

The first integral in (6.8) can be computed as

$$\int_{\widehat{Q}/\widehat{P}}^{\infty} \sigma_g^2 e^{-\sigma_g^2 x} dx = e^{-\frac{\sigma_g^2\widehat{Q}}{\widehat{P}}}, \tag{6.9}$$

and the second integral in (6.8) becomes [98]

$$\int_{\frac{\widehat{Q}}{\widehat{P}}}^{\infty} \sigma_g^2 e^{-\sigma_g^2 x} \sqrt{\frac{\widehat{Q}}{\widehat{Q}+\sigma_n^2 x(k+1)}}dx = \sqrt{\frac{\sigma_g^2\widehat{Q}\pi}{\sigma_n^2(1+k)}}\, e^{\frac{\sigma_g^2\widehat{Q}}{\sigma_n^2(1+k)}} \mathrm{erfc}\left(\sqrt{\frac{\sigma_g^2\widehat{Q}}{\widehat{P}}+\frac{\sigma_g^2\widehat{Q}}{\sigma_n^2(1+k)}}\right), \tag{6.10}$$

where $\mathrm{erfc}(x) = \frac{2}{\sqrt{\pi}}\int_x^{\infty} e^{-t^2}dt$ is the complementary error function.

Inserting (6.8)-(6.10) and $\mathcal{K}=2$ in (6.7), the analytical expression of the average SER for the BPSK modulation can be written as

$$\begin{aligned}\overline{\mathrm{SER}} = \frac{K}{2}\sum_{k=0}^{K-1}\frac{(-1)^k\binom{K-1}{k}}{k+1}\Bigg[1-\sqrt{\frac{\widehat{P}}{\widehat{P}+\sigma_n^2(k+1)}}\left(1-e^{-\frac{\sigma_g^2\widehat{Q}}{\widehat{P}}}\right)\\ -\sqrt{\frac{\sigma_g^2\pi\widehat{Q}}{\sigma_n^2(1+k)}}e^{\frac{\sigma_g^2\widehat{Q}}{\sigma_n^2(1+k)}}\,\mathrm{erfc}\left(\sqrt{\frac{\sigma_g^2\widehat{Q}}{\widehat{P}}+\frac{\sigma_g^2\widehat{Q}}{\sigma_n^2(1+k)}}\right)\Bigg].\end{aligned} \tag{6.11}$$

6.1.2 The Case of QPSK Modulation

Inserting $\mathcal{K}=4$ in (6.7), the analytical expression of the average SER for the QPSK modulation can be simplified as

$$\begin{aligned}\overline{\mathrm{SER}} = \frac{3K}{4}\sum_{k=0}^{K-1}\frac{(-1)^k\binom{K-1}{k}}{k+1}\\ \cdot\Bigg\{\left(1-e^{-\frac{\sigma_g^2\widehat{Q}}{\widehat{P}}}\right)\left[1-\frac{4}{3\pi}\sqrt{\frac{\widehat{P}}{2\sigma_n^2(k+1)+\widehat{P}}}\left(\frac{\pi}{2}+\tan^{-1}\left(\sqrt{\frac{\widehat{P}}{2\sigma_n^2(k+1)+\widehat{P}}}\right)\right)\right]\\ +\int_{\widehat{Q}/\widehat{P}}^{\infty}\sigma_g^2 e^{-\sigma_g^2 x}\left[1-\frac{4}{3\pi}\sqrt{\frac{\widehat{Q}}{2\sigma_n^2 x(k+1)+\widehat{Q}}}\left(\frac{\pi}{2}+\tan^{-1}\left(\sqrt{\frac{\widehat{Q}}{2\sigma_n^2 x(k+1)+\widehat{Q}}}\right)\right)\right]dx\Bigg\}.\end{aligned} \tag{6.12}$$

To the best of our knowledge, there exists no closed-form expression of the integral in (6.12). The value of $\overline{\mathrm{SER}}$ is therefore computed numerically.

6.2 Numerical Results

In this section, we provide numerical results of the SER performance. In the simulations we assume that the values of σ_n^2 and σ_g^2 are both equal to one.

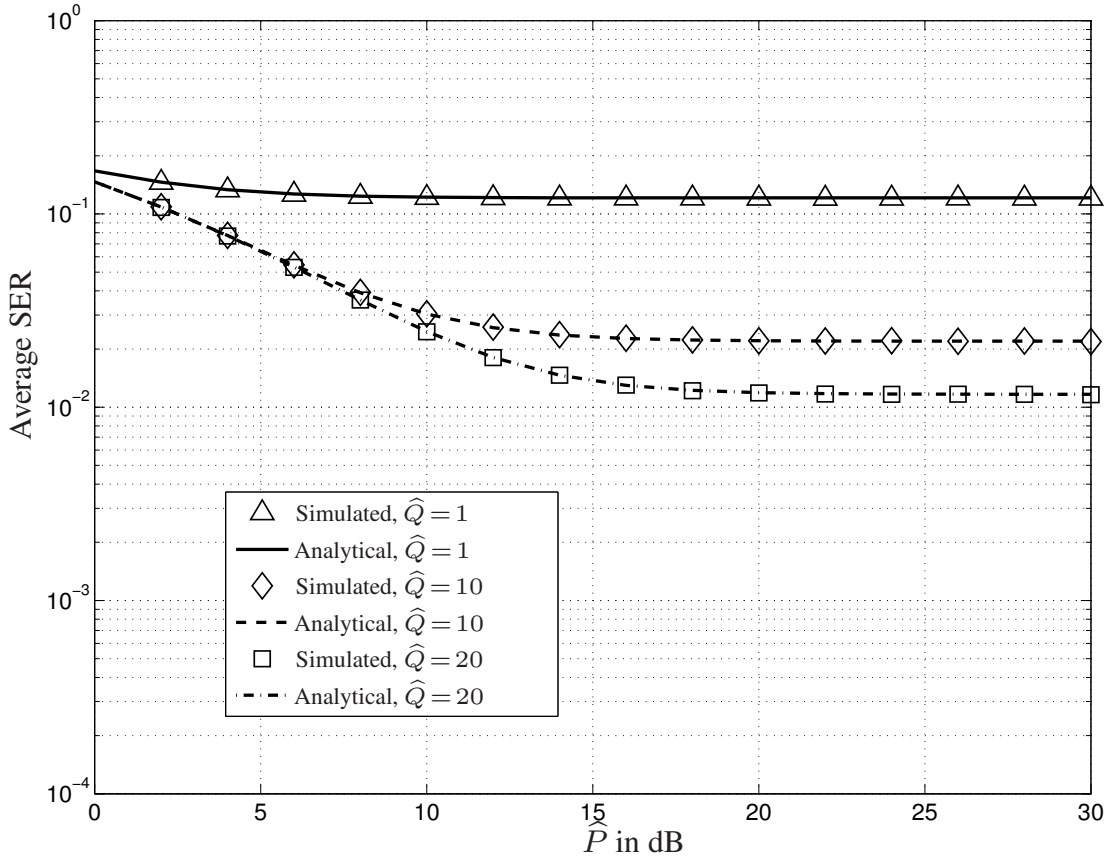

Figure 6.1: SER of BPSK versus transmitted power threshold $\widehat{P}$ for $K = 1$.

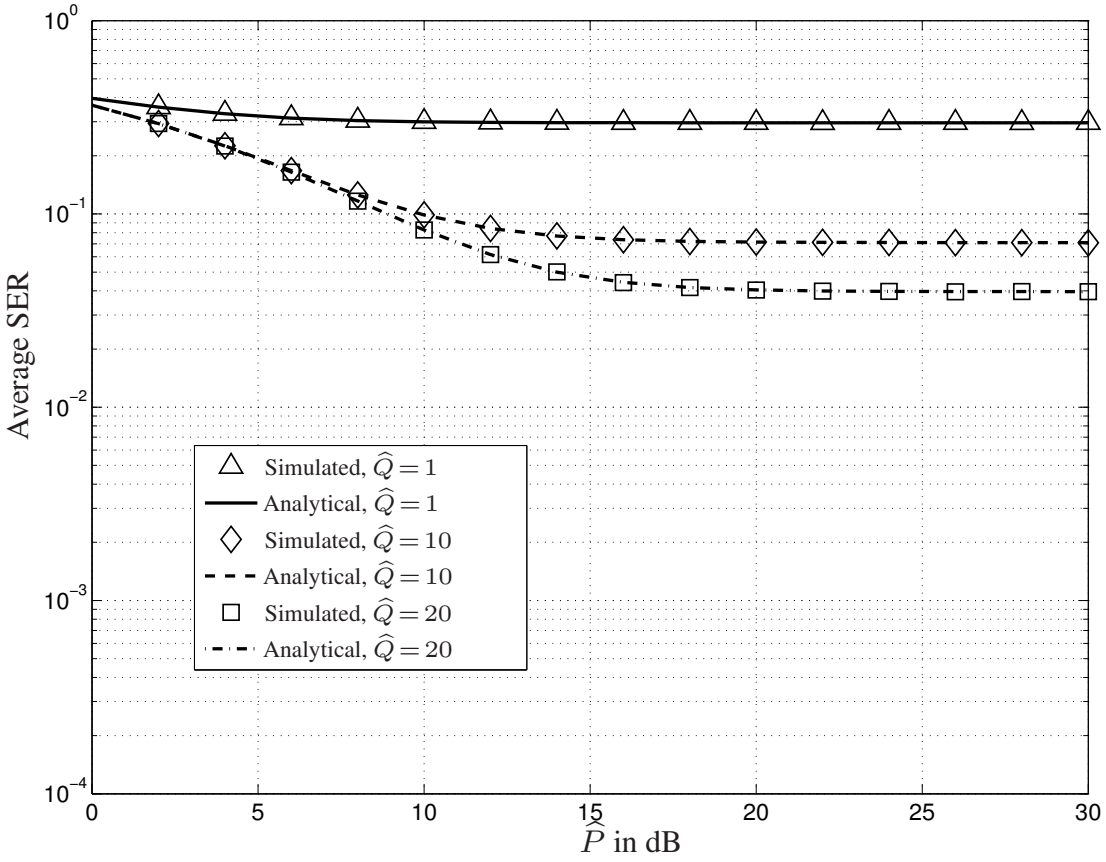

Figure 6.2: SER of QPSK versus transmitted power threshold $\widehat{P}$ for $K = 1$.

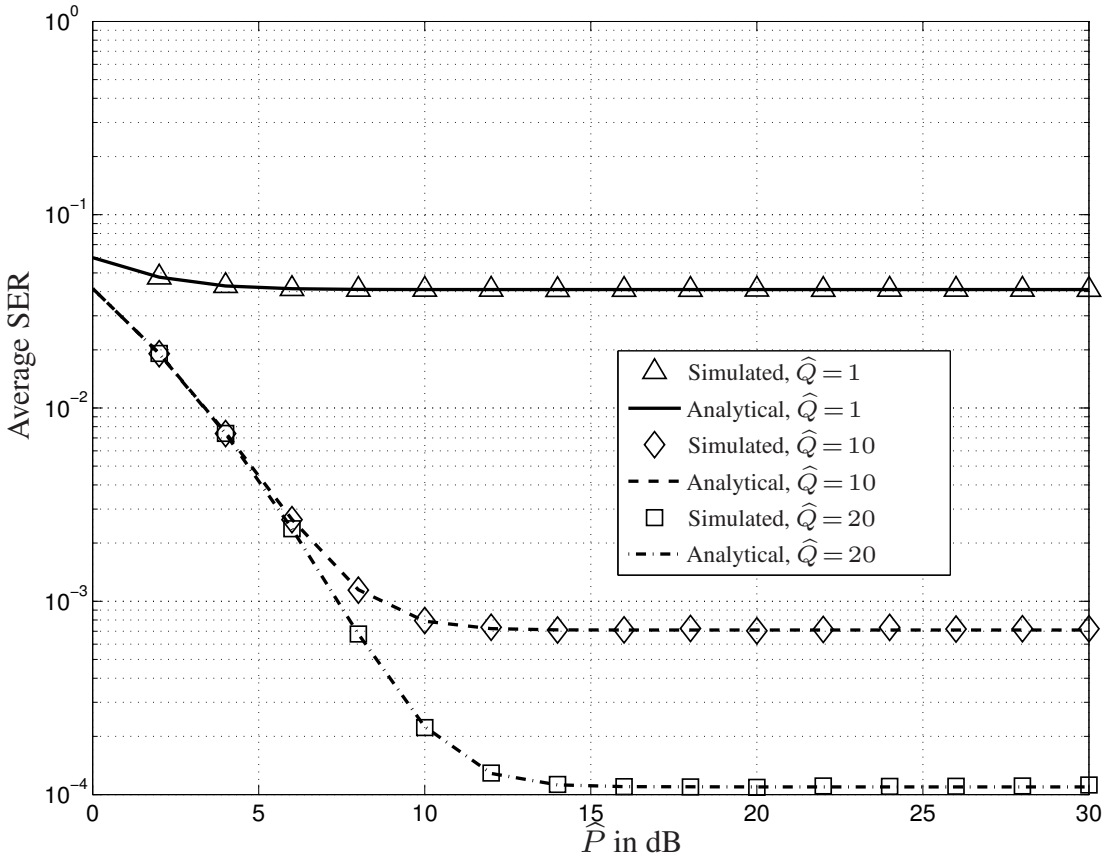

Figure 6.3: SER of BPSK versus transmitted power threshold $\widehat{P}$ for $K = 4$.

In Fig. 6.1 and Fig. 6.2, the SER is displayed versus the transmitted power threshold $\widehat{P}$ for the BPSK and the QPSK modulations, respectively, for the case of a single SR, i.e., $K = 1$. The analytical SER expressions given by (6.11) and (6.12) are plotted along with the results obtained from Monte-Carlo simulations. From these two figures, it can be observed that the simulated SER values match very well with the analytical results. Moreover, the SER decreases with the increasing PR interference threshold $\widehat{Q}$ as intuitively expected.

The SER performance of a multiple-receiver underlay cognitive system is illustrated in the Fig. 6.3 and Fig. 6.4. The values of the SER are plotted versus the transmitted power threshold $\hat{P}$ for the BPSK and the QPSK modulations, respectively. The number of users is equal to four, i.e., $K = 4$. The analytical SER expressions given by (6.11) and (6.12)

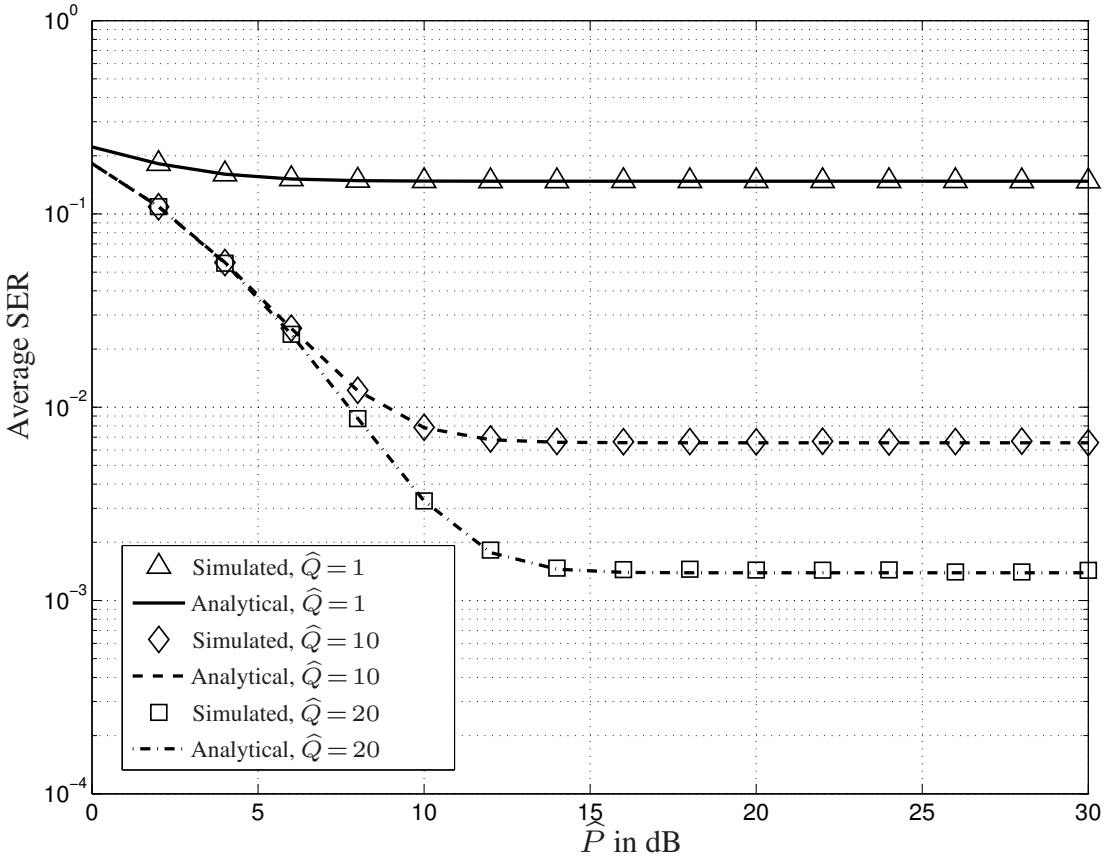

Figure 6.4: SER of QPSK versus transmitted power threshold $\widehat{P}$ for $K = 4$.

are compared with the simulation results for several different values of $\widehat{Q}$. From these two figures, we can see again that the analytical SER results match very well with the results obtained from Monte-Carlo simulations. Comparing the results for $K = 1$ and $K = 4$ in Figs. 6.1-6.4, we conclude that the opportunistic scheduling can improve the SER performance of a multiple-receiver system.

From Figs. 6.1-6.4, it can be observed that there exists a regime for the peak transmitted power threshold $\widehat{P}$ where the SER curves approach to constant values. This is due to the fact that the system is operating in the interference limited regime in which the actually transmitted power $\widehat{P}$ is mainly affected by constraint (6.1) and, therefore, does not increase significantly with the power threshold $\widehat{P}$. Figs. 6.1-6.4 further illustrate that if the remaining parameters such as the transmitted power P and the interference threshold $\widehat{Q}$ have the same values for both modulation types, then the SER values obtained for the BPSK modulation are generally lower than that for the QPSK modulation.

6.3 Chapter Summary

In this chapter, we have studied the SER performance of an underlay CR network where an opportunistic scheduler manages the data transmission making use of multiuser diversity. Exact analytical expressions of SER have been derived for general PSK modulations under the assumption that the peak interference power and the peak transmitted power does not exceed given thresholds. To date, the performance analysis for CR networks is mainly focused on the system throughput and channel capacity, a thorough study on the SER performance of the CR system is still missing. Our pioneering work in this area may attract further research interests and facilitate the future scheduler design.

Chapter 7

Conclusions and Future Work

In this final chapter, conclusions of this thesis are summarized and some future work is outlined.

7.1 Conclusions

In Chapter 3, we have studied the transmit diversity techniques in a point-to-point communication system. In the case of error-free feedback, it has been shown that the SER performance can be substantially improved by means of the TAS and the combined TAS-PA techniques compared with the OSTBC. In the erroneous feedback case, improved robustness against the feedback errors can be obtained by embedding the OSTBC in the applied transmit diversity techniques.

Multiuser diversity obtained by opportunistic scheduling has been investigated in Chapter 4. In a multiuser downlink system with homogeneous Rayleigh flat-fading channels, we have proved that the SER performance can achieve a maximal diversity order equal to the number of receivers K and a maximal multiuser diversity gain equal to the average SNR A. In the erroneous feedback case, it has been demonstrated that even in the case of a rather high feedback error probability, the opportunistic scheduling strategy outperforms the scheduling schemes that do not take any advantage of multiuser diversity such as random scheduling and round-robin scheduling.

The underlay CR has been studied in Chapter 5 and Chapter 6. In these two chapters, we have investigated the multiuser diversity achieved by opportunistic scheduling in terms of the channel capacity and the SER, respectively. In Chapter 5, we have computed the sum capacity of the underlay cognitive BC. In the case of homogeneous Rayleigh fading, we have also investigated the asymptotic behavior of the ergodic sum capacity C. In the regime of a large number of SRs K and a fixed number of PRs U, the ergodic sum capacity C has been shown to scale as $\ln \ln K$ with $K \to \infty$. This means that the same asymptotic gain can be obtained from the multiuser diversity in the underlay CR BC as in the conventional BC. In the asymptotic regime of $U \to \infty$ and fixed K, we have shown that C decreases with increasing U and asymptotically converges to a certain limit. In the case of average IPCs at the PRs, this capacity limit is equal to the ergodic sum capacity of a conventional BC with the average transmitted power not greater than the available power budget of the cognitive BC. In the case of peak IPCs at the PRs, C is upper bounded by $\ln\left(1 + \frac{a}{\ln U}\right)$ and converges to 0 as $U \to \infty$, where a is a constant independent of U. This means that the limit is equal to 0 in this case.

The SER performance of the underlay CR BC has been studied in Chapter 6. In this chapter, we have considered an underlay cognitive BC similar to that in Chapter 5 and assumed that there exist a single PR, i.e., $U = 1$. We have analyzed the opportunistic scheduling scheme and derived the SER expressions for the $\mathcal{K}$-PSK modulation. The derived expressions have been verified by the simulations.

Transmit and multiuser diversity find wide applications in wireless communication. The results from this thesis and the previous study have shown that fading should be reconsidered as a phenomenon facilitating the wireless communication instead of a kind of channel impairment. Making use of fading, transmit diversity based techniques can enhance the system performance while providing robustness against the feedback errors. Channel-aware scheduling, which exploits multiuser diversity in a fading environment, can significantly improve the overall system performance. In CR systems, transmit and multiuser diversity also find their applications to increase the overall system performance. In future wireless communication systems, diversity based transmit and scheduling schemes will play an important

role and contribute significantly to the high-performance wireless data service.

7.2 Future Work

A natural extension of the SER analyses presented in Chapters 3, 4 and 6 is to study the SER for other modulation and fading types besides the PSK and Rayleigh fading. For example, it is interesting to investigate whether the derived scaling laws in Chapter 4 also hold for other modulation types and other fading types. Further, all SER results in this thesis derived for the multiuser case are based on the assumption of a homogeneous network, extensions to heterogeneous network will be very interesting future work. To date, the link reliability in terms of the SER is mainly studied for the point-to-point communication system. A thorough study on the link reliability in other communication systems such as the multiuser MIMO system and the CR system is still missing. For example, in a multiuser MIMO system, it is interesting to analyze the impact of scheduling more than one users at the same time on SER performance. Future work in this area will surely contribute many interesting results.

As an emerging paradigm of the modern wireless communication, the CR has already attracted much attention. However, many important questions regarding its theoretical limits remain open and there is a variety of future work in this area. In the information theoretical aspect, it is important to further study the capacity regions of different CR systems. In the aspect of signal processing, more advance transmit and receive techniques have to be developed to enable the practical implementation of CR. For example, extending the results in Chapters 5 and 6 to the MIMO case will be a challenging work and future results on diversity and multiplexing gains will certainly provide new insights into the CR. Future efforts on this area will be very helpful to eventually commercialize the wireless CR systems.

Bibliography

[1] 2010 ICT Market Review & Forecast, available online at www.tiaonline.org.

[2] D. Tse and P. Viswanath, *Fundamentals of Wireless Communication*, Cambridge University Press, 2005.

[3] M. K. Simon and M. S. Alouini, *Digital Communication over Fading Channels: A Unified Approach to Performance Analysis*, John Wiley & Sons, 2000.

[4] B. L. Stüber, *Principles of Mobile Communication*, 2nd Edition, Kluwer Academic Publishers, 2002.

[5] J. S. Seybold, Introduction to RF Propagation, John Wiley & Sons, 2005.

[6] C. Oestges and B. Clerckx, *MIMO Wireless Communications: From Real-World Propagation to Space-Time Code Design*, Academic Press, 2007.

[7] J. Mitola, "Cognitive radio: An integrated agent architecture for software defined radio," Ph.D dissertation, KTH, Stockholm, Sweden, 2000.

[8] S. Haykin, "Cognitive radio: Brain-empowered wireless communications," *IEEE J. Sel. Areas Commun.*, vol. 23, no. 2, pp. 201-220, Feb. 2005.

[9] B. A. Fette, *Cognitive Radio Technology*, 2nd Edition, Academic Press, 2009.

[10] G. J. Foschini and M. J. Gans,"On limits of wireless communications in a fading environment when using multiple antennas,"*Wireless Personal Commun.*, vol. 6, no. 3, pp. 311-335, March 1998.

[11] E. Dahlman, S. Parkvall, J. Sköld, and P. Beming, *3G Evolution: HSPA and LTE for Mobile Broadband*, Elsevier Academic Press, 2008.

[12] E. Dahlman, S. Parkvall, J. Sköld, and P. Beming, *4G: LTE/LTE-Advanced for Mobile Broadband*, Elsevier Academic Press, 2011.

[13] T. K. Moon, *Error Correction Coding: Mathematical Methods and Algorithms*, John Wiley & Sons, 2005.

[14] B. Vucetic and J. Yuan, *Turbo Codes: Principles and Applications*, Springer, 2000.

[15] H. Schulze and C. Lüders, *Theory and Applications of OFDM and CDMA: Wideband Wireless Communications*, John Wiley & Sons, 2005.

[16] J. Proakis, *Digital Communications*, 4th Edition, McGraw Hill, 2001.

[17] P. Popovski, H. Yomo and R. Prasad, "Strategies for adaptive frequency hopping in the unlicensed bands," *IEEE Wireless Commun.*, vol. 13, no. 6, pp. 60-67, Dec. 2006.

[18] M. Bengtsson and B. Ottersten, "Optimal and suboptimal transmit beamforming," chapter in the book *Handbook of Antennas in Wireless Communications*, L. Godara (Editor), CRC Press, 2002.

[19] A. B. Gershman, "Adaptive beamforming for multiantenna communications," chapter in the book *Adaptive Signal Processing for Wireless Communications*, M. Ibnkahla (Editor), CRC Press, 2009.

[20] E. G. Larsson and P. Stoica, *Space-Time Block Coding for Wireless Communications*, Cambridge University Press, 2003.

[21] B. Vucetic and J. Yuan, *Space-Time Coding*, John Wiley & Sons, 2003.

[22] A. Paulraj, R. Nabar, and D. Gore, *Introduction to Space-Time Wireless Communications*, Cambridge University Press, 2003.

[23] A. B. Gershman and N. D. Sidiropoulos, Editors, *Space-Time Processing for MIMO Communications*, John Wiley & Sons, 2005.

[24] S. M. Alamouti, "A simple transmit diversity technique for wireless communications," *IEEE J. Sel. Areas Commun.*, vol. 16, no. 8, pp. 1451-1458, Oct. 1998.

[25] V. Tarokh, H. Jafarkhani, and A. R. Calderbank, "Space-time block codes from orthogonal designs," *IEEE Trans. Inf. Theory*, vol. 45, no. 5, pp. 1456-1467, July 1999.

[26] G. Jöngren, M. Skoglund and B. Ottersten, "Combining beamforming and orthogonal space-time block coding," *IEEE Trans. Inf. Theory*, vol 48, no. 3, pp. 611-627, March 2002.

[27] S. Zhou and G. B. Giannakis, "Optimal transmitter eigen-beamforming and space-time block coding based on channel mean feedback," *IEEE Trans. Signal Proc.*, vol. 50, no. 10, pp. 2599-2613, Oct. 2002.

[28] G. Ganesan, P. Stoica, and E. G. Larsson, "Diagonally weighted orthogonal space-time block codes," in *Proc. Asilomar Conf. Sign., Syst., and Comp.*, California, USA, vol. 2, pp. 1147-1151, Nov. 2002.

[29] D. Gore and A. Paulraj, "MIMO antenna subset selection with space-time coding," *IEEE Trans. Signal Proc.*, vol. 50, no. 10, pp. 2580-2588, Oct. 2002.

[30] Y. Xue and A. B. Gershman, "Alamouti-type wireless communication system with one-bit feedback," in *Proc. IEEE SAM 2004*, Sitges, Spain, pp. 143-147, July 2004.

[31] Y. Rong, S. A. Vorobyov, and A. B. Gershman, "Adaptive OFDM techniques with one-bit-per-subcarrier channel state feedback," *IEEE Trans. Commun.*, vol. 54, no. 11, pp. 1993-2003, Nov. 2006.

[32] D. J. Love, R. W. Heath, W. Santipach, and M. L. Honig, "What is the value of limited feedback for MIMO channels?" *IEEE Commun. Magazine*, vol. 42, no. 10, pp. 54-59, Oct. 2003.

[33] D. J. Love, R. W. Heath, V. K. N.. Lau, D. Gesbert, B. D. Rao, and M. Andrews, "An overview of limited feedback in wireless communication systems," *IEEE J. Sel. Areas Commun.*, vol. 26, no. 8, pp. 1341-1365, Oct. 2008.

[34] M. Gharavi-Alkhansari and A. B. Gershman, "Fast antenna subset selection in MIMO wireless systems," *IEEE Trans. Signal Proc.*, vol. 52, no. 2, pp. 339-347, Feb. 2004.

[35] T. L. Marzetta and B. M. Hochwald, "Capacity of a mobile multiple-antenna communication link in Rayleigh flat fading," *IEEE Trans. Inf. Theory*, vol. 45, no. 1, pp. 139-157, Jan. 1999.

[36] A. Goldsmith, S. A. Jafar, N. Jindal, and S. Vishwanath, "Capacity limits of MIMO channels," *IEEE J. Sel. Areas Commun.*, vol. 21, no. 5, pp. 684-702, June 2003.

[37] A. D. Dabbagh and D. J. Love, "Feedback rate-capacity loss tradeoff for limited feedback MIMO systems," *IEEE Trans. Inf. Theory*, vol. 52, no. 5, pp. 2190-2202, May 2006.

[38] A. F. Molish, M. Z. Win, C. Yang-Seok and J. H. Winters, "Capacity of MIMO systems with antenna selection," *IEEE Trans. Wireless Commun.*, vol. 4, no. 4, pp. 1759-1772, May 2005.

[39] E. A. Neasmith and C. Beaulieu, "New results on selection diversity," *IEEE Trans. Commun.*, vol. 46, no. 5, pp. 695-704, May 1998.

[40] Q. Ma, and C. Tepedelenlioglu, "Antenna selection for space-time coded systems with imperfect channel estimation," *IEEE Trans. Wireless Commun.*, vol. 6, no. 2, pp. 710-719, Feb. 2007.

[41] 3rd Generation Partnership Project, available online at www.3gpp.org.

[42] P. Viswanath, D. Tse and R. Laroia, "Opportunistic beamforming using dumb antennas," *IEEE Trans. Inf. Theory*, vol. 48, no. 6, pp. 1277-1294, June 2002.

[43] R. Knopp and P. Humblet, "Information capacity and power control in single cell multiuser communications," in *Proc. IEEE ICC 2005*, Seattle, WA, USA, vol. 1, pp. 331-335, June 1995.

[44] D. Tse, "Optimal power allocation over parallel Gaussian broadcast channels," in *Proc. IEEE ISIT 1997*, Ulm, Germany, p. 27, June 1997.

[45] L. Yang and M. S. Alouini, "Performance analysis of multiuser selection diversity," *IEEE Trans. Vehicular Tech.*, vol. 55, no. 6, pp. 1848-1861, Nov. 2006.

[46] S. Sanayei and A. Nosratinia, "Opportunistic downlink transmission with limited feedback," *IEEE Trans. Inf. Theory*, vol. 53, no. 11, pp. 4363-4372, Nov. 2007.

[47] T. Yoo, N. Jindal, and A. Goldsmith, "Multi-antenna downlink channels with limited feedback and user selection," *IEEE J. Sel. Areas Commun.*, vol. 25, no. 7, pp. 1478-1491, Sept. 2007.

[48] T. M. Cover, "Broadcast channels," *IEEE Trans. Inf. Theory*, vol. 18, no. 1, pp. 2-14, Jan. 1972.

[49] T. M. Cover, "Comments on broadcast channels," *IEEE Trans. Inf. Theory*, vol. 44, no. 6, pp. 2524-2530, Oct. 1998.

[50] G. Caire and S. Shamai, "On the achievable throughput of a multiantenna Gaussian broadcast channel," *IEEE Trans. Inf. Theory*, vol. 49, no. 7, pp. 1691-1706, July 2003.

[51] H. Weingarten, Y. Steinberg, and S. Shamai, "The capacity region of the Gaussian multiple-input multiple-output broadcast channel," *IEEE Trans. Inf. Theory*, vol. 52, no. 9, pp. 3936-3964, Sept. 2006.

[52] M. Sharif and B. Hassibi, "On the capacity of MIMO broadcast channels with partial side information," *IEEE Trans. Inf. Theory*, vol. 51, no. 2, pp. 506-522, Feb. 2005.

[53] M. Sharif and B. Hassibi, "A comparison of time-sharing, DPC, and beamforming for MIMO broadcast channels with many users," *IEEE Trans. Commun.*, vol. 55, no. 1, pp. 11-15, Jan. 2007.

[54] R. Zhang, S. Cui, and Y. C. Liang, "On ergodic sum capacity of fading cognitive multiple-access and broadcast channels," *IEEE Trans. Inf. Theory*, vol. 55, no. 11, pp. 5161-5178, Nov. 2009.

[55] N. Jindal, S. Vishwanath, and A. Goldsmith, "On the duality of Gaussian multiple-access and broadcast channels," *IEEE Trans. Inf. Theory*, vol. 50, no. 5, pp. 768-783, May 2004.

[56] O. C. Ugweje, "Selection diversity for wireless communications in Nakagami-fading with arbitrary parameters," *IEEE Trans. Vehicular Tech.*, vol. 50, no. 6, pp. 1437-1448, Nov. 2001.

[57] A. Sendonaris, E. Erkip, and B. Aazhang, "User cooperation diversity - part I: System description," *IEEE Trans. Commun.*, vol. 51, no. 11, pp. 1927-1938, Nov. 2003.

[58] A. Sendonaris, E. Erkip, and B. Aazhang, "User cooperation diversity - part II: Implementation aspects and performance analysis," *IEEE Trans. Commun.*, vol. 51, no. 11, pp. 1939-1948, Nov. 2003.

[59] J. N. Laneman, D. Tse, and G. W. Wornell, "Cooperative diversity in wireless networks: Efficient protocols and outage behavior," *IEEE Trans. Inf. Theory*, vol. 50, no. 12, pp. 3062-3080, Dec. 2004.

[60] F. H. P. Fitzek, M. D. Katz, *Cooperation in Wireless Networks: Principles and Applications*, Springer, 2006.

[61] M. O. Hasna and M. S. Alouini, "End-to-end performance of transmission systems with relays over Rayleigh-fading channels," *IEEE Trans. Wireless Commun.*, vol. 2, no. 6, pp. 1126-1131, Nov. 2003.

[62] M. O. Hasna and M. S. Alouini, "Harmonic mean and end-to-end performance of transmission systems with relays," *IEEE Trans. Commun.*, vol. 52, no. 1, pp. 130-135, Jan. 2004.

[63] M. O. Hasna and M. S. Alouini, "Optimal power allocation for relayed transmissions over Rayleigh-fading channels," *IEEE Trans. Wireless Commun.*, vol. 3, no. 6, pp. 1999-2004, Nov. 2004.

[64] P. A. Anghel and M. Kaveh, "Exact symbol error probability of a cooperative network in a Rayleigh-fading environment," *IEEE Trans. Wireless Commun.*, vol. 3, no. 5, pp. 1416-1421, Sept. 2004.

[65] T. Tsiftsis, G. Karagiannidis, P. T. Mathiopoulos, and S. A. Kotsopoulos, "Nonregenerative dual-hop cooperative links with selection diversity," *EURASIP J. Wireless Commun. & Networking*, vol. 2006, Article ID 17862, Jan. 2006.

[66] Y. Zhao, R. Adve, and T. J. Lim, "Symbol error rate of selection amplify-and-forward relay systems," *IEEE Commun. Lett.*, vol. 10, no. 11, pp. 757-759, Nov. 2006.

[67] B. Barua, H. Q. Ngo, and H. Shin, "On the SEP of cooperative diversity with opportunistic relaying," *IEEE Commun. Lett.*, vol. 12, no. 10, pp. 727-729, Oct. 2008.

[68] A. Ribeiro, X. Cai, and G. B. Giannakis, "Symbol error probabilities for general cooperative links," *IEEE Trans. Wireless Commun.*, vol. 4, no. 3, pp. 1264-1273, May 2005.

[69] T. Wang, A. Cano, G. B. Giannakis, and J. N. Laneman, "High-performance cooperative demodulation with decode-and-forward relay," *IEEE Trans. Commun.*, vol. 55, no. 7, pp. 1427-1438, July 2007.

[70] Z. Yi and I. Kim, "Diversity order analysis of the decode-and-forward cooperative networks with relay selection," *IEEE Trans. Wireless Commun.*, vol. 7, no. 5, pp. 1792-1799, May 2008.

[71] C. Cordeiro, K. Challapali, and D. Birru, "IEEE 802.22: An introduction to the first wireless standard based on cognitive radios," *J. of Commun.*, vol. 1, no. 1, pp. 38-47, April 2006.

[72] C. Stevenson, G. Chouinard, Z. Lei, W. Hu, S. Shellhammer, and W. Caldwell, "IEEE 802.22: The first cognitive radio wireless regional area network standard," *IEEE Commun. Magazine*, vol. 47, no. 1, pp. 130-138, Jan. 2009.

[73] A. Goldsmith, S. A. Jafar, and S. Srinivasa, "Breaking spectrum gridlock with cognitive radios: An information theoretic perspective," *Proc. of the IEEE*, vol. 97, no. 5, pp. 894-914, May 2009.

[74] A. Ghasemi and E. S. Sousa, "Fundamental limits of spectrum-sharing in fading environments," *IEEE Trans. Wireless Commun.*, vol. 6, no. 2, pp. 649-658, Feb. 2007.

[75] N. Devroye, P. Mitran, and V. Tarokh, "Achievable rates in cognitive radio channels," *IEEE Trans. Inf. Theory*, vol. 52, no. 5, pp. 1813-1827, May 2006.

[76] A. Jovicic and P. Viswanath, "Cognitive radio: An Information theoretic perspective," *IEEE Trans. Inf. Theory*, vol. 55, no. 9, pp. 3945-3958, Sept. 2009.

[77] C. E. Shannon, "A mathematical theory of communication," *Bell Sys. Tech. Journal*, vol. 27, pp. 379-423, 623-656, 1948.

[78] T. M. Cover and J. A. Thomas, *Elements of Information Theory*, John Wiley & Sons, 1991.

[79] I. E. Telatar, "Capacity of multi-antenna Gaussian channels," *European Trans. Telecommun.*, vol. 10, pp. 585-596, Nov. 1999.

[80] A. Goldsmith and P. Varaiya, "Capacity of fading channels with channel side information," *IEEE Trans. Inf. Theory*, vol. 43, no. 6, pp. 1986-1992, Nov. 1997.

[81] E. Biglieri, J. Proakis, and S. Shamai, "Fading channels: Information-theoretic and communications aspects," *IEEE Trans. Inf. Theory*, vol. 44, no. 6, pp. 2619-2692, Oct. 1998.

[82] H. A. David and H.-N. Nagaraja, *Order Statistics*, 3rd Edition, John Wiley & Sons, 2003.

[83] S. Kotz, and S. Nadarajah, *Extreme Value Distributions: Theory and Applications*, Imperial College Press, 2000.

[84] P. Billingsley, *Convergence of Probability Measures*, 2nd Edition, John Wiley & Sons, 1999.

[85] Z. Chen, J. Yuan, and B. Vucetic, "Analysis of transmit antenna selection/maximal-ratio combining in Rayleigh fading channels," *IEEE Trans. Vehicular Tech.*, vol. 54, no. 4, pp. 1312-1321, July 2005.

[86] Z. Chen, J. Yuan, B. Vucetic and Z. Zhou, "Performance of Alamouti scheme with transmit antenna selection," in *Proc. IEEE PIMRC 2004*, vol. 2, pp. 1135-1141, Sept. 2004.

[87] D. Olive, *Applied Robust Statistics*, available online at www.math.siu.edu/olive/ol-bookp.htm.

[88] V. Chakravarthy, X. Li, R. Zhou, Z. Wu and M. Temple, "A novel hybrid overlay/underlay cognitive radio waveform in frequency selective fading channels," in *Proc. IEEE CROWNCOM 2009*, pp. 1-6, June 2009.

[89] M. H. Islam, Y. C. Liang, and A. T. Hoang, "Combining eigen-beamforming and orthogonal space-time block coding for secondary usage of spectrum," in *Proc. IEEE ICC 2008*, pp. 830-834, May 2008.

[90] P. Ligdas, and N. Farvardin, "Optimizing the transmit power for slow fading channels," *IEEE Trans. Inf. Theory*, vol. 46, no. 3, pp. 565-576, March 2000.

[91] P. Borjesson and C.-E. Sundberg, "Simple approximations of the error function Q(x) for communications applications," *IEEE Trans. Commun.*, vol. 27, no. 3, pp. 639-643, March 1979.

[92] D. P. Bertsekas, A. Nedic, and A. E. Ozdaglar, *Convex Analysis and Optimization*, Belmont, MA, Athena Scientific, 2003.

[93] D. P. Bertsekas, *Nonlinear Programming*, 2nd Edition, Belmont, MA, Athena Scientific, 1999.

[94] S. Boyd and L. Vandenberghe, *Convex Optimization*, Cambridge University Press, 2004.

[95] M. Grant and S. Boyd, *CVX: Matlab software for disciplined convex programming*, http://cvxr.com/cvx.

[96] G. Dimic and N. D. Sidiropoulos, "On downlink beamforming with greedy user selection: Performance analysis and a simple new algorithm," *IEEE Trans. Signal Proc.*, vol. 53, no. 10, pp. 3857-3868, Oct. 2005.

[97] Q. Spencer, A. L. Swindlehurst and M. Haardt, "Zero-forcing methods for downlink spatial multiplexing in multiuser MIMO channels," *IEEE Trans. Signal Proc.*, vol. 52, no. 2, pp. 461-471, Feb. 2004.

[98] I. S. Gradshteyn, I. M. Ryzhik, A. Jeffrey and D. Zwillinger, *Table of Integrals, Series, and Products*, 7th Edition, Academic Press, 2007.

[99] L. Li, S. A. Vorobyov and A. B. Gershman, "Adaptive resource allocation in MIMO communication systems using low rate channel state feedback," in *Proc. IEEE SPAWC 2007*, Helsinki, Finland, pp. 1-5, June 2007.

[100] L. Li, S. A. Vorobyov, and A. B. Gershman, "Transmit antenna selection based strategies in MISO communication systems with low-rate channel state feedback," *IEEE Trans. Wireless Commun.*, vol. 8, no. 4, pp. 1660-1666, April 2009.

[101] L. Li and A. B. Gershman, "Downlink opportunistic scheduling with low-rate channel state feedback: Error rate analysis and optimization of the feedback parameters," in *Proc. IEEE SPAWC 2008*, Recife, Brazil, pp. 356-360, July 2008.

[102] L. Li, M. Pesavento, and A. B. Gershman, "Downlink opportunistic scheduling with low-rate channel state feedback: Error rate analysis and optimization of the feedback parameters," *IEEE Trans. Commun.*, vol. 58, no. 10, pp. 2871-2880, Oct. 2010.

[103] L. Li, M. Pesavento, and A. B. Gershman, "On ergodic sum capacity of underlay cognitive broadcast channels," in *Proc. IEEE PIMRC 2010*, Istanbul, Turkey, pp. 2710-2714, Sept. 2010.

[104] L. Li, M. Pesavento, and A. B. Gershman, "Sum capacity limits for underlay cognitive radio SISO broadcast channels," *IEEE Trans. Inf. Theory*, submitted, April 2011.

[105] L. Li and M. Pesavento, "The sum capacity of underlay cognitive broadcast channel," in *Proc. IEEE CROWNCOM 2011*, Osaka, Japan, pp. 390-394, June 2011.

[106] L. Li, P. I. Derwin, and M. Pesavento, "Symbol error rate analysis in multiuser underlay cognitive radio systems," in *Proc. IEEE PIMRC 2011*, Toronto, Canada, Sept. 2011.

Curriculum Vitae

Personal information

Name	Liang Li
Date of birth	02 Nov. 1981

Education

Nov. 2006-present	Ph. D. student in Communication Systems Group Technische Universität Darmstadt, Germany
Oct. 2002-Nov. 2006	Diploma in Electrical Engineering Technische Universität Darmstadt, Germany Overall Classification: Very good
Sep. 2000-Oct. 2002	Electrical Engineering, Tongji University, Shanghai, China

Teaching Experiences

Nov. 2004-present	Teaching assistant at Technische Universität Darmstadt

Academic Awards

2010	Chinese government award for outstanding self-financed students abroad

Supervised Theses

Yuefeng Qian	Feedback optimization in multiuser downlink channels
Qichao Li (external)	CQI estimation for MIMO transmission in the presence of receiver impairments
Yin Zhu	Optimal downlink beamforming in OFDM systems
Philemon Ivan Derwin	Derwin Symbol error rate analysis in multiuser underlay cognitive radio system
Jun Ma	Symbol error rate of underlay cognitive radio system
Peng Jin	The application of game theory to the OFDM based cognitive radio systems
Javier Chiquero	Applying game theory for spectrum sharing in cognitive radio